Doctoral theses at NTNU, 2013:250

Mette Eltvik

Sediment erosion in Francis turbines

Doctoral Thesis

Mette Eltvik

ISBN 978-82-471-4623-1 (printed version)
ISBN 978-82-471-4625-5 (electronic version)
ISSN 1503-8181

NTNU – Trondheim
Norwegian University of
Science and Technology

NTNU – Trondheim
Norwegian University of
Science and Technology

Doctoral theses at NTNU, 2013:250

NTNU

NTNU
Norwegian University of Science and Technology
Thesis for the degree of Philosophiae Doctor
Faculty of Engineering Science & Technology
Department of Energy and Process Engineering

Mette Eltvik

Sediment erosion in Francis turbines

Thesis for the degree of Philosophiae Doctor

Trondheim, July 2013

Norwegian University of Science and Technology
Faculty of Engineering Science & Technology
Department of Energy and Process Engineering

NTNU – Trondheim
Norwegian University of
Science and Technology

NTNU
Norwegian University of Science and Technology

Thesis for the degree of Philosophiae Doctor

Faculty of Engineering Science & Technology
Department of Energy and Process Engineering

ISBN 978-82-471-4623-1 (printed version)
ISBN 978-82-471-4625-5 (electronic version)
ISSN 1503-8181

Doctoral theses at NTNU, 2013:250

Printed by Skipnes Kommunikasjon as

To my grandpa, Clarence Yggeseth

CHAPTER

Preface

The work has been conducted at the Waterpower Laboratory, Department of Energy and Process Engineering at the Norwegian University of Science and Technology(NTNU) in Trondheim. This thesis is a product of papers submitted during the project period lasting from August 2010 to July 2013. The work is funded by Energy Norway, which is a non-profit industry organization representing companies from the renewable energy sector in Norway.

The research has also been part of the RenewableNepal project *Development of Hydraulic Turbines with a new design philosophy as a foundation for turbine manufacturing in Nepal*. The project is a co-operation with Katmandu University, NORAD Cooperation, SINTEF and NTNU. The candidate's role, as a supporting researcher, was to contribute knowledge within turbine design criteria, programming and numerical simulations.

CHAPTER

Abstract

Sediment erosion is a major challenge for run-of-river power plants, especially during flood periods. Due to the high content of hard minerals such as quartz and feldspar carried in the river, substantial damage is observed on the turbine components. Material is gradually removed, thus the efficiency of the turbine decreases and the operating time of the turbine reduces. Hydro power plants situated in areas with high sediment concentration suffer under hard conditions, where turbine components could be worn out after only a short period of three months. This short life expectation causes trouble for energy production since the replacement of new turbine parts is a time consuming and costly procedure.

It is desirable to design a Francis runner which will withstand sediment erosion better than the traditional designs. The literature states that an expression for erosion is velocity to the power of three. By reducing the relative velocities in the runner by 10%, the erosion will decrease almost 30%. The objective is to improve the design of a Francis turbine which operates in rivers with high sediment concentration, by looking at the design parameters in order to reduce erosion wear. A Francis turbine design tool was developed to accomplish the parameter study. In the search for an optimized Francis runner, several design proposals were compared against a reference design by evaluating the turbine's performance. The hydraulic flow conditions and the prediction of erosion on the turbine components are simulated by analyzing the models with a Computational Fluid Dynamic (CFD) tool. A Fluid Structure Interaction (FSI) analysis ensures that the structural integrity of the design is within a desired value. Results from this research show that it is feasible to design a runner with an extended lifetime, without affecting the main dimensions and hydraulic efficiency.

Keywords: Hydraulic Turbines, Francis runner design, sediment erosion, CFD, FSI

CHAPTER

Acknowledgements

During these years there have been many people who contributed with support, advice and encouragement. I would like to express my gratitude to Professor Ole Gunnar Dahlhaug for good discussions, knowledge transfer and motivation through all these years. Professor Torbjørn K. Nielsen deserves the same appreciation for always having the door open and time to discuss problems in details. Thanks to Professor Emeritus Hermod Brekke and Arne Kjølle for conveying good experiences and keeping the old stories alive. I am very grateful to have had the opportunity to be part of the Water Power Laboratory community as a student and PhD candidate. Thanks to all old and new students and friends that made the days cheerful with encouraging talk, productive discussions and enjoyable coffee breaks.

During the project period, the author has been a co-supervisor for several master students. Their work was linked to topics relevant in this PhD project, and their contributions have been vital. Working together with Kristine Gjøsæter and Biraj Singh Thapa, the software Khoj emerged. This made it possible to accomplish the parameter study and investigate the effects of changing design variables. Later Peter Joachim Gogstad made improvements to the software which made it more collaborative with CAD software. Helene Palmgren Erichsen and Jonas Bermann-Paulsen worked on the mechanical design of the Francis turbine.

Thanks to Bjarne Børresen and Energy Norway for financial support of the project. Great thanks to Ola G. Thorvaldsen and Per Egil Skaare at Dynavec for their help and support on numerical problems and discussions. Special thanks to Kjell Tore Fjærvold at Statkraft for involving me in inspiring discussions on sediment problems at Norwegian power plants, and for allowing me work at their office at Lysaker when I needed break from Trondheim. Thanks to Professor Bhola Thapa and the staff at Turbine Testing Lab at Kathmandu University, and to Meg B. Bishwakarma and his staff at Hydro Lab for making my stay in Nepal a memorable time. I will surly go back to Nepal as often as possible. Thanks to Stian Breilo and Rainpower Peru for their hospitality and kindness during my short stay at their office in Lima. Thanks to Viggo Mossing at SN Power for reminding me to keep both feet on the ground.

Special thanks to all my friends in Trondheim for making the student life an unforgettable and happy adventure. My family and friends in Oslo also need a great thanks for always being there and supporting me in the choices I have made.

The thesis is dedicated to my grandpa, Clarence Yggeseth, because he always talked about Eulers equation and inspired me to work with hydro power.

Mette Eltvik
Trondheim, July 2013

CHAPTER

List of publications

This thesis is a collection of four papers, either presented at conferences or submitted for publication in journals. The complete papers are enclosed in Part II of the thesis. Additional papers, where the author has contributed with research related to the same topic, are found in Part III.

Papers - Main author

1. **Eltvik, M.**, Dahlhaug, O.G., Neopane, H.P., "Prediction of sediment erosion in Francis turbines", 4^{th} *International Meeting on Cavitation and Dynamic Problems in Hydraulic Machinery and Systems*, Belgrade, Serbia, October 26-28, 2011

2. **Eltvik, M.**, Thapa, B.S., Dahlhaug, O.G., Gjøsæter, K., "Numerical analysis of effect of design parameters and sediment erosion on a Francis runner", *Fourth International Conference on Water Resources and Renewable Energy Development in Asia*, Chiang Mai, Thailand, March 25-26, 2012

3. **Eltvik, M.**, Nielsen, T., Dahlhaug, O.G., "Hydraulic design of a Francis runner exposed to sediment erosion", submitted

4. **Eltvik, M.**, Dahlhaug, O.G., Nielsen, T., "Numerical analysis of Francis runners exposed to sediment erosion", submitted

Papers - Co-author

Thapa, B.S., Gjøsæther, K., Eltvik, M., Dahlhaug, O.G., "Effect of turbine design parameters on sediment erosion of Francis runner", *2nd International Conference on the Developments in Renewable Energy Technology*, IEEE, Bangladesh, January 5-7, 2012

Thapa, B.S., Eltvik, M., Dahlhaug, O.G., Thapa, B., Gjøsæter, K., "Design optimization of Francis runner for sediment handling", *Fourth International Conference on Water Resources and Renewable Energy Development in Asia*, Chiang Mai, Thailand, March 25-26, 2012

Thapa, B.S., Thapa, B., Eltvik, M., Gjøsæter, K., Dahlhaug, O.G., "Optimizing runner blade profile of Francis turbine to minimize sediment erosion", *The 26th IAHR Symposium on Hydraulic Machinery and Systems*, Beijing, China, August 19 – 23, 2012

Supervision of Master thesis

- **Co-adviser MSc. Thesis**: Kristine Gjøsæter, "Hydraulic design of Francis turbine exposed to sediment erosion", NTNU, Trondheim, Norway, 2011
- **Co-adviser MSc. Thesis**: Biraj Singh Thapa, "Hydraulic design of Francis turbine to minimize sediment erosion", NTNU, Trondheim, Norway, 2011
- **Co-adviser MSc. Thesis**: Helene P. Erichsen, "Mechanical design of Francis turbine exposed to sediment erosion", NTNU, Trondheim, Norway, 2011
- **Co-adviser MSc. Thesis**: Njål Vangdal, "Sediment erosion in a centrifugal pump", NTNU, Trondheim, Norway, 2011
- **Co-adviser MSc. Thesis**: Jonas Bergmann-Paulsen, "Mechanical design of Francis turbine exposed to sediment erosion" NTNU, Trondheim, Norway, 2012

Contents

List of Figures

List of Tables

PART I

Summary

CHAPTER I

Introduction

► This chapter gives an introduction to the erosion problem in Francis turbines and the motivation for this project. The objective and methods are briefly described, along with the outline of the thesis and a review of earlier work and the status of ongoing research in the field.

1.1 Background

The world's population has passed 7.2 billion, and is gradually growing, and expected to reach 9.6 billion by 2050 [38]. The energy demand will surly increase along with the population growth, which turns out to be larger than first predicted. As economies and prosperity are growing, the need for energy will increase even more. Recently there has been a large focus on sustainable energy, with the aim to secure future energy and reduce greenhouse-gas emissions. None of the renewable energy sources are as reliable and flexible as hydropower, with its large storage capacity, high efficiency, low operation and maintenance costs. Although the technology has been utilized through the ages and is relatively mature compared to other renewable sources, new barriers emerge such as public acceptance, and political and environmental challenges [21].

The potential of hydropower in the world is almost 4 000 GW, only one fifth of which is currently in use. The technical potential is estimated to 15 955 TWh/year, which is 4.8 times larger than today's production [22]. A large potential of unexploited hydro power is found in Asia, South America and Africa. Already there has been a growth of hydro power generation in the emerging and developing countries [21]. New problems arise, which today's turbine equipment manages poorly: the high content of hard minerals in the rivers, which rapidly wear down the turbine parts.

As a consequence of the increase in population and wealth, the amount of climate gases has increased and extreme weather is more common all over the world [27]. Monsoon seasons are highly connected with the weather variation, and the precipitation will increase in the near future and affect a larger areas than today [19].The melting of glaciers has become a larger problem for hydro power plants, due to the global changes and rises in temperature. As the glacier moves along the rock face, rocks erode and are transported further with the glacial stream. Especially

in alpine areas such as the Alps, the Andes and the Himalaya, rivers cause problems for the power plants. These mountain ranges have a large amount of hard minerals such as quartz and feldspar, which wear out the turbine components. The sediment transported in the rivers increase drastically during the monsoon season due to intense rainfall, steep topography and fragile geology. The reservoir capacity decreases due to the settling of huge loads of sediments, even though a system exists for handling this problem [33]. There is usually a desander at the intake filtering out the particles from the flow. However, there will be unsettled particles in the flow passing through the turbines. The erosion wear occurs where the velocities are highest, typically in the guide vanes and in the runner. This results in worn out mechanical parts, vibration problems and reduced performance, which often lead to often shut downs and costly repairs. CFD is a numerical simulation tool that gives a quantitative prediction of the flow pattern in the turbine, and of which areas on the turbine are most vulnerable to sediment erosion. Elasticity and structural analysis are solved by FSI simulations and indicate stresses and displacement of the turbine blade. By using these tools in the turbine design process, an optimized turbine design, which is more resistant to erosion, is achievable.

1.2 Objective

Sediment erosion in hydro power plants is a wide topic which involves research on, among other topics, sediment flow, mineral properties, turbine materials, coatings, operation conditions, head work, and maintenance procedures. Through studies of earlier work no research was found on the design of Francis runners with regard to the sediment erosion problem. The aim of this PhD-project is to search for a new approach for Francis runner design, in order to minimize wear due to sediment erosion. To improve the Francis turbine which operates in sand-laden rivers, a study of the design parameters is necessary to gain a proper understanding of the erosion phenomena in the runner. The research will be favorable for both the economic and energy production aspects for turbines operating in sand laden rivers.

The main objectives of the work are to:

Goal 1: Develop a new design of a Francis runner to minimize sand erosion
- Create a Francis turbine design software, and carry out a study of the design parameters, with the aim of decreasing the relative velocity in the runner

Goal 2: Verify the hydraulic design
- CFD simulations analyze the flow conditions and predictions of erosion in the runner designs.

Goal 3: Verify the mechanical design
- The stress and strain analysis of the runner using FSI simulations, involving hydraulic pressure from the CFD results

1.3 Outline of thesis

This thesis is divided into four parts. Part I is a summary which gives an overall understanding of the sediment erosion problem in Francis turbines, covering the background, motivation, theory and methods relevant to this project. A short resume of each paper is given, followed by a thorough discussion of the results. Finally, there is a conclusion of the work with recommendations for further research.

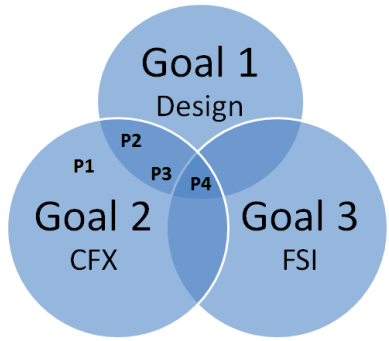

Figure 1.1: *The coherence between project goals and paper content*

In Part II, the four papers submitted for this work are presented. The coherence between the three goals and the papers (denoted as P) is illustrated in Fig 1.1. The work has been done in the following manner:

Paper 1. Prediction of Sediment Erosion in Francis Turbines
Mette Eltvik, Ole Gunnar Dahlhaug and Hari Prasad Neopane
This paper was presented at the 4^{th} International Meeting on Cavitation and Dynamic Problems in Hydraulic Machinery and Systems in Belgrade in October 2011. The author is responsible for the entire content in the paper. The co-authors have had a consultative contribution.

Paper 2. Numerical analysis of effect of design parameters and sediment erosion on a Francis runner
Mette Eltvik, Biraj Singh Thapa, Ole Gunnar Dahlhaug and Kristine Gjøsæter
The paper was presented in Thailand in March 2012 at the Fourth International Conference on Water Resources and Renewable Energy Development in Asia. The author is responsible for the main work of the thesis. B. S. Thapa and K. Gjøsæter contributed with the design parameter study by helping with the completion of the design software *Khoj*.

Paper 3. Hydraulic Design of a Francis Runner Exposed to Sediment Erosion
Mette Eltvik, Torbjørn Nielsen and Ole Gunnar Dahlhaug
The author is responsible for the entire work in the paper, under the guidance of the co-authors.
Submitted.

Paper 4. Numerical Analysis of Francis Runners Exposed to Sediment Erosion
Mette Eltvik, Ole Gunnar Dahlhaug and Torbjørn Nielsen
The author is responsible for the entire work in the paper, under the guidance of the co-authors.
Submitted.

In Part III three papers are enclosed, written by Biraj Singh Thapa. The candidate has had a close collaboration with this work as a supervisor, and has contributed to all three papers. The results from these papers are not discussed in this thesis.

The documentation of the Francis turbine design software that was developed during this project is found in Part IV.

1.4 Earlier work

Damage to the material surface due to the impact of a fluid laden with solid particles, is defined as solid particle erosion. This is a complex wear mechanism, and the phenomena is found in many different engineering disciplines. For decades there have been experiments investigating the problems due to the erosion in pipelines transporting oil, gas or coal, as well as pumps and turbines operating with steam, gas or water, propellers for airplanes, gas turbines, and jet engines etc.

Since Reynolds [32] published his work on sandblasting in 1873, numerous articles on erosion wear can be found in the literature [15]. Wellinger et.al [40] were the first to get proper results from the test data with experiments about the erosion effects of a stream of particles hitting various types of steel plates with varying angles of impingement. They found that the ductile materials wore more than the brittle materials at small angles, while the inverse was true for large angles. Other researchers also to similar conclusions from their experiments, but none explained the basic principles of erosion before Finnie [14]. His paper from 1960 is seen as a pioneering work within the understanding of the erosion process on surfaces and its complexities. To reduce the sediment erosion problem, it is essential to understand the physics of the sediment transport and erosion phenomena; thus, knowledge about the influence of fluid flow conditions, material and particle properties is important. Bitter's papers from 1962 [4, 5] give a thorough study on the fundamentals of deformation wear and cutting wear on brittle and ductile surfaces. Bitter also takes into account the particle size, shape and hardness to find a correlation with the erosion phenomena.

There were also other researchers who worked on the erosion phenomena seen from other perspectives. Smith [34] wrote a report on erosion in the gas turbines in 1952, where he discussed the correlation of particle size and blade erosion. In 1969, Goodwin et.al [16] published their work on the erosion on gas turbines operating

in dusty environments. Truscott [37] presented his work in 1972 regarding wear theory and the hydraulic performance of pumps exposed to erosion. Brekke [6] discussed the choice of hydraulic turbines operating in sand laden rivers in 1978, and continued working on the design of both the Francis and Pelton turbines exposed to erosion. Since then, he has contributed with a significant number of papers on the sediment erosion problem and solutions regarding turbine design, turbine performance and material properties [7, 9]. One of the pioneering works in the field of erosion in hydraulic turbines, is the paper by Duan [12] from 1981. The extensive report involves a theory on erosion mechanisms, erosion trends on turbine parts, design criteria and material resistance. Together with Karelin, he presented additional research work on the erosion in hydraulic machinery in 2002 [23]. The doctoral thesis of Thapa [36] gives an in-depth study of the erosion mechanism in hydraulic turbines, comparing theory with observation at turbines in Nepal. Thapa also presented his experimental work with a high velocity jet on different materials and coating types, and a study of particle separation in swirl flow. Neopane [29] continued the work of Thapa and compared the theoretical and experimental data of the effect of particle size, shape and concentration with numerical simulations.

To reduce the erosion process, the choice of material and type of coating for hydraulic turbines is important. Tungsten Carbide is found to be the most resistant coating to apply on turbine components in order to extend the lifetime. Research proves that erosion damage is drastically reduced on turbines with a coating layer [11]. Often these turbines are based on traditional design concepts, with the aim of high efficiency, without take into consideration the erosion phenomena. Hence a more thorough research on optimized design solutions, combining a numerical evaluation of erosion prediction and structural behavior, is needed.

The erosion theories of Bitter and Finnie were not only used as a foundation for the theoretical estimation of erosion wear on hydraulic turbine components [41], but also in the numerical prediction of erosion. There exist several research papers on the numerical analysis of erosion on pipelines [13], elbows [10, 17] and gas turbines [2, 18] which show that the numerical prediction is in a good agreement with the measured data from the experiments. Publications regarding the numerical prediction of erosion in hydraulic turbine components [25, 26] are scarce and few examples are verified experimentally, thus more research to verify the numerical models is required.

CHAPTER II

Theoretical background

► This chapter gives a concise definition of the erosion theory, which is needed to better understand the erosion pattern observed at the Francis turbine components, and to be able to investigate new design concepts in order to diminish the erosion problem.

2.1 Wear theory

The general definition of wear is the loss of material due to the mechanical impact on the surface. There are many forms of the wear mechanism, but regarding hydraulic turbines the principal mechanism is the mechanical wear which involves abrasive and erosive wear. The removal of material due to damage on the surface by hard particles carried in the water is defined as *abrasive wear*. A bed of particles slides over the surface with a velocity vector parallel with the surface, and the material is removed by cutting. *Erosion wear* is the effect of particles colliding with the surface. Particles hit the material with a velocity and angle. The continuous impact of hard particles sliding along or colliding with the material surface, results in material deformation, cutting, fatigue cracking or a combination of them. The surfaces damage first appears as small pitting, and gradually takes shape as fish-scale or wave-shaped grooves, and with time, small amounts of material tear away. The extent of the eroded material is influenced by various circumstances such as flow conditions, and particle and material properties, listed in Tab 2.1 [35].

Flow conditions	Flow velocity, impingement angle, forces acting such as turbulence, centrifugal, cavitation, viscosity
Particle properties	Particle size, shape, hardness, concentration
Material properties	Material hardness, strength, ductility, coating

Table 2.1: *Parameters affecting the extent of the erosion on the surface*

These parameters are used in theoretical erosion models in order to give an estimation of the eroded material. The literature agrees that the most influencing factor affecting the erosion is the velocity of the particle at the time of the collision

with the surface, defined in Eq. 2.1 [37]:

$$Erosion \propto Velocity^n \tag{2.1}$$

The value of the exponent *n* depends on the flow conditions and material properties, but is often set to three. Numerous more advanced equations calculating the erosion rate exist, but an accurate mathematical model is difficult to achieve and the results may only be used as a qualitative estimate.

2.2 Erosion phenomena in Francis turbines

As described in the literature [9, 23, 30], the erosion patterns on Francis turbines operating in sand laden rivers all over the world share similarities. The erosion patterns found can be caused by the different flow phenomena which occur in the turbine, described in Tab. 2.2. An evaluation of these flow phenomena gives a better understanding of the erosion problems in the turbine; thus, flow conditions and the erosion trends in the turbine are briefly described.

Erosion phenomena	**Definition**
Turbulence erosion	Due to turbulence: - In the boundary layer, the particles get high rotational velocities - Smaller particles less than $60\ \mu\mathrm{m}$ cause harsh abrasive erosion
Acceleration erosion	Due to acceleration/deceleration: - Forces particles to diverge from the main flow, normal to the streamline, and collide with the wall. - Larger particles above $500\ \mu\mathrm{m}$ cause severe wear damage.
Secondary flow vortex erosion	Due to secondary flow: - Combination of turbulence and acceleration erosion, can induce horse shoe vortex near blade root - Both small and large particles induce deep grooves

Table 2.2: *Definition of flow phenomena [9]*

The purpose of the spiral casing is to have an even distribution of the flow towards the center of the turbine, hence the design of the spiral casing is cochlear. Due to the friction forces along the wall, there is an energy loss, and a secondary flow occurs. In old designs, the secondary flow in the spiral casing gave incorrect flow angles at the stay vane inlet, thus the blade roots of the stay vanes were prone to erosion. To improve the flow pattern, modern spiral casing has a stay ring between the stay vane cover and the spiral casing, as illustrated in Fig. 2.1. The results were a more uniform flow and less erosion on the stay vane inlet. Only minor erosion tends to be

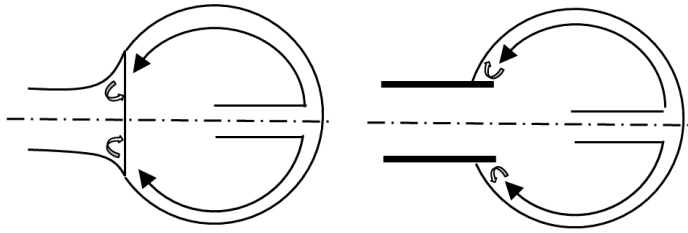

Figure 2.1: *Old and modern stay vane design*

found at the welding joints in the spiral casing. The purpose of the stay vanes is to direct the water flow towards the guide vane without disturbing the flow; hence, a smooth blade design is desirable. To tolerate the maximal axial forces which occur in the spiral casing under full load operation, a certain cross section area is required. Due to the secondary flow in the spiral casing, typically fine scale surface erosion is found, located in the inlet areas and at the blade roots of the stay vanes where paint flakes are torn away. The erosion trend in the spiral casing and stay vanes is fairly low compared to those of other turbine components.

Figure 2.2: *Guide vanes at Cahua Power Plant*

The load variation of the turbine output is governed by the guide vane mechanism. The conversion of pressure energy to kinetic energy in the guide vane channels induces high absolute velocities and acceleration of the water. Thus, the blade surfaces experience heavy erosion, as seen in Fig. 2.2. A typical phenomena in the guide vanes is the secondary flow vortex, which occurs at the stagnation point of the guide vane's inlet. This flow phenomena creates a so-called horse shoe vortex

erosion which make grooves on the covers along the blade root, associated with the shape of a horse shoe. Through the clearance between guide vanes and covers, leakage flow occurs due to the pressure difference over the blade. The leakage flow induces turbulence and a separation flow which will intensify the horse shoe vortex effect at the suction side, thus the grooves on the covers increase. As the clearance increases due to heavy erosion, the hydraulic efficiency decreases drastically. Even when the guide vanes are closed, the leakage flow through the gap increases and accelerates the erosion damage. Heavy erosion is also observed at the guide vane shaft due to the above mentioned flow phenomena, thus the bearings are vulnerable to erosion damage.

Erosion trends at the runner are seen in Fig. 2.3. In the gap between the stationary and rotating parts, erosion will occur at the runner ring due to turbulent flow, and thus the labyrinth seals are also worn out. As hydraulic losses increase and the runner seals erode, the hydraulic efficiency decreases. The particles are accelerated through the guide vanes and collide with the runner inlet region, where they cause a high rate of erosion. Due to the pressure difference between the suction and pressure side of the blade, a stagnation point at the inlet edge occurs, and induces a separation flow with particles that wear out the blade roots. Velocities in relative directions, accelerate through the runner vane and turbulence erosion arises at the outlet. When the particles reach the vane outlet, the centrifugal forces will force them to the outer diameter and severe erosion occurs. An incorrect blade leaning angle creates a cross flow from the hub to the shroud, and the horse-shoe vortex will intensify the erosion grooves at the blade roots.

Figure 2.3: *Eroded runner from Cahua Power Plant*

2.3 Design methods to diminish erosion

The International Electrotechnical Commission (IEC) has come up with a guide for dealing with erosion in hydraulic machines [20]. The guide presents erosion theory and theoretical models, recommendations on the operation mode of turbines, design suggestions in order to diminish wear, choice of material and coating, and inspection and maintenance routines. Other researchers [7, 8, 28] also give recommendations on the design of such runners by modifying a runner designed for operation in clean water. Many of the suggestions will increase the overall cost of the power

plant. However, the cost of overhauling eroded turbine parts will become even more expensive, both in the cost of the repair and the loss of power production.

According to the erosion theory, the relative velocity is the main parameter affecting the erosion wear in the runner. Hence designing a runner with the aim of the reduction of this parameter should give better results regarding the erosion wear. Table 2.3 and Tab. 2.4 list suggested design modification found in the literature.

Hydraulic design parameter	**Design proposal**
Velocity	Reducing peripheral speed
Acceleration	Lower the rate of change of velocity
Inlet condition	Minimizing the angle of incidence
Blade shape	Reducing blade curvature at outlet
Blade length	Longer blade decreases the peak velocity
Blade number	Reducing number of blades
Blade thickness	Thicker blades at trailing edge

Table 2.3: *Hydraulic design recommendations from literature [7, 8, 20, 28, 31]*

Mechanical design parameter	**Design proposal**
Specific speed	Low specific speed reduces flow velocity
Submergence	Increase submergence level
Coating	Protect the material surface
Easy to dissemble	Optimize the down time
Offering plate	Renew during maintenance
Splitter blades	Improves the pressure distribution
Production method	Easier to apply coating on a bolted runner

Table 2.4: *Mechanical design recommendations from literature [20, 28, 31]*

Mode of turbine operation

The given design recommendations are most relevant for the new hydro power projects, which are open to innovative solutions to withstand sand erosion on turbine components. On existing power plants there are limited design modifications to be implemented. However, it is possible to affect the extent of erosion damage by adjusting the turbine operation.

Operation outside the design point is connected with reduced efficiency, high velocities and increased accelerations. At part load and over load, the water velocity is high and turbulence level increase, thus the particle flow will be more chaotic and induces erosion damage. The inlet flow angle from the guide vanes is not favorable, and separation at the leading edge is likely to occur. Under part load conditions, the pressure difference on the guide vanes is large, thus the leakage flow between the guide vane and the facing plates increases and creates an undesirable inlet flow on the runner.

Few starts and stops of power plants are recommended because waterway oscillations in the system will unsettle particles resting in the tunnel system and channels. However, during monsoon periods, it is recommended to shut down units in order to avoid too much damage on turbine components.

CHAPTER III

Design method

► This chapter briefly presents the numerical methods utilized to investigate the hydraulic and mechanical performance of the Francis runner designs. Jhimruk Power Plant, which was chosen as a reference case, is presented.

3.1 Numerical methods

The aim of the thesis is to investigate the design parameters in order to design a Francis runner which will tolerate erosion better than the traditional designs do. The work flow of the design process is illustrated in Fig. 3.1. Three programs are used to accomplish the process to an approved runner design. The Francis turbine design software, *Khoj*, is developed special for this project. The fluid and strucutral simulations are analyzed with *Ansys 14.0*. The geometry needed for structural analysis is modeled with the commercial CAD program *Pro/Engineer Wildfire 5.0* (Creo Parametric).

Turbine design software

A parameter study on selected design variables were necessary in order to achieve an optimal design of a Francis runner with an extended life time. Thus, the Francis turbine design software *Khoj* was created to be able to accomplish a thorough study of Francis runner design. The software is programmed in Matlab and has a graphical user interface to make it more convenient for the designer to develop the designs. For a given net head and flow rate, the main dimensions and velocity triangles are calculated. Additional design modifications involving blade shape, load distribution and blade leaning, can be varied. Several graphs and 2D- and 3D plots of the design make the adjustment and comparisons more efficient. When a satisfied design is achieved, *Khoj* generates files which can be exported to *Ansys* and *ProEngineer* for further hydraulic and mechanical analysis. A more thorough documentation of the program is found in Part IV.

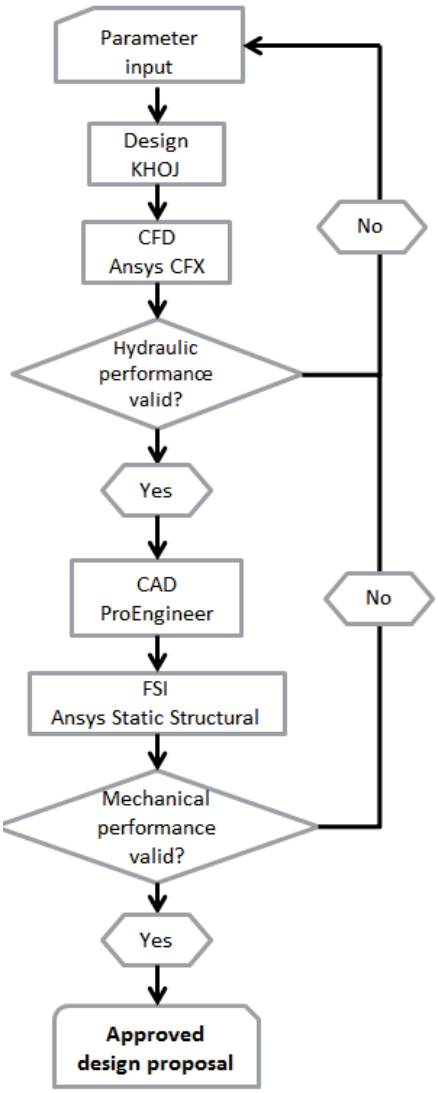

Figure 3.1: *Flowchart of the design process*

Mesh generation

Initially, a mesh is generated with *Ansys Turbogrid*, which is an automated hexahedral mesh generator, specially made for turbo machinery blades [1]. Curve files defines the blade shape and are imported from *Khoj*. The automatic topology and meshing feature(*ATM Optimized*) were utilized to generate the mesh. Compared to traditional methods, were different topology grid types must be chosen and adjusted manually, the *ATM Optimized* method is a fast and simple process, which automatically generates high quality mesh with minimal effort. The traditional methods also

have trouble generating mesh of the runner blade designs with too large curvatures.

The mesh quality depends on the flow conditions and the physical phenomena emerging, therefore the selection of element size and turbulence models must be done with care. In the prediction of sediment erosion, the near-wall modeling has a great influence on the results. Since the erosion models use the particle velocity and impact angle at the time of collision, the results depend on how this is numerically solved. It is a complex phenomena to describe numerically when the flow changes from turbulent to laminar. The numerical near-wall equations solve this problem by dividing the areas into layers where the velocities are derived differently [39]. Close to the wall, the flow is almost laminar since the viscosity forces have the greatest influence, thus, a linear approximation describes the particle velocity. In the mixing layer between the laminar and turbulent flow, a logarithmic relation of the velocities gives the best prediction of the chaotic flow. As in all numerical models, there exist cases where the model fails. In the near-wall prediction, this is found where the viscosity and turbulent forces are equal, and the model fails in the intersection of the two equations. A grid independence test must be carried out to prove the quality of the simulation. The choice of turbulence models and an illustration of the near wall phenomena is found in Paper 2.

Flow analysis

To verify the hydraulic performance of the turbine, CFD simulations were executed with the commercial program *Ansys CFX*. The mesh was imported from *Ansys Turbogrid*, and the boundary conditions are defined in *Turbomode*. As recommended for simulations of hydraulic machines [1], a mass flow rate is defined at the blade inlet, and a static pressure is set at the blade outlet. The turbine operation is determined by the flow direction at the blade inlet, specified by cylindrical coordinates. Therefore, an iteration process must be carried out for each simulation case to find the right values of the velocity components. By using the goal driven optimization method available in *Ansys Workbench*, the desired operation condition is found by an iteration process.

To simplify the computational model, a periodic boundary condition couples two adjacent blades and only one set of blades is analyzed. The hub, shroud and vanes are defined as smooth walls with no-slip condition. The fluid velocities near the wall will then be affected by the wall friction. To predict the erosion on the blades, an erosion model has to be selected. Two erosion models are available in Ansys CFX, *Finnie's erosion model* and *Tabakoff and Grant erosion model*. The choice of erosion models are discussed in Paper 1.

Lagrangian particle tracking is a multiphase model that calculates the particles trajectories through the turbine. Quartz particles are uniformly injected at the inlet with the same conditions as the fluid. The particles will follow through the turbine and exit at the outlet. The particles are defined as solid particles and the size distribution is uniform in diameter. The turbulence dissipation force is activated, and the *Schiller Naumann model* calculates the drag force acting on the particle. The method is most suitable for steady state analysis since each particles are tracked from an injection point to a final destination.

After defining the boundary conditions and the simulations has achieved the given convergence criteria, the results can be evaluated and approved for further analysis.

Structural analysis

If the runner design has a satisfactory hydraulic performance, a Computer Aided Design(CAD) model of the runner blade must be sketched in *ProEngineer*, and then exported to *Ansys Static Structural* for FSI analysis. A mechanical mesh is first generated and verified according to the recommended values found in the Ansys meshing guide [1]. The hydraulic pressure is included by importing the results from the CFD analysis, ensuring that the mechanical performance at different turbine operation modes are considered. The mechanical performance is controlled by the FSI simulation, which is a structural analysis estimating the stress, strain, displacement and forces acting on the runner blade. An approved design proposal is accomplished if the mechanical performance is valid.

3.2 Jhimruk Power Plant

Jhimruk Power Plant is situated in the Pyuthan district in Nepal, owned by Butwal Power Company (BPC). The construction of the run-of-river power plant started in 1989 and was put into operation in 1994. Three horizontal Francis units, each of $4\ \mathrm{MW}$ were designed for a net head of $201.5\ \mathrm{m}$ and a discharge of $2.35\ \mathrm{m^3/s}$. The annual energy production is $87\ \mathrm{GWh}$.

Figure 3.2: *Dam site, Jhimruk Power Plant*

The dam site is located in the Jhimruk river, as seen in Fig. 3.2. To obtain optimal flow conditions, a $1\ \mathrm{km}$ long channel was built upstream from the sediment chamber. The flow velocities decrease such that the sediment particles have time to settle before entering the head race tunnel. Jhimruk Power Plant was the first to install a settling chamber with the S4-model, designed by Håkon Støle [33]. A flush system

drains the chambers for sediment when needed. Often the sediment transport is much higher than expected and the chambers fill up quickly, so flushing is frequently necessary.

During the monsoon period, which lasts from April to September, 83 % of the annual precipitation occurs. Hence, the sediment content in the river drastically increases, and erosion damages are observed on the turbine components, as can be seen in Fig. 3.3. The sediment concentration is measured by a hydro meter at the inlet gate, and the annual sediment load is $35\ \mathrm{kg/m^3}$. Sixty percent of the sediment minerals that pass through the turbines are quartz, and 90% of the sediments are smaller than $0.1\ \mathrm{mm}$ [24, 33]. If the sediment content exceeds 3000 ppm, the turbines are shut down to save them from severe erosion damage.

All three units are under operation in the wet season, but in the dry season only two turbines operate due to less discharge. Once a year the turbine runners and guide vanes are changed out. The time for overhauling is dependent on the pressure in the spiral casing. A value of $100\ \mathrm{MPa}$ is normal, and below $70\ \mathrm{MPa}$ indicates large leakage. The plant owner states that it is preferable to have a high efficiency in the period with the highest production, therefore, the exchange often takes place during March or April, and 5-7 days are needed to change each turbine [24]. There are 3 turbines from China and 4 turbines from Norway. While one set of turbines is operating, the others are sent for repair to the Nepal Hydro Electric (NHE) workshop in Butwal.

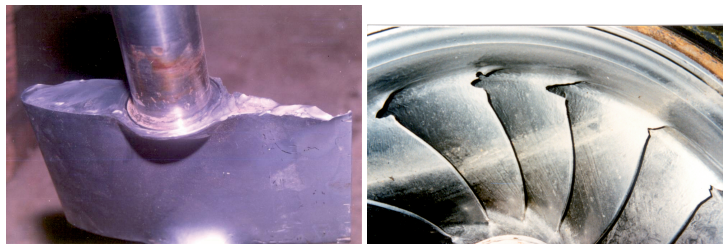

(a) Guide vane (b) Runner

Figure 3.3: *Erosion damage on turbine components at Jhimruk Power Plant*

CHAPTER IV

Summary of papers

► This chapter gives a summary of the content in the four submitted papers. The papers are found in Part II in this thesis.

4.1 Summary of paper 1

Prediction of sediment erosion in Francis turbines
Mette Eltvik, Ole Gunnar Dahlhaug and Hari Prasad Neopane
4^{th} International Meeting on Cavitation and Dynamic Problems in Hydraulic Machinery and Systems, October 26-28th, 2011, Belgrade, Serbia

The paper presents the numerical prediction of erosion wear in a Francis turbine. The numerical methods and boundary conditions are described, and different turbulence models and erosion models are discussed.

Numerical prediction of erosion

The numerical prediction of erosion gives an overview of where on the turbine blade the erosion occurs. Comparisons between the numerical model and the turbine at Cahua Power Plant show a similar erosion pattern. Thus, numerical models can be utilized to predict which areas on the turbine blade are most vulnerable for sediment erosion.

Two different erosion models were compared and gave unequal results. Even though a relative comparison gives applicable values, Finnie's erosion model overestimates the absolute erosion rate. Tabakoff and Grant erosion model is a more complex equation which takes into account for the reference values and material properties; hence, the model gives more realistic absolute values on the amount of eroded material. In general, the erosion models only give a qualitative rate of eroded material, but are useful as a tool in the design process to predict areas that are more exposed to erosion.

Over a period of nine years, sediment samplings have been gathered daily from the river near Cahua Power Plant. With this data available it was possible to get a more accurate analysis of the erosion wear in the turbine. By knowing the amount of sediments passing through the turbine during a given period, a similar prediction can

be achieved by simulating the same sediment concentration. The paper compares turbine operation between the design point and the full load, and the results show that the turbine surface is more eroded at full load operation than at best efficiency point where the flow conditions are more optimal. The whole turbine operation scheme can be simulated to find out which operation conditions are best and to get an indication of when the next overhaul is needed.

4.2 Summary of paper 2

Numerical analysis of effect of design parameters and sediment erosion on a Francis runner

Mette Eltvik, Biraj Singh Thapa, Ole Gunnar Dahlhaug and Kristine Gjøsæter
Fourth International Conference on Water Resources and Renewable Energy Development in Asia, Thailand, March 25-26, 2012

The paper evaluates the numerical methods in the CFD analysis of erosion prediction in a Francis runner. Five different hydraulic designs of runner blades are evaluated by changing the blade loading, and observing how it effects the erosion rate. Two turbulence models were tested, and results from the grid independence analysis show the limitations of these numerical models.

Mesh control

A grid independence test of the numerical mesh is important to assure the quality of the numerical results. This is accomplished by analyzing several mesh with different qualities and comparing vital parameters such as head, hydraulic efficiency and erosion prediction. In this paper, ten different mesh were tested with the number of nodes between 90 thousand up to 10 million. The two turbulence models compared in this research, were the k-ϵ model and the Shear Stress Transport (SST) model.

The results show that a too fine mesh with a low y+ value fails to predict erosion on the surface. If the first node is too close to the wall, the particle velocity is almost zero, thus the kinetic energy in the particle is small and there is no indication of erosion on the surface. A mesh with a y+ value outside the numerical deviation area optimized for the SST-model will give the best results for predicting erosion on the turbine surface.

Design parameters

The five runner blade designs presented in the paper are based on traditional design concepts with the aim to reduce the relative velocity and erosion wear. As presented in Paper 1, the Tabakoff and Grant erosion model gives reliable results of erosion prediction, thus creating the possibility for a design optimization by comparing designs and erosion prediction. Compared to the reference design, two blade designs have 20-30% less erosion, and the hydraulic efficiency deviation is within 0.8%. These results emphasize that it is possible to design a Francis runner which tolerates erosion better, without changing the main dimensions.

4.3 Summary of paper 3

Hydraulic design of a Francis runner exposed to sediment erosion
Mette Eltvik, Torbjørn Nielsen and Ole Gunnar Dahlhaug
Submitted

The paper gives an analytic evaluation and numerical analysis on how the hydraulic performance will be affected by choosing design parameters outside the traditional ranges.

Hydraulic turbine design concepts and empirical values

In the design process of a Francis runner, it is usual to begin with the Euler's turbine equation and continuity equation, which determine the main dimensions. The blade geometry is shaped after the designer's knowledge and use of empirical values evolve from manufactures' experiences during decades of turbine production. By looking at the effect of changing the reaction ratio and peripheral velocity at the outlet of the runner, a better overview of the velocity distribution through the runner is achieved. According to the empirical values, the optimal inlet angle should be between 50 and 70 degrees. If the blade angle inlet is too large or too small in proportion to the guide vane angle, separation and cavitation at the inlet can occur. Traditionally, a wide operation range with high efficiency is a requirement, but for a runner exposed to sediment flow, it is desirable to operate the turbine at the design point to avoid too much erosion wear on the turbine components. Thus nontraditional angles can be chosen, giving a design which can tolerate wear better than an optimal design can.

To determine which design parameters are best, an evaluation of the hydraulic performance is necessary. Hence a CFD-analysis of the selected designs were examined. The three runner shapes presented in the paper have quite different design values outside the recommended ranges, because it is desirable to evaluate how this affects the hydraulic and mechanic performance of the turbine. The short blade with a large blade inlet angle turned out to be the best design regarding hydraulic efficiency and erosion prediction. Although the acceleration is higher in the blade cascade, less erosion occurs due to a lower velocity, hence the particles have less kinetic energy. Since the blades are shorter, the particles strikes less surface area than on the other designs.

4.4 Summary of paper 4

Numerical analysis of Francis runners exposed to sediment erosion
Mette Eltvik, Ole Gunnar Dahlhaug and Torbjørn Nielsen
Submitted

This paper presents a structural analysis of three Francis runner designs to verify the structural behavior. The same geometries presented in Paper 3 have been evaluated and discussed concerning of hydraulic performance and principal stress and strain.

Static structural analysis

Designing a Francis runner adapted to operation in a river containing heavy loads of sediment, is a challenging task. There are large expectations of the hydraulic performance, fatigue life and reliable energy production. The hydraulic evaluation of the designs gives an overview of the flow distribution and particle path through the runner, thus the designer is given the opportunity to discover the influence of the parameter variation. The next step is to verify the mechanical strength by accomplishing a FSI simulation involving the effects from the hydraulic forces.

Three designs which have design parameters exceeding the recommended limitations are presented in Paper 3. Results from the structural analysis state that the designs are within the required limits. The stress and strain distribution corresponds to the known energy distribution on the blades, and bad trends can be traced. The results show that a shorter blade is preferable to a long blade, both regarding the erosion and blade strength. Although this design has a large curvature at the inlet and higher acceleration through the runner, which differs from the design suggestions, this is the preferred design proposal. Further research must be carried out involving model testing to confirm the numerical conclusions.

CHAPTER V

General discussions

► This chapter discusses Francis runner design concepts based on the results of the papers and recommended design methods. A proposal on the operation and maintenance routine for Jhimruk Power Plant is given.

5.1 Design concept

The aim of the research was to look at the design of a Francis runner which is exposed to sediment erosion in order to minimize the damage due to wear. Traditional design concepts and empirical values have been considered, and form the basis for examining the design parameters. Recommended design criteria from other researchers are evaluated along with the chosen design parameters, with the intention of getting a better comprehension of the erosion phenomena in Francis runners.

As stated in the literature, reducing the relative velocity will reduce the erosion rate in turbines. Therefore, a parameter study was accomplished with the purpose of reducing this velocity and observing the extent of the erosion damage in the runner. The conversion of hydraulic energy to mechanical energy in the runner can be adjusted by changing the blade loading and reaction ratio. Varying these parameters demonstrates that it is possible to design a runner which is more durable against sediment erosion without affecting the turbine dimensions.

Blade angle distribution

Adjusting the blade angle distribution has large influence on the blade loading; hence, the blade shape is affected as well. As presented in Paper 2, five different blade shapes and their erosion tendency is analyzed and compared to the reference design. Two of the shapes evinced signs of withstanding the erosion better with 20-30% less wear than the reference design, and without a too large deviation of hydraulic efficiency. The shape with the least erosion even had a relatively high acceleration of velocity at the outlet, where most of the conversion of hydraulic forces were localized at the first blade half. The second best design had an opposite energy conversion, where the forces were balanced out at the blade outlet region.

A structural analysis of the selected designs was conducted examining nontraditional blade loading [3]. A blade which converts most of the energy at the outlet

region of the blade, may exceed the mechanical strength, and cracks may occur; thus, the blade may be thicker towards the outlet. The drawbacks are a reduced efficiency, and the probability that the von Karman vortexes increase. An analysis of blades with a thickness at the leading edge of 15 mm decreasing to 8 mm towards the trailing edge were compared with those having only $10\ \mathrm{mm}$ and $6\ \mathrm{mm}$, repectively. The simulations of the blades were performed at the design point, and at a full load condition, to assure that the structural behavior was below the maximal yield strength for different flow conditions. The yield strength at both blades was lower than $120\ \mathrm{MPa}$, which was set as a safety value. The hydraulic efficiency was not influenced by the increased thickness. Hence, a blade designed with an unconventional energy conversion could be considered, since the structural integrity and hydraulic efficiency is ensured.

Reaction ratio

The reaction ratio also has an effect on the conversion of the hydraulic energy in the turbine. This will modify the blade shape, but in a different way than does the blade angle distribution. As the results from the research presented in Paper 3 show, a reaction ratio of 0.5 or below comes out as a better design regarding the erosion prediction. A low reaction ratio increases the blade angle at the inlet, which is off the empirical limits and creates a large curvature at the first part of the blade. However, this design has a high hydraulic efficiency and less erosion than the other designs. Consequently, a low reaction ratio may affect the erosion tendency in the guide vanes, which for the high head Francis is already a risk zone for sediment erosion.

Along with the reaction ratio, the blade length increases, which according to the literature is favorable for a runner operating in these conditions. The highest velocities are observed in the long blades, resulting in a high erosion tendency. Higher acceleration acts in the runner with short blades, but less erosion occurs. This shows that the erosion is more influenced by the flow velocity than the acceleration effect. Therefore, a short blade is preferable to a long blade with high velocities, even though the curvature at the inlet is larger, and the acceleration higher.

General design improvements

One way to decrease the flow velocities in the turbine is to reduce the *specific speed*, which will increase the turbine dimensions. Larger turbine runners are less exposed to sand erosion than smaller turbines with the same specific speed, since relatively less particles are in contact with the blade surface, and the acceleration is lower due to a larger radius and curvature. However, there will be no changes of the velocity in the guide vanes and inlet of the runner, hence for a high head Francis runner, changing the specific speed is not vital. For a low head Francis turbine, the erosive wear commonly takes place in the runner, and thus the choice of specific speed is more important. The disadvantage of increasing the turbine dimensions is cost escalation, since it involves the enlargement of other turbine components.

Turbines operating in water with a high mineral content are more prone to cavitation damage than those operating in clean water, due to the synergy between

erosion and cavitation. Water with sand particles forms cavitation bubbles at an earlier stage than clean water. Hence, increasing the *submergence* of the turbine is recommended to avoid cavitation erosion. For existing power plants, this is not a solution, but for new projects it should be considered even though the expenses increase.

Coating of wet surfaces is a good, but expensive solution. In the beginning of the operating period, the hydraulic efficiency will be less due to higher surface roughness, but after some time, when the particles have polished the surface, the efficiency will increase. Curved parts such as runner blades are difficult to coat, thus a runner with bolted blades is a good solution, since it gives better access to spraying on a proper coating layer.

A runner with *fewer runner blades* is suggested to simplify the coating process, but this may induce an unfavorable pressure distribution in the blade channel. Thus, *splitter blades* are more favorable, since they will level out the pressure, which gives improved flow conditions and reduces the erosion effect.

To optimize the process of maintenance and repair of the turbine parts, it is essential to design vertically shafted turbines to be disassembled from underneath at the draft tube. Therefore, the *replacements of worn out parts* such as the runner, guide vanes, upper and lower cover, and offering plates are less time consuming. Spare parts must be available to make the replacement as quick as possible, and worn out parts have to be repaired and re-coated till the next overhaul period.

5.2 Numerical methods

Mesh generation and turbulence models

The numerical prediction of flow near surfaces is complex, and thus there exist several turbulence models adapted to various flow conditions. Some models require a very fine mesh near the wall, hence a low y+ value most be chosen. For other models, which are less accurate on near wall prediction, it is sufficient with a larger y+ value, outside the numerical deviation area. There is a correlation between the chosen turbulence model and the mesh quality, which has a large influence on the outcome of the simulation.

Results from Paper 2 conclude that the SST turbulence models give a more reliable evaluation of erosion prediction than the k-ϵ model. Owing to the fact that turbulence models have numerical limitations, there is no need to obtain the finest grid with the lowest y+ values. However, it is necessary to accomplish a grid analysis in order to optimize the numerical mesh by fine tuning the mesh according to vital parameters.

Erosion models

Two erosion models were compared in Paper 1, and the analysis of erosion prediction in Francis turbines is presented. The erosion trends look similar, but the predicted amount of eroded material is unequal. Finnie's erosion models overestimate the quantity of material eroded, and estimate a value far above what is physically

possible. The model allows the user to set the value of the velocity influence, but even recommended values give inadequate results. Tabakoff and Grant erosion model is more receptive to adjustments, and even has reference values for some common minerals and steel types, which give a better and more realistic evaluation of the erosion quantity.

5.3 Proposal to Jhimruk Power Plant

New custom made runners with a compromise of the old and new design suggestions just discussed, along with a Tungsten Carbide coating, could be a good solution for the sediment problem that exists at Jhimruk Power Plant today. Before new runners can be installed, model testing of the recommended design modification is necessary. Meanwhile, an optimization of the operation conditions and overhaul routines can be implemented in order to reduce the wear.

In the dry periods of the year, the energy demand is higher due to the cold winter temperatures. The energy production is lower since the rivers are dry, and the rationing of electricity is necessary, also known as load shedding. To limit the period of load shedding, which lasts up to 17 hours a day, the energy production could be improved. In hydro power turbines, it is desirable to have a high hydraulic efficiency as long as possible through-out the year. Instead of changing the turbine components right before the monsoon period, it is more appropriate to replace the turbine when the peak concentration of sediments in the river has decreased. Thus the hydraulic efficiency will be high in a longer period of the year, and not be worn out during the first months of the wet season.

Running the turbine close to the design point gives better flow conditions and will spare the turbine components for severe damage. As seen in Paper 1, when the best efficiency operation and full load operation were compared, there were large differences in the amount of eroded material. The effect of sediment concentration was also evaluated, and illustrates the process of erosion damage during the whole year of operation. These findings can be used in order to determine the next time for overhaul, and to be aware of which areas are most exposed to erosion and need inspection.

Installing a sediment control system will simplify the sediment sampling process and give sediment concentration values rapidly. During periods of floods when sediment concentration increases, the system alerts when the concentration is too high, and the turbines can be shot down more quickly in order to spare turbine components.

The desilter system at the intake reduces the particle concentration and filters out the largest minerals; however, the size of the basins are often under-dimensioned. Enlarging these basins will reduce the concentration of particles even more, and extend the lifespan of the turbine parts.

CHAPTER VI

Conclusions

The aim of the parameter study was to investigate the influence of hydraulic design in order to obtain a Francis runner which is more resistant to sediment erosion compared to the reference design. According to what the literature states, the fluid velocity which has the most influence on the phenomena, was decreased with the intent to diminish the sand erosion intensity. To understand the erosion phenomena, and how to decrease the intensity, numerous design parameters were altered and compared with regard to hydraulic and mechanical performance.

Based on traditional turbine design equations, several designs were generated without considering the empirical values and limitations to find out which parameter has the most influence on the sand erosion phenomena. The designs were evaluated by comparing the hydraulic performances simulated with a CFD software. Selected designs were further analyzed with regard to their strength properties.

The results from the parameter study indicate that small changes in the hydraulic design are enough for the runner to endure longer than traditional runner designs operating in sand laden rivers. The effect of varying the blade loading and reaction ratio seems to be a convincing method to postpone the sediment erosion damages, without expanding the turbine size and exceeding the structural integrity.

A combination of optimized runner design modification, coating of surfaces and restriction on the operation point, would reduce the sediment erosion wear, and extend the lifetime of the turbine components, which makes the power production more reliable and economical. Model testing of suggested runner modifications must be completed before producing a prototype.

CHAPTER VII

Future work

The consequence of changing the reaction ratio relocates the erosion problem. Due to a higher potential flow conversion in the guide vane, erosion wear may increase. A more thorough study on the guide vane design with respect to the sediment erosion problem and the change of runner design is needed.

Numerical analysis on a wider turbine load variation will give a more proper understanding of the erosion effect at different operation points. Transient simulations are also of interest, but such an analysis involving particles is not available in the versions of Ansys that were used in this project.

To keep the degree of difficulty to a moderate level, not all of the available functions in the design software *Khoj* were utilized in this project. For example, the individual change of streamlines in the axial view of the runner blade will complicate the design comparison, thus this is excluded. Observing how the erosion trends in the runner are affected by varying the stay vane and guide vane design would be of interest. Further development of Khoj is necessary in order to improve and validate existing functions.

The next stage of the project is to approve the new design concepts by running model tests. At Katmandu University, a testing lab has been built and is currently being instrumented and prepared for model testing. A Francis runner model, designed by the Francis team in Trondheim 2011, was manufactured by Nepal Hydro and Electric Limited (NHE). The model test will verify the numerical computation of the hydraulic design and efficiency. It may not be possible to demonstrate the reduction of erosion wear before a full scale turbine is installed at Jhimruk Power Plant.

Bibliography

[1] ANSYS . *Ansys Meshing User's Guide*, 2011. Release 14.0.

[2] ANSYS . Predicting turbimachinery erosion rate. *Ansys Advantage*, 5(2):pp. 31–33, 2011.

[3] BERGMAN-PAULSEN J. Mechanical design of a Franics turbine exposed to sediment erosion. Master's thesis, Norwegian University of Science and Technology(NTNU), Trondheim, 2012.

[4] BITTER J. A study of erosion phenomena Part I . *Wear*, 6(1):pp. 5 – 21, 1963.

[5] BITTER J. A study of erosion phenomena Part II. *Wear*, 6(3):pp. 169–190, 1963.

[6] BREKKE H. Discussion of pelton turbine versus francis turbines for high head turbines. In *IAHR ASME*, 1978. Colorado Stat Univ.

[7] BREKKE H. Hydraulic design strategy for francis turbines. *Hydropower and Dams*, pages pp. 38–42, 1996.

[8] BREKKE H. *Hydraulic turbines - Design, Erection and Operation*. Hydropower laboratory, NTNU, 2012.

[9] BREKKE H., CAI B. Y., AND WU Y. L. *Design of hydraulic machinery working in sand laden water*, chapter 4, pages pp. 155–233. Imperial College Press, London, 2002.

[10] CHEN X., MCLAURY B. S., AND SHIRAZI S. A. Application and experimental validation of a computational fluid dynamics CFD-based erosion prediction model in elbows and plugged tees. *Computers & Fluids*, 33(10):pp. 1251 – 1272, 2004. ISSN 0045-7930.

[11] DAHLHAUG O., SKÅRE P., MOSSING V., AND GUTIERREZ A. Sediment resistive francis runner at cahua power plant. *Int. J. Hydropower and Dams*, Issue 2:pp. 109–112, 2010.

[12] DUAN C. Sand particle erosion of water turbines. Technical report, Press of Tsinghua University, Beijing, 1988.

[13] EDWARDS J., MCLAURY B., AND SHIRAZI S. Modeling solid particle erosion in elbows and plugged tees. *J Energ Resour*, 123:pp. 277–284, December 2001.

[14] FINNIE I. Erosion of surfaces by solid particles. *Wear*, 3(2):pp. 87 – 103, 1960.

[15] FINNIE I. Some reflections on the past and future of erosion. *Wear*, 186–187, Part 1:pp. 1 – 10, 1995.

[16] GOODWIN J. E., SAGE W., AND TILLY G. P. Study of erosion by solid particles. *Proceedings of the Institution of Mechanical Engineers*, 184(1):pp. 279–292, 1969.

[17] GRAHAM L., LESTER D., AND WU J. Quantification of erosion distributions in complex geometries. *Wear*, 268(9-10):pp. 1066 – 1071, 2010. ISSN 0043-1648.

[18] HAMED A. A., TABAKOFF W., RIVIR R. B., DAS K., AND ARORA P. Turbine blade surface deterioration by erosion. *ASME Conference Proceedings*, 2004 (41677):pp. 329–337, 2004.

[19] HSU P.-C., LI T., AND WANG B. Trends in global monsoon area and precipitation over the past 30 years. *Geophysical Research Letters*, 38(8), 2011. ISSN 1944-8007.

[20] *IEC 62364: Hydraulic Machines - Guide for dealing with hydro-abrasive erosion in Kaplan, Francis and Pelton turbines*. International Electrotechnical Commission(IEC), 2012.

[21] *Technology roadmap - Hydropower*. International Energy Agency(IEA), 2012.

[22] *Hydropower*. International Renewable Energy Agency (IRENA), June 2012.

[23] KARELIN V. Y., WU Y. L., AND DENISOV A. I. *Fundamentals of hydroabrasive erosion theory*, chapter 1, pages pp. 1–52. Imperial College Press, London, 2002.

[24] KARICI S. B. Senior Operator. Personal communication during inspection at Jhimruk Power Plant, 2012.

[25] KUROSAWA S., NAKAMURA K., AND WEI P. Sand erosion prediction for hydraulic Turbine runner. *The 11thAsian International Conference on Fluid Machinery and The 3rd Fluid Power Technology Exhibition*, 2011. Chennai, India.

[26] MACK R., DRTINA P., AND LANG E. Numerical prediction of erosion on guide vanes and in labyrinth seals in hydraulic turbines. *Wear*, 233-235:pp. 685 – 691, 1999. ISSN 0043-1648.

[27] MIN S.-K., ZHANG X., ZWIERS F. W., AND HEGERL G. C. Human contribution to more-intense precipitation extremes. *Nature*, 470:pp. 378–381, 2011.

[28] NAIDU B. *Silt erosion problems in hydro power stations and their possible solutions*, chapter 1, pages pp. 3–17. Central Board of Irrigation and Power, 1996. New Delhi, India.

[29] NEOPANE H. P. *Sediment Erosion in Hydro turbines*. PhD thesis, 2010.

[30] PADHY M. K. AND SAINI R. A review on silt erosion in hydro turbines. *Renewable and Sustainable Energy Reviews*, 12(7):pp. 1974 – 1987, 2008. ISSN 1364-0321.

[31] PANDE V. AND RAMANATHAN S. Prediction of erosion severity for hydro turbine components operating in silty conditions. *Int. seminar on sediment handling technique*, 1999. NHA, Kathmandu.

[32] REYNOLDS O. On the action of a blast of sand in cutting hard materials. *Philos.Mag*, 46:pp 337–343, 1873.

[33] RUUD J. Sediment handling problems jhimruk hydroelectric center. Master's thesis, Norwegian University of Science and Technology, Norway, 2004.

[34] SMITH M. A theoretical note upon the mechanism of deposition in turbine blade fouling. *Nat. Gas Turbine Estab.*, M-145, 1952. Report.

[35] STACHOWIAK G. AND BATCHELOR A. W. *Engineering tribology*. Butterworth-Heinemann, 2011.

[36] THAPA B. *Sand Erosion in Hydraulic Machinery*. PhD thesis, Norwegian University of Science and Technology, Faculty of Engineering Science and Technology, 2004.

[37] TRUSCOTT G. A literature survey on abrasive wear in hydraulic machinery. *Wear*, 1:pp 29–50, 1972.

[38] *World Population Prospects: The 2012 Revision*. United Nations, 2013.

[39] VERSTEEG H. K. AND MALALASEKERA W. *An introduction to computational fluid dynamics: the finite volume method*. Harlow: Prentice Hall, 2007.

[40] WELLINGER K. AND BROCKSTEDT H. C. Versuche zur ermittlung des verschleisswiderstandes von wekestoffen für blasversatzsohr sowie des einflusses der rohrverlegung bei blasversatzanlangen. *Glückauf*, 78, 1942.

[41] WU Y. L., DENISOV A. I., AND KARELIN V. Y. *Calculation of Hydraulic Abrasion*, chapter 2, pages pp. 53–94. Imperial College Press, London, 2002.

PART II

Papers

CHAPTER VIII

Paper 1

Prediction of sediment erosion in Francis turbines
Eltvik, M., Dahlhaug, O.G., Neopane H.P.
4^{th} International Meeting on Cavitation and Dynamic Problems in Hydraulic Machinery and Systems, Belgrade, Serbia, October 26-28th, 2011

4-th International Meeting on
Cavitation and Dynamic Problems in Hydraulic Machinery and Systems,
October, 26-28, 2011, Belgrade, Serbia

Prediction of Sediment Erosion in Francis Turbines

Mette Eltvik[1], Ole Gunnar Dahlhaug[1] and Hari Prasad Neopane[2]

[1]Department of Energy and Process Engineering, Norwegian University of Science and Technology
Alfred Getz Vei 4, Trondheim, 7491, Norway, mette.eltvik@ntnu.no, ole.g.dahlhaug@ntnu.no
[2]Department of Mechanical Engineering, Kathmandu University, Dhulikhel, Nepal, hari@ku.edu.np

Abstract

Sediment erosion is a complicated problem and depends upon several factors. To reduce the sediment erosion problem it is important to understand the physics of sediment transport and erosion phenomena. Computational Fluid Dynamic (CFD) is a numerical simulation tool that can predict which areas on the turbine that is most vulnerable to sediment erosion. This is investigated by implementing particles in ANSYS CFX and by utilizing Lagrangian particle tracking one can follow the particles path through the turbine. Erosion models shows the erosion areas and degree of intensity of erosion. The paper will explain how the numerical simulations can give reasonably prediction of erosion trends in a Francis runner. The relationships between the sediment erosion and operating conditions of the turbine are investigated. It has been found that the erosion process is strongly dependent on the operating conditions of the turbines.

Keywords: Francis turbines, CFD, Erosion

1. Introduction

Sediment erosion in hydraulic turbines is a large problem for run of river power plants neighboring mountain ranges such as the Himalaya and the Andes. During the monsoon period the concentration of sediments in the river increases radically. A large amount of the minerals consists of hard and sharp minerals such as quartz and feldspar which are vulnerable for the turbine material. The result is worn out blades, vibration problems and reduced performance which can lead to often shut downs and costly repairs.

SN Power has invested in power plants in Peru and rehabilitates turbines which are exposed to erosion. An example is the Cahua Power Plant in Peru, were tons of sediments passes through each of the two Francis units every day. In March 2009 a coated turbine delivered by Dynavec, were installed. After 131 000 tons of sediments has passed through the turbine, less erosion were observed compared to the uncoated turbine. [1]

To reduce the sediment problem in turbines it is important to start at the design stage. A numerical simulations tool is used to get an optimum fluid flow through the turbine and can also give a prediction of abrasive erosion in the turbine. This paper presents the results of CFD simulations of the Francis turbine situated at Cahua Power Plant, and will be compared with the turbine at the power plant.

2. Numerical method

All simulations are accomplished with three-dimensional Navier Stokes solver Ansys CFX 13.0. To achieve a second order accuracy of the grid and sufficient numerical stability, the High Resolution scheme is applied for discretization of the grid. The algebraic equations are solved iteratively with the approach called Monotone Upstream centered Scheme for Conservative Laws (MUSCL), which is second order accurate. All simulations are at steady state with viscous and incompressible flow.

Particles are inserted in the fluid flow and the Lagrangian particle tracking function is a multiphase model used to calculate the particles trajectories through the turbine. An erosion model calculates the kinetic energy of the particles when they collide with the vanes and gives a prediction of the erosion areas.

2.1 Numerical mesh and boundary conditions

Ansys Turbogrid is utilized to make the mesh of each vane. The turbine consists of 20 stay vanes and guide vanes, and 17 runner vanes. Only one channel of blades, including stay vane, guide vane and runner vane, is modeled to simplify the simulations, see Figure 1.

DOI: *to be inserted by the publisher*

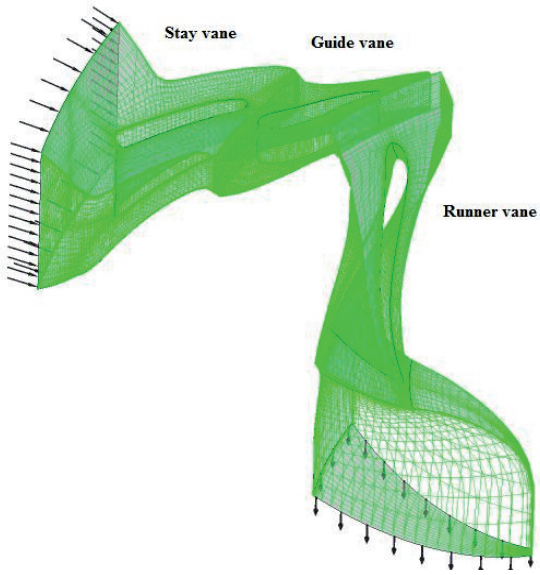

Figure 1: Mesh of the simulation domains

The inlet conditions are set as mass flow rate per passage with velocity components and a constant total pressure at the outlet of the runner. Quarts particles are uniformly injected at the stay vane inlet with the same conditions as the fluid. The particles will follow through the domains and exit at the outlet. The quarts particles are defined as solid particles and the size distribution is uniform in diameter. The turbulence dissipation force is activated, and the Schiller Naumann model calculates the drag force acting on the particle. The coupling between the water and particles is divided into two sets, one-way coupled and fully coupled.

The covers, hub, shroud and vanes are defined as smooth walls with no-slip condition. Fluid velocities near the wall will then be decreased by the wall friction. The runner has an angular velocity of 600 rad/s, while the stay vane and guide vane are stationary domains. Two operation points are compared, design load with guide vane opening at 16° and full load at 22° opening. A periodic boundary condition is set to couple two adjacent blades. This simplifies the computational model and only one set of blades needs to be analyzed. To predict the erosion on the blades, an erosion model has to be selected. Two erosion models are tested in these simulations; the Finnie's and Tabakoff's erosion models. In Table 1 the boundary conditions are listed [2].

Variable	Value
Fluid density	997 kg/m^3
Particle density	2.65 g/cm^3
Particle dimension	0.1-0.2 mm
Mass flow of fluid through turbine	540 kg/s
Mass flow of particles	0.5, 3, 20. 50 kg/s
Flow direction at stay vane inlet (a, r, θ)	0, 0.4, 0.9165 m/s

Table 1: Boundary conditions

Every day over a period of nine years sediment samples have been taken from the river Rio Pativilca, where Cahua Power Plant is located. Analysis of the samples gives the percentage of the different mineral types and distribution of particle size. Quartz, feldspar, hornblende are the dominating minerals in the river which have a hardness of 5-7 at the Mohs scale [3]. The result is high abrasive wear on the turbines which are stopped when the concentration exceeds 3000 ppm [4] of sediments to prevent damage on the turbines.

Since the particle size and density are known, the total number of particles in the simulation can be calculated. The concentration of particles is varied from 0.5 kg/s to 50 kg/s and gives different amount of particle concentration. Comparing the simulated concentration with the sediment data from Cahua Power Plant [4], the different simulated concentration rates can be linked to amounts of sediments passing the turbines at Cahua Power Plant during different periods of a year, see Table 2. Thus it is possible to predict when the turbine needs maintenance.

DOI: *to be inserted by the publisher*

Concentration rate in the simulations	Tons of sediments	Equivalent to concentration of particles passing the turbines at Cahua power plant
0.5kg/s	700	An average day during the monsoon period
3kg/s	4300	One month during dry season
20kg/s	28 800	One month in the monsoon period
50kg/s	72 000	Three intense months during the monsoon period

Table 2: Concentration rate

2.2 Turbulence models

Numerical simulations of turbulence are complicated and many models adjusted for different problems are available. The models have weaknesses and strengths, but it all comes down to a compromise between accuracy and computational cost. The Reynolds averaged Navier-Stokes equations (RANS) models are computational cheap but unfortunately the accuracy is low compared to Direct Numerical Simulations (DNS) and Large-Eddy Simulations (LES). As the name denote, the RANS models uses an average of the Navier-Stokes equations which gives a reasonable accuracy and are at the same time robust. The k- ε model is a two-equation model within the RANS models and is considered as industry standard due to its stable and numerical robust calculations.

In the near wall regions, a scalable wall-function is provided. Limitations for the model are boundary layer separation, flows over curved surface and rotating fluids. A model which takes care of these phenomena is the Shear-Stress-Transport model (SST). In the near wall region, the model uses an automatic near-wall function which switches between k- ε and k-ω depending on the distance to the wall. The model is more computational expensive than k- ε, but gives a better accuracy and is more robust [5]. When introducing particles in the domain, the treatment near the wall is important and no loss of data is desirable. Therefore a SST model is preferable since it gives a more accurate prediction of the flow in these areas. For turbomachinery simulations, literature recommends a y+ value between 20 and 200 to avoid numerical errors [6]

2.3 Particle Transport Model

Lagrangian particle tracking is a multiphase model used to calculate the particles trajectories through the turbine. The overall mass flow rate of the particles is shared amongst the representative particles being tracked. By dividing by the (initial) mass of the particle, this means that each representative particle has a Particle Number Rate, $\dot{N}$. This quantity is used internally in the code for calculating overall sources to the continuous phase, and is also used in post-processing for calculating mass flows of particles through boundaries, forces on walls, etc. The fluid contains high concentration of sediment, but only representative number of particles is calculated in the simulation to save computer performance.

Each particle follows an individual path through the domains, representing a sample of particles. As the particles collide with the wall, the impingement information (velocity and location) is treated by a set of empirical erosion equations. These equations determines the material mass losses caused by the particle impact, and take into account the particle velocity, shape, impact angle, density and mechanical properties of the wall material. The method is most suitable for steady state analysis since each particle is tracked from an injection point to a final destination.

All simulations have been accomplished under these assumptions:

- No particle-particle interaction or particle breakup.
- Only spherical particles are considered.
- The sliding effect of particles along the wall is not possible to simulate.
- No geometry modification due to removed material.

2.5 Erosion models

Prediction of erosion wear on material is a complex function of properties of the wall and particle. The most crucial factor is the particle impact angle and particle velocity at impact point. Two different models are available in Ansys CFX [5]; Model of Finnie and Model of Tabakoff and Grant.

Finnie's erosion model calculates the erosion rate according to the relation:

$$E = k \cdot V_p^n \cdot f(\gamma) \qquad [-] \qquad (1)$$

E is dimensionless mass as a function of eroded wall material and particle mass. V_p is the particle impact velocity. For metals, the exponents value, *n*, can be between 2.3 to 2.5, but for Francis turbines the exponential value is recommended to be 3[7]. This factor defines in what extent the particle velocity impacts the erosion factor. $f(\gamma)$ is a dimensionless function of the impact angle which is defined as the angle between the particle and the wall, described as:

DOI: *to be inserted by the publisher*

$$f(\gamma) = \frac{1}{3} \cdot \cos^2 \gamma \qquad if\ \tan\gamma > \frac{1}{3} \qquad [-]$$
$$f(\gamma) = \sin(2 \cdot \gamma) - 3 \cdot \sin^2 \gamma \qquad if\ \tan\gamma \leq \frac{1}{3} \qquad [-] \qquad (2)$$

Tabakoff and Grant erosion model has another more complex and adapted erosion prediction. Tabakoff were able to find reference constants depending on combination of colliding particles and wall material properties. Tabakoff and Grant state that the erosion rate is given by [8]:

$$E = f(\gamma) \cdot \left(\frac{V_p}{V_1}\right)^2 \cos^2\gamma (1 - R_T^2) + f(V_{pn}) \qquad [-] \qquad (3)$$

Where

$$f(\gamma) = [1 + k_2 \cdot k_{12} \cdot \sin\left(\gamma \cdot \frac{\pi/2}{\gamma_0}\right)]^2 \qquad [-] \qquad (4)$$

$$R_T = 1 - k_4 \cdot \left(\frac{V_p}{V_3}\right) \cdot \sin\gamma \qquad [-] \qquad (5)$$

$$f(V_{pn}) = \left(\frac{V_p}{V_2} \cdot \sin\gamma\right)^4 \qquad [-] \qquad (6)$$

$$k_2 = \begin{cases} 1 & if\ \gamma \leq 2 \cdot \gamma_0 \\ 0 & if\ \gamma > 2 \cdot \gamma_0 \end{cases} \qquad [-] \qquad (7)$$

Table 3 shows the reference values for k and γ_0 that take into account the erosion effect of quartz particles on stainless steel, ST 304[8].

Variable	Value
Constant k_{12}	0.293328 [-]
Ref velocity V_1	123.72 [m/s]
Ref velocity V_2	352.99 [m/s]
Ref velocity V_3	179.29 [m/s]
Angle of maximum erosion γ_0	30 [°]

Table 3: Reference values for Tabakoff erosion model for quartz particles and stainless steel

The general erosion calculation in Ansys CFX is a relation between the particle mass m_p and the number rate $\dot{N}$, described as:

$$ErosionRate = E \cdot \dot{N} \cdot m_p \qquad [\text{kg/s/m}^2] \qquad (8)$$

The erosion rate is given as kilograms of eroded material per seconds, kg/s. In the post-processor, CFX- Post, contour plots on the vane of the erosion rate density is possible. The erosion rate density is given as kg/s/m^2 and is a qualitative guide to erosion rate [5]. A streamline tracks the particles paths through the domain and is useful to trace the mean flow and detect turbulent behavior or other phenomena.

3. Results

The erosion models calculates the forces that acts when the particles collides with the wall. The erosion rate signifies loss of material per square meter per second, and is seen as colored spots on the vane. This indicates the erosion intensity, were blue denote zero erosion and red is high erosion intensity. Figure 2 shows the result from simulation at design load calculated with the Tabakoff's erosion model. The prediction of erosion rate for concentration equivalent to an average day during dry season is seen in Figure 2a), and the erosion rate for one month during monsoon period in Figure 2b). At the surface of the blade, abrasive erosion is most present at the pressure side. Due to increasing velocities in the runner channel, the erosion intensity will increase from the middle of the blade towards the trailing edge. At the outlet region the relative velocities are the highest, thus the erosion rate increases, seen in Figure 2a) as growth of red spots near the trailing edge.

DOI: *to be inserted by the publisher*

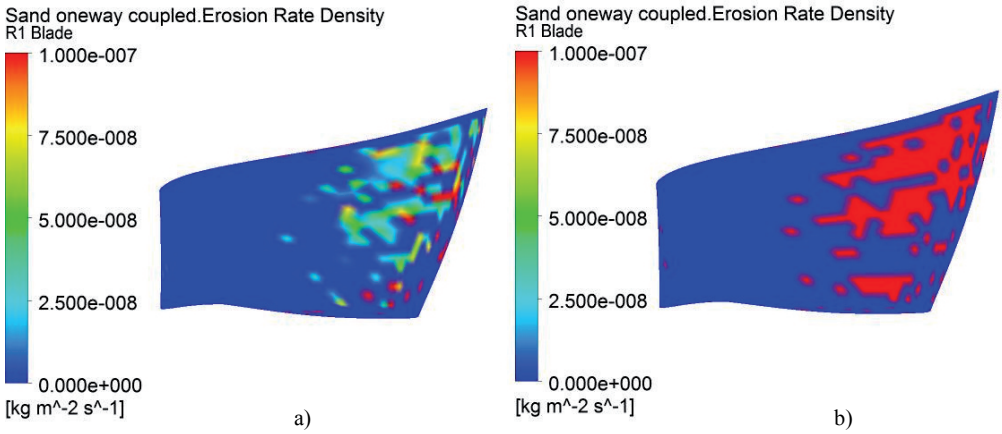

Figure 2: Erosion on pressure side of runner vane at design load for a) 0.5 kg/s and b) 20kg/s.

Similar erosion trends were observed during the inspection at Cahua Power Plant in 2009, see Figure 3. Especially the outlet region is exposed to erosion wear due to high relative velocities and material is worn out. Cracks occurs and parts of the vane brakes off. Operation at off design causes a higher erosion rate due to the increased turbulence, and secondary flows and vortices are likely to occur.

Figure 3: Erosion on outlet region on the runner vane, Cahua Power Plant [4]

Table 4 shows the relative erosion rates for different turbine operations and erosion models. Both the concentration of particles and turbine operation has large influence on the erosion intensity. Minor erosion is detected for best efficiency point, but at full load the erosion rate grows and more spots is found. At full load the flow condition is not optimal and likely the erosion rate increases.

	Design Load		**Full Load**	
Mass flow of particles	*0.5 kg/s*	*20 kg/s*	*0.5 kg/s*	*20 kg/s*
Finnie's erosion model	1,20E+08	5,62E+09	2,88E+08	1,18E+10
Tabakoff's erosion model	1,00E+00	1,24E+01	1,13E+00	4,76E+01

Table 4: Relative erosion rates for different turbine operations and erosion models

Both Finnie's and Tabakoff's erosion models are tested in the simulations, but indicate disparate values for erosion rate. Finnie's erosion model overestimates the erosion prediction where over 1E+08 kg of the material is eroded per square meter every second more than Tabakoff's model. These unrealistic values can be explained by the mathematics behind the models. The most influencing factors in the models are the velocity and material constants. In Finnie's erosion model, the erosion rate is highly dependent on the velocity component exponent, *n,* see Eq. 1. The exponent relies on individual experiments and material properties. The IEC guide [9], the exponential value is recommended to be 3 for Francis turbines, but in Ansys Solver Guide [5], a value between 2.3 and 2.5 for steel material is suggested. The simulations implementing Finnie's erosion model are tested for all these values, but the erosion prediction is improbable. With the Tabakoff's erosion model the simulation takes into account the influence of quartz particles colliding with stainless steel 304. This prediction is closest to the uncoated turbine at Cahua Power Plant because of the properties of the material.

Conclusion

The numerical analysis of sediment erosion in Francis turbines gives an indication of relative erosion intensity and zones on the runner vane. As expected, the erosion rate magnifies with increasing sediment concentration and is greatest for full load operation. The results coincide with observation at the turbines at Cahua Power Plant.

Comparing the two available erosion models it turns out that the Tabakoff's erosion model gives the most reliable results. The only mineral implemented in the simulations is quartz. For the real case in Cahua, the river contains about 30% of quartz. To get a better erosion rate prediction of an existing turbine, the exact amount of the different minerals should be included.

Further work

When designing a Francis turbine for sediment laden rivers, a numerical erosion prediction gives a good indication of the possible amount of erosion damage of the turbine. By including CFD and FEM analysis in the design process, an optimized turbine design which is more resistant to erosion wear can be achieved. The work with making a design program and couple the analysis results in the process is commenced.

Nomenclature

a	Axial velocity component [-]	r	Radial velocity [-]
E	Dimensionless mass of eroded material [-]	V_p	Particle velocity [m/s]
k_i	Erosion constant (i=1, 2, 3) [-]	V_i	Velocity components (i=1, 2, 3) [m/s]
m_p	Particle mass [kg/m]	γ	Particle impact angle [°]
$\dot{N}$	Particle number rate [-]	γ_0	Maximum angle of impact angle [°]
n	Erosion exponent [-]	θ	Theta velocity component [-]

References

[1] Dahlhaug O.G., Skåre P.E., Development of a sediment-resistant Francis runner, Hydro 2009, Lyon
[2] Eltvik, M., Sediment Erosion in Francis Turbines, Master Thesis, NTNU, Trondheim, Norway, 2009.
[3] Mindat, Mineral and locality database, 2011 (http://www.mindat.org)
[4] Cáceres H. P., Personal conversations, Plant Manager, Cahua power plant, SN Power, Peru, 2009.
[5] Ansys CFX Release 13.0, Ansys CFX-Solver Modeling Guide, 2010
[6] CFD-Online, Best practice guidelines for turbomachinery CFD, 2011 (http://www.cfd-online.com/Wiki/Best_practice_guidelines_for_turbomachinery_CFD
[7] Bajracharya T.R., Efficiency Deterioration in Small Pelton Turbines due to Sand Particles Led Bucket Erosion, PhD Thesis, Tribhuvan University, Nepal, 2007
[8] Tabakoff W., Wenglarz R., Hamed A., Erosion and deposition in turbomachinery, Journal of propulsion and power, 2006.
[9] IEC62364 rev.7. Hydraulic Machines - Guide for dealing with abrasive erosion in water, 2008.

CHAPTER IX

Paper 2

Numerical analysis of effect of design parameters and sediment erosion on a Francis runner

Eltvik, M., Thapa, B.S., Dahlhaug, O.G., Gjøsæter, K.

Fourth International Conference on Water Resources and Renewable Energy Development in Asia, Chiang Mai, Thailand, March 25-26th, 2012

Numerical analysis of effect of design parameters and sediment erosion on a Francis runner

Mette Eltvik
Waterpower Laboratory
Norwegian University of Science and Technology
Trondheim, Norway

Biraj Singh Thapa
Turbine Testing Lab
Kathmandu University
P.O. Box 6250
Dhulikhel, Nepal

Ole Gunnar Dahlhaug
Waterpower Laboratory
Norwegian University of Science and Technology
Trondheim, Norway

Kristine Gjøsæter
Waterpower Laboratory
Norwegian University of Science and Technology
Trondheim, Norway

Abstract
In mountain regions in Asia and South America the sediment contents in the rivers increase drastically during monsoon periods. This causes a large problem for the hydropower operation and especially the run-of-river power plants suffer. Due to the amount of hard minerals such as quarts and feltspar, substantial damage is observed on the turbine components. The consequences are reduced turbine performance, standstill due to replacement of equipment and costly repairs. If these effects where diminished, the lifespan of the turbine could be extended and the power production increase. Hence the power company can make a profit and the consumer's access to energy be improved.

To reduce the erosion problem it is important to understand the particle flow conditions in the turbine and the erosion phenomena. Studies show a cubic relation between the erosion wear and velocity [1]. The aim is to reduce the relative velocities in the runner without affecting the efficiency. Computational Fluid Dynamic (CFD) is a numerical simulation tool which analyses the fluid flow and predicts which areas on the turbine that are most vulnerable to sediment erosion. This is investigated in Ansys CFX by implementing particles in the fluid domain.

Numerical evaluation of blade loading has been investigated and a grid independency study with regard to the erosion prediction effect has been utilized. This paper presents a relation between design parameters and its effect on erosion wear on the runner blade. The aim is an optimum runner design which is more resistant to abrasive wear than original turbines.

Key Words: Francis runner, design optimization, erosion, CFD, RenewableNepal

1. Introduction
Due to the global changes in temperature, melting of glaciers has become a larger problem for hydro power plants as the mineral contents in the river increases. Especially the rivers in alpine areas like the Alps, the Andes and the Himalaya, gives problems for run-of-river power plants. These mountain ranges have a large amount of hard minerals such as quartz and feldspar which harms the turbine material. The concentration of minerals increases during monsoon season due to higher sedimentation transports in the rivers. The result is worn out components, vibration problems and reduced performance which can lead to often shut downs and costly repairs.

Computational Fluid Dynamic (CFD) is a numerical simulation tool which analyses the fluid flow and predicts which areas on the turbine that are most vulnerable to sediment erosion. This is investigated in Ansys CFX by implementing particles in the fluid domain. By utilizing the Langrangian particle tracking method, the path of particles through the turbine can be predicted. The Tabakoff's erosion model shows the erosion areas and degree of erosion intensity on the runner blade surface.

The work is a part of the RenewableNepal project, which is a cooperation between Norwegian University of Science and Technology(NTNU) and Kathmandu University funded by Norad and Sintef. The aim of the project is to come up with an improved design of a Francis turbine runner that will have less erosion worn than traditional turbine design. As a reference case, Jhimruk Power Plant in Nepal is chosen since this is a representative power plant which suffers from erosion problems in the Himalaya.

1.1. Referanse design
Jhimruk Power Plant is a 12MW run-of- river power plant located in the Pyuthan district of Mid-Western region of Nepal. Three Francis runners with splitter blades are installed, each on 4.2 MW. The turbine data is listed in table 1. Due to the high sediment content in the Jhimruk River, the turbines need maintenance yearly. 83% of the annual rainfall occurs during the monsoon period and the sediment content in the Jhimruk River increases

drastically. The dominating minerals in the area are quarts (70%) and feldspar (7%) which is hard minerals with Mohs scale value 6-7. The sediment concentration in the monsoon period exceeds 4000PPM [2].

Head	201.5 m
Flow rate	2.35 m^3/s
Rotational speed	1000 rpm
Number of blades	17
Speed number	0.3220
Diameter inlet / outlet	0.890 m / 0.540 m
Thickness at leading edge / trailing edge	15 mm / 8 mm

Table 1: Turbine data, Jhimruk Power Plant

It is of interest to design a new erosion resistant Francis turbine for Jhimruk Power Plant. A reference design is created according to the turbine data given in table buy using the open source program Khoj [3]. Due to limitations in the design software, the splitter blades are excluded and 17 ordinary blades is considered.

2. Numerical method

2.1. Near wall modelling

Definition of boundary conditions is necessary to solve the governing model equations. Near the wall this poses a problem due to variation of dependent variables, such as velocity and wall shear stress. The boundary layer close to the wall consists of two layers, see figure 1. Closest to the wall is the viscous sub-layer where viscosity has greatest influence since the flow is practically laminar. In this region a linear approximation is used to define the dimensionless velocity close to the wall, the log law:

$$u^+ = y^+ \qquad [-] \tag{1}$$

In the logarithmic layer the mixing turbulence is the dominating variable. The logarithmic relation for the near wall velocity is given by [4, 5]:

$$u^+ = \frac{U_t}{u_\tau} = \frac{1}{\kappa}\ln(y^+) + B \quad [-] \tag{2}$$

$$y^+ = \frac{\rho \Delta y u_\tau}{\mu} \quad [-] \tag{3}$$

$$u_\tau = \sqrt{\frac{\tau_\omega}{\rho_{flow}}} \quad [-] \tag{4}$$

u^+ is the near wall velocity, u_τ is the friction velocity, U_t is the tangential velocity, and κ is the von Karman constant. y^+ is a dimensionless factor that defines the distance between the wall and the first node. B is the log-layer constant depending on the wall roughness and τ_ω is the wall shear stress. For smooth wall the von Karman constant κ =0.4 and the constant B=5.5. Figure 2 illustrates the use of the two wall equations.

In between these two layers is a region called the buffer layer, were both viscosity and turbulence has equal influence to the flow. In this layer, where $5< y^+ < 30$, none of the near wall models holds, thus less accurate results are expected. The largest error occur at the intersection of the two equations, at $y^+ = 11.63$ which is where laminar and turbulent flow blends and none of the numerical models yield [4, 5].

For flow with high Reynolds number it can be difficult to resolve the grid close to the wall due the very thin viscous layer. Two approaches are commonly used to model the near wall flow. Wall functions use empirical formulas and are based on the assumption that the first grid point off the wall is located in the logarithmic region. The fluid shear stress

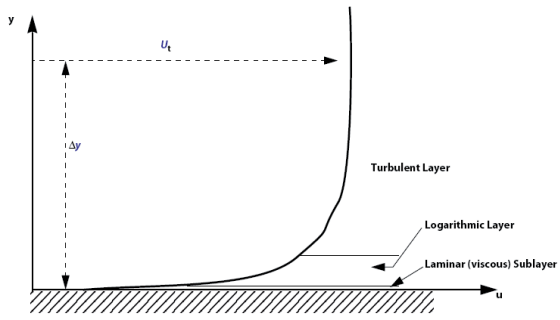

Figure 1: Boundary layers near wall [5]

is numerical computed as a function depending on the velocity at a given distance from the wall. The advantage with this model is the low number of required cells and computer storage and runtime is reduced.

The second approach available is the low Reynolds number model which is based on standard k-ε model with additional viscous damping function to improve the computation in the near wall region. Since the model resolves the grid near the wall by using very thin inflation layers, this requires a very fine mesh and a low y^+ value close to the wall, but need better computational power.

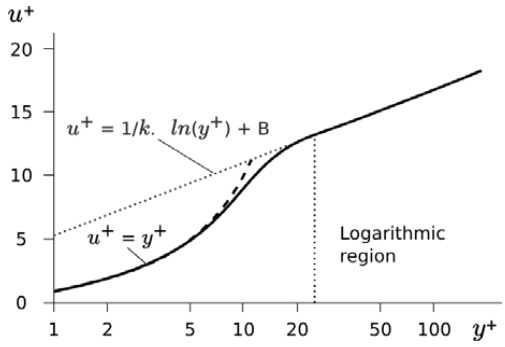

Figure 2: Law of the wall [6]

2.2. Turbulence models

Selecting suitable turbulence models for turbomachinery simulations is challenging since there is no model which is appropriate for all types of flow phenomena. When introducing particles in the domain, the treatment near the wall is important and no loss of data is desirable. Two equitation models is the best choice for accurately prediction of separating flow, secondary flow, rotating flow and similar cases [4]. These equations may have problems with over-prediction of turbulent energy around leading edge and suction side of the blade, where strong acceleration is detected. The two most common turbulence models are the k-ε and Shear Stress Transport (SST).

The k-ε model is often used by the industry because it is numerically robust, while it also is computational accurate. The model does not resolve all the way through to the wall since it uses universal law to solve the wall functions. The drawback is its limitations with rotating domain, curved surfaces and separation prediction. This model is suitable for y^+ values above 30 as the first cell near the wall is intended to be inside the log-layer.

The SST model calculates the conditions near the wall by using an automatic near-wall treatment, which gradually blends between the low Reynolds number model and wall functions. The k-ω model is used at the viscous sub-layer, and the k-ε model in the free stream. The treatment of low Reynolds number is more accurate and robust, and it requires $y^+ \leq 2$ and at least 15 nodes in the boundary layer near the wall to avoid numerical errors.

Different sources recommend various limits for the y^+ values depending on the particular case. Best practice guides for design iteration simulation on a one-singled blade, 100 000 nodes are sufficient with a y^+ between 20 and 200, but also $30< y^+<300$ is approved [6]. For more accuracy analyses with low-Reynolds mesh, one million nodes with a y^+ below 1 is proposed. Accordingly it is impossible to obtain a constant y^+ value on the whole blade surface, but as long as most of the surface are within the recommended limits, the mesh ought to be approved. Anyhow, Eltvik [7] managed to get reliable results for a similar case with only 150 000 nodes and y^+ values outside the recommended range.

2.3. Grid independency test

It is important to assess the grid quality before performing a large and complex CFD analysis. The choice of properties will affect the accuracy and convergence of the solution. A grid independent test will ensure verification of the mesh quality by refining the mesh until some parameters relevant to your problem no longer changes. A turbine design process require numerous of simulations and it is desirable to save computer memory and run time. There is not found any good references which give a best practice of grids generating with the aim on erosion analysis.

The grids are generated in Ansys Turbogrid 13.0 using the ATM optimization mesh method. The turbine at Jhimruk Power Plant is chosen as a reference case and the grid independency test is based on one runner blade. Eleven different grids are made which span from 90 thousand to 10 million nodes. Same mesh method is used for all grids. To specify the near wall element size, the y^+ method are conducted with a Reynolds number of 500 thousand and y^+ value 1. An expansion ratio at 1.25 will ensure a smooth transition between the small and larger nodes. At the trailing edge it was necessary to change the curve type to be piece wise linear instead of b-spline due to dent near the outlet region.

All simulations are accomplished with Ansys CFX 13.0. By using periodic boundary conditions, only one blade channels is taken into account to save computational process. Best practice guide for CFD analysis on Francis

turbines [5, 6] recommend to set a mass flow rate at the inlet and a static pressure at the outlet. The hub, shroud and blade are defined as walls with no-slip conditions. Two turbulence models are tested; k-ε model and SST turbulence model, and parameters are compared for all grids.

To predict the erosion trend in the turbine, solid particles are uniformly injected at the inlet with the same flow conditions as the fluid. Langrangian partical tracking is a multiphase model used to calculate the particles trajectories through the domain. When the particles collide with the blade, the kinetic energy implies erosion damage on the surface. Two different erosion models are available in Ansys CFX [5], Finnies and Tabakoffs erosion model. These models determine the amount of material loss caused by the particle impact based on the particle velocity, impact angle, shape, density and material properties. The latter model gives the best prediction of abrasive erosion on the turbine blade [8] and values for quarts particles colliding with stainless steel are considered. The turbulence dissipation force is activated, and the Schiller Naumann model calculates the drag force acting on the particle. All simulations presented have the same input parameters.

2.4 Design parameters

When designing a high head Francis turbine, it is appropriate to shape the blade in such a way that the hydraulic energy is utilized at the beginning of the blade. In these areas, large pressure differences will occur and the blade has to tolerate high tensions. As the tension decreases towards the trailing edge, the blade gets thinner. For a Francis turbine exposed to erosion, new design trends need to be investigated to reduce the risk of erosion wear. Thus a parameter study which looks at the effect of chosen variables and their effect on erosion extent is necessary.

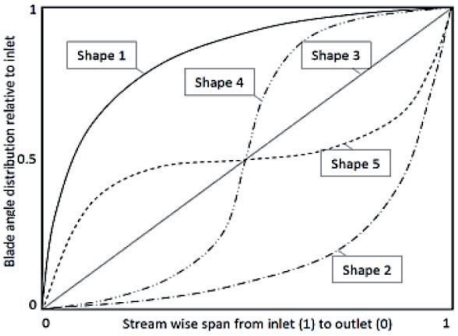

Figure 3: Blade shapes [3]

In Thapa et.al (2011), a parameter study is presented with the aim to optimize a Francis runner which can handle abrasive erosion better than traditional design. This paper will focus on the effect of varying the blade angle distribution which defines the blade shape from inlet to outlet. Figure 3 show five different blade angel shapes that have been investigated. The blade angle affects how the hydraulic energy is converted to mechanical energy along the blade. For example a runner blade design based on shape 1 will convert half of the hydraulic energy from the middle of the blade towards the outlet, while shape 2 will convert the energy at the beginning of the blade to the middle. A linear blade angle distribution, shape 3, is chosen as a reference design.

The design program indicates quantification of *erosion tendency* for a given design by calculating the relative flow velocity W_i for each segment area A_i of the runner blade, equation (5). An *erosion factor* gives the ratio between the erosion tendency on the new design and the reference design, equation (6). With these factors, different design philosophies for an optimized turbine design exposed to erosion can be compared already at the design process. The erosion tendency, E_t, and erosion factor, E_f, is give as [9]:

$$E_t = \frac{\sum_{i=1}^{n} w_i^3 * A_i}{\sum_{i=1}^{n} A_i} \ [\mathrm{m^3/s^3}] \tag{5}$$

$$E_f = \frac{(E_t)\ New\ design}{(E_t)\ Reference\ design} \ [-] \tag{6}$$

3. Results

3.1 Grid independency test

Total eleven grids where tested for both turbulence models. As the grid refines, the y^+ value decreases, shown in graph 1. The average y^+ values for the grids below 600 000 are all out of the recommended range. The 2 million and 5 million grids have y^+ values in the numerical error area. It is unachievable to have the same value all over the blade, and the maximum values can be disregarded since this yields only some spots at the leading edge and trailing edge [3].

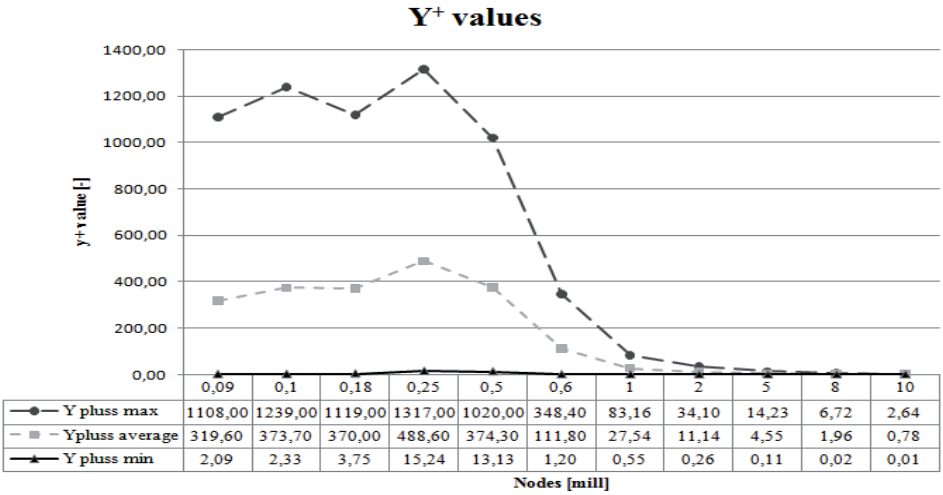

	0,09	0,1	0,18	0,25	0,5	0,6	1	2	5	8	10
Y pluss max	1108,00	1239,00	1119,00	1317,00	1020,00	348,40	83,16	34,10	14,23	6,72	2,64
Ypluss average	319,60	373,70	370,00	488,60	374,30	111,80	27,54	11,14	4,55	1,96	0,78
Y pluss min	2,09	2,33	3,75	15,24	13,13	1,20	0,55	0,26	0,11	0,02	0,01

Graph 1: Grid independency test, y^+ values

Erosion prediction comparison between the k-ε and SST turbulence model is seen in graph 2. The erosion factor is logarithmic, normalized in proportion to the 1 million grid with the SST turbulence model. General it is only minor changes between the two turbulence models for the grids with high y^+ values. As the y^+ values increase, the erosion prediction decreases, and it seems like the changes is larger for high y^+ values. The k-ε model had problem detecting the erosion on the very fine grids, where the y^+ value is lower than recommended, thus no results are given for grids above 5 million nodes. Similar for both turbulence models is the numerical error on the 2 million grid, where the erosion is either over-predicted (SST model) or under predicted (k-ε model). It was also observed that the finer grids showed less or no traces of erosion wear on the runner blade, yielding both turbulence models. In addition to be computational expensive, these grids frequently have more numerical problems and fail to solve relevant parameters.

Other factors like efficiency and head is evaluated and given in graph 3 and graph 4. The variations of head are best predicted with the SST model for grids with 600 000 nodes and below, which is closer to the design head at 201.5m. The efficiency trend is varying up till 250 000 nodes, where it becomes more stable around 96.2%.

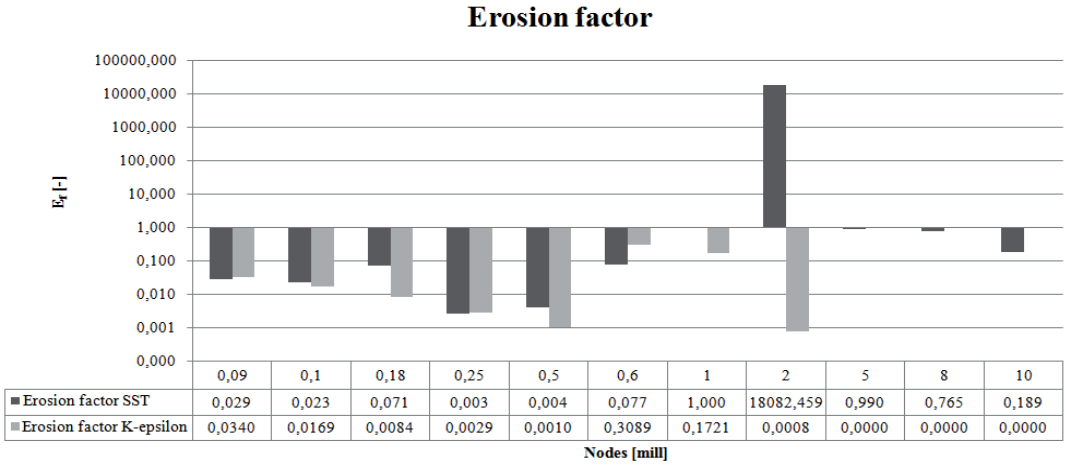

	0,09	0,1	0,18	0,25	0,5	0,6	1	2	5	8	10
Erosion factor SST	0,029	0,023	0,071	0,003	0,004	0,077	1,000	18082,459	0,990	0,765	0,189
Erosion factor K-epsilon	0,0340	0,0169	0,0084	0,0029	0,0010	0,3089	0,1721	0,0008	0,0000	0,0000	0,0000

Graph 2: Erosion prediction with SST and K-epsilon

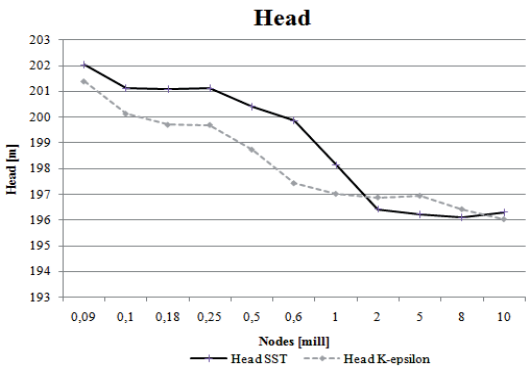

Graph 4: Head estimated with SST and K-epsilon model

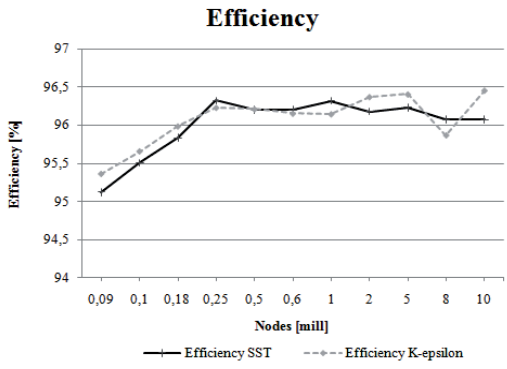

Graph 3: Efficiency estimated with SST and K-epsilon model

3.2 Design parameter

The parameter study of various blade shapes has been conducted. The grids where made on the same bases as the grid independency test. For a design optimalization study, it is appropriate to use as course mesh as possible to reduce the computational time. Approximately 600 000 nodes where chosen for this parameter study as the grid independency test showed that finer grids gave unpredictable results. Only the SST turbulence model has been utilized due to more reliable results than the k-ε model.

In graph 5 the erosion factors for each blade shape from Khoj and CFD analysis is presented with the efficiency, normalized to the reference design. The design program and CFD analysis does not concur on erosion prediction. According to the design program Khoj, the shape 1 and shape 5 where pointed out to be a better resistant for erosion. CFD analyses shows that shape 4 and shape 5 seem to be a better choice. The commercial CFD program has more advanced models than the open source design program, thus these values are more reliable. The erosion factor on Khoj is dependent on the discretization of the control volumes on the blade surface.

On shape 1, the energy is converted at the end of the blade which may require a thicker blade at the outlet area. The relative velocities slightly increase at the beginning of the blade and accelerate near the trailing edge due to the high curvature at the blade outlet. This is the shape which has the highest efficiency.

Shape 5 has almost the same trends as shape 1, but with a more smooth increase of relative velocities on the whole blade, accelerating a bit at the end. The efficiency is the same as the references design and the erosion rate has reduced by 20%.

Compared to the reference design, the erosion rate on shape 4 is 30% less, but consequently the efficiency also decreased. The relative velocities have minor changes at the first half of the blade, thereafter suddenly accelerate towards the outlet.

Traditionally runner design converts most of the hydraulic energy at the beginning half of the blade, similar to shape 2. This design has the highest erosion factor in this comparison.

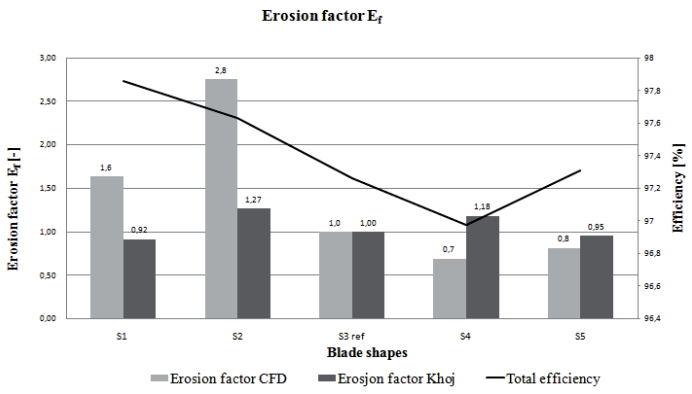

Graph 5: Erosion factor on blade shapes

4. Conclusion

Generally a fine mesh with low y^+ values is recommended in literature. However considering erosion, these values give poor results. The grid independency test shows that a grid with nodes from 600 000 to 1 million are within the recommended y^+ values for simulations on turbomachinery components. Two turbulence models where tested, SST and k-e turbulence model, where the former were found to be general better for these types of simulations.

As regards erosion prediction, finer grids appear to fail and no erosion spots are seen on the runner blade. The grids with high y^+ values emerge to give better and more equal results. The grid with 2 million illustrates the expected numerical error as the erosion estimation is either over or under predicted depending on the turbulence model. In a design optimization process it is essential to observe the variation in erosion trend for each design. Thus it is unsuitable to generate fine grids if the objective is to do a design analyses or erosion prediction.

It is found that a runner with a blade angle distribution equal to shape 4 will have reduced erosion by 60%, but efficiency will be adversely influenced. Shape 5 is the other alternative with 20% reduced erosion and no change in efficiency.

Erosion prediction in turbines is very complicated. Numerical models exist but an exact estimation is unachievable. Due to the diverse outcome of the blade shape analysis from the design program and the CFD analysis, there is no doubt that a discussion on numerical methods is needed.

Further work

Strength analysis (Finite Element Method (FEM) and Fluid Structure Interaction (FSI)) has to be performed to determine if the blade is strong enough to handle the pressure forces. If such analysis show that the blade fails, a more moderate shape of the blade angle distribution or another thickness distribution has to be chosen for the blade.

Nomenclature

A_i	Area [-]	η	Efficiency [%]
B	Log-layer constant [-]	κ	von Karman constant [-]
E_t	Erosion tendency [m^3/s^3]	μ	Dynamic viscosity [kg/ms]
E_f	Erosion factor [-]	ρ	*Density [*kg/m³*]*
U_t	Tangential velocity [m/s]	τ	Wall shear stress [Pa]
u_τ	Friction velocity []		
u^+	Near wall velocity []		
W_i	Relative velocity [-]		

References

1. **IEC standard**,"*Hydraulic machines- guide for dealing with abrasive erosion in water* ", Technical report, International Electrotechnical Commission, 2008.
2. **Neopane, H.P.**, "*Sediment Erosion in Hydro Turbines*", Doctoral thesis, NTNU, Trondheim, 2010.
3. **Gjosater K.**, "*Hydraulic design of Francis Turbine Exposed to Sediment Erosion*", Master's Thesis, NTNU, 2011.
4. **Versteeg, H.K. Malalasekera, W.M.**, "*Computational Fluid Dynamics*", Pearson, second edition, 2007
5. **Ansys** CFX Release 13.0, CFX-"*Solver theory guide*", Technical report, Ansys, November 2010.
6. **CFD**-online, "*Best practice guidelines for turbomachinery*", http://www.cfd-online.com/Wiki/Best_practice_guidelines_for_turbomachinery_CFD, September 2011
7. **Eltvik M.**, "*Sediment Erosion in Francis Turbines"*, Master's thesis, NTNU, 2009
8. **Eltvik M., Thapa B., Dahlhaug O.G.,** "*Prediction of Sediment Erosion in Francis Turbines*", 4th IAHR Cavitation and Dynamic Problems in Hydraulic Machinery and Systems, Belgrade, October 2011
9. **Thapa B., Eltvik M., Gjosater K., Dahlhaug O.G.**, *" Design Optimization of Francis Runners for Sediment Handling "*, Fourth International Conference on Water Resources and Renewable Energy Development in Asia, Thailand, March 2012

CHAPTER X

Paper 3

Hydraulic design of a Francis runner exposed to sediment erosion
Eltvik, M., Nielsen, T., Dahlhaug, O.G.
Submitted

Is not included due to copyright

CHAPTER XI

Paper 4

Numerical analysis of Francis runners exposed to sediment erosion
Eltvik, M., Dahlhaug, O.G., Nielsen, T.
Submitted

Is not included due to copyright

PART III

Co-authored papers

CHAPTER XII

Paper A

Effect of turbine design parameters on sediment erosion of Francis runner
Thapa, B.S., Gjøsæter, K., Eltvik, M., Dahlhaug, O.G.
2nd International Conference on the Developments in Renewable Energy Technology, IEEE, Bangladesh, January 5-7, 2012

EFFECTS OF TURBINE DESIGN PARAMETERS ON SEDIMENT EROSION OF FRANCIS RUNNER

Biraj Singh Thapa[1], Kristine Gjosater[2], Mette Eltvik[2], Ole Gunnar Dahlhaug[2]

[1]Turbine Testing Laboratory, Kathmandu University, Nepal
[2]The Waterpower Laboratory, Norwegian Institute of Science and Technology, Norway
Corresponding author: bst@ku.edu.np

ABSTRACT:

Problems of sediment erosion in the hydropower industry across Asia and South America have become a major technical challenge. One of the emerging solutions to prevent the erosion of hydro turbines is to reduce the relative velocity inside the runner by improving hydraulic design. It is important to evaluate relation of the turbine design parameters on sediment erosion so as to identify those parameters that can be attuned to reduce the erosion. A new design program named as "Khoj" has been developed to facilitate this study. A method to include sediment erosion as a design parameter is devised. Analytical design of Francis runner has been made for a reference case. Each hydraulic design parameter is varied within a pre-defined range and changes in erosion relative to the reference design have been evaluated. It is found that the runner outlet diameter, peripheral velocity at inlet, and blade angle distribution have the highest effect on sediment erosion of Francis runner. Results of this study can be utilized to develop better Francis turbines to handle sediments.

Key Words: *turbine, erosion, design, optimization*

1. INTRODUCTION:

Hard particles as quartz are present with a high concentration in the rivers of the Asian and South American subcontinents [1]. This has very crucial effects on hydropower plants across these regions. Wear of turbine runner and damage of associated components are the major effects of the sediment particles [2]. This leads to a drop in turbine efficiency and often is a cause for shutdown of power plants during monsoon period to prevent severe damage [3].

Different types and designs of hydraulic turbines are eroded by sediments in different ways. In general Francis turbines are more sensitive to the effects of sediment erosion [4]. Studies have shown some possibilities to reduce sediment erosion in Francis turbines. Neopane [5] has estimated that a 20% increase in runner outlet diameter reduces the total sediment erosion in the runner by 60%. Dahlhaug [6] has reported satisfactory improvements in performance in sediment handling of the Francis runner manufactured with a new technology. Several design methods [7]-[10] have been proposed for improving hydraulic efficiency of Francis turbines avoiding cavitation. However these methods do not include sediment erosion as a design parameter.

Literatures [11],[12] have shown that the erosion in hydraulic machineries is proportional to the cube of the flow velocity. This relation can be used as a fundamental basis for comparison of relative erosion in turbine runner keeping the sediment properties to be constant.

In this paper we establish a means to include sediment erosion as one of the design parameters of Francis runners. The design methodology discussed in [7],[13],[14] and some improvements proposed in [15] is used as the reference method to design the runner of Francis turbine for this study.

2. PROPOSED METHODOLOGY

In the proposed methodology the following two terms are defined as the indicator and the means of comparison of relative erosion in the Francis turbine runner.

Erosion Tendency (E_t)

It is quantification of tendency of a specific design of runner to be eroded in similar sediment conditions. Erosion tendency is defined as follows:

$$E_t = \frac{\sum W_i^3 * A_i}{\sum A_i} \qquad [m^3/s^3] \qquad (1)$$

Where W_i is the relative velocity of flow in each segment area (A_i) of the runner blade surface. Segment area is the area between the intersection of stream lines and stream points in the runner blade surface.

Erosion Factor (E_f)

It is ratio of erosion tendency of each new design with respect to the reference design. Erosion factor is defined as follows:

$$E_f = \frac{(E_t)_{New\ Design}}{(E_t)_{Refrence\ Design}} \qquad [-] \qquad (2)$$

The erosion factor estimates a quantitative difference in sediment erosion of runner with the change in hydraulic design alone.

In this study the erosion factor is used as a means to compare the relative erosion in the optimized designs of runner with respect to the reference design.

Reference design

Jhimruk Hydroelectric Center (JHC) in Nepal is considered as the reference case for this study. JHC is a typical power plant suffering from sediment erosion of high head Francis turbine in South Asia. It has three units of splitter blade Francis runners of 3 MW each. With the basic design data presented in Table 1 and values of hydraulic design parameters presented in Table 2, a reference design to suit this site is created. Full blade runner has been considered as the reference design instead of splitter blade due to limitation of the design program. The erosion factor for the reference design is 1.

Table 1. Basic design data for JHC

S.N.	*Parameters*	*Symbol*	*Unit*	*Value*
1	Net design head	H	m	201.5
2	Net discharge per unit	Q	m^3/s	2.35
3	Design efficiency	n	%	96

Design optimization range

The hydraulic design parameters are varied within a defined range and its effects on erosion factor is evaluated. Table 2 lists the range of variation of the design parameters considered for this study.

Table 2. Hydraulic design parameters

S.N.	*Parameters*	*Symbol*	*Unit*	*Value for Reference design*	*Range of optimization*
1	Outlet diameter	D_2	m	0.54	0.4 - 0.75
2	Number of pole pairs in generator	Z_P	0	3	3 - 12
3	Reduced peripheral velocity at inlet	$\underline{U_1}$	-	0.74	0.65 - 1
4	Acceleration of flow through runner	Acc	%	35	0-50
4	Height of runner	b	m	0.16	0.05-0.4
5	Blade angle distribution	β	0	linear	4 different nonlinear

Design optimization process

A graphic user interface (GUI) program to create and modify design of Francis runner has been developed. The program is named as "Khoj" and is able to create a 3-D runner profile based on the given basic design data listed in Table 1 and optimization parameters listed in Table 2. The GUI provides enough flexibility to change these input parameters and is able to compute the erosion factor for each new design. The program is also featured to save the summary of the design and export it to CFD and CAD programs for further analysis.

In this study the reference design, is created by "Khoj". The optimization parameters are varied within the range as given in Table 2. Only one parameter is considered at a time and the new runner design is created with its corresponding erosion factor. Several designs are developed and analyses of the results are done to draw the conclusions.

3. RESULTS AND DISCUSSION

Consequences of variation in each design parameter are evaluated from the design program. Effect of the variation on the erosion factor is of primary interest. However, the effects on other relevant deign parameters is also observed. The results of the study are analyzed as follows.

a. Effects of varying the outlet diameter

An increase in outlet diameter reduces erosion factor significantly and reaches to a minimum value, then remains constant. Fig. 1 shows the effect of varying out let diameter on relative velocity at inlet and outlet of runner. Fig. 2 shows the effect on erosion factor and submergence (H_s) required.

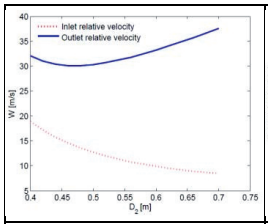

Fig. 1. Effect on relative velocity at inlet and outlet

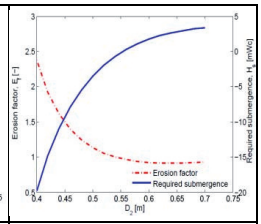

Fig. 2. Effect on erosion factor and submergence

Increasing the outlet diameter reduces relative velocity at inlet and increases relative velocity at outlet. There exists a maximum diameter of outlet for which the erosion factor is minimum. Increasing outlet diameter reduces the submergence. As also indicated by Neopane [5], increasing outlet diameter is a solution to reduce the sediment erosion in Francis runner. However, bigger diameter may increase financial investments. Hence the maximum runner diameter has to be limited from the financial analysis.

b. Effects of varying the number of pole pairs

Number of pole pairs in generator has a reverse effect on rotational speed. That means increasing number of pole pairs cause reduction in relative velocity inside the runner and hence lower erosion factor. This also cause to lowering in speed number of the runner. Fig. 3 shows effect of number of pole pairs on speed number (Ω) and Fig. 4 shows the effect on erosion factor and submergence required.

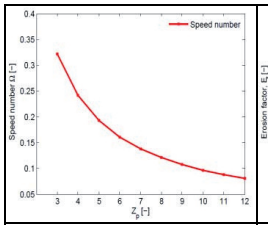

Fig. 3 Effect on speed number

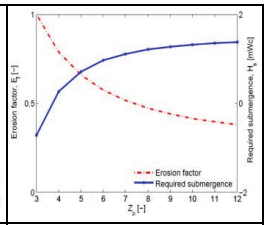

Fig. 4 Effect on erosion factor and submergence

Increase in pole pairs seems to be a promising option to reduce the erosion factor. But speed number below 0.2

causes increased friction losses for a Francis turbine and is generally avoided [7]. For speed numbers below 0.15, Pelton turbines are usually preferred. Lowering speed number also causes diameter of runner to increase. Hence maximum number of pole pairs to be selected has a limiting value.

c. *Effects of varying reduced peripheral velocity at inlet*

Varying the inlet peripheral speed does not affect the outlet conditions, but it does affect the reaction ratio, the inlet dimensions and the inlet velocity triangle. Fig. 5 shows effect of reduced inlet peripheral velocity on inlet height (B_1) and inlet diameter (D_1) and Fig. 6 shows the effect on erosion factor and reaction ratio. Lowering of $\underline{U_1}$ causes reduction of the erosion factor, reaction ratio and the inlet diameter. The inlet height is increased to maintain the continuity. However, change in inlet velocity triangle due to lower $\underline{U_1}$ causes radical changes in blade profile if the inlet angle becomes lower than 90^0 [7].

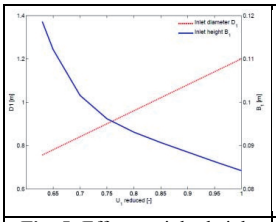

Fig. 5. Effect on inlet height and inlet diameter

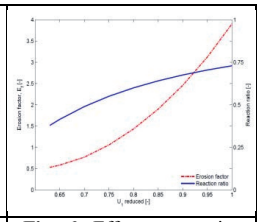

Fig. 6. Effect on erosion factor and reaction ratio

Lowering the reaction ratio causes lower change of potential energy into mechanical energy inside the runner. This means higher conversion of potential energy into kinetic energy at guide vanes, which causes higher flow velocity around it. This increases erosion in the guide vanes. Hence detailed analysis should be done to limit the lower value of $\underline{U_1}$.

d. *Effects of varying acceleration of flow through runner*

Changing acceleration through the runner causes a change in meridional flow velocity and also the relative velocity. Due to continuity, this causes a change in inlet area as well. Fig. 7 shows the effect of varying the acceleration on inlet velocities and Fig. 8 shows the effect on the erosion factor.

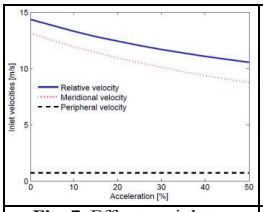

Fig. 7. Effect on inlet velocities

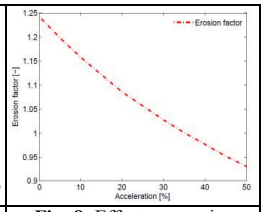

Fig. 8. Effect on erosion factor

For an increasing acceleration in flow, the inlet relative velocity is decreased, which cause the erosion factor to decrease as well. A substantial reduction in erosion factor can be expected by this. However, higher acceleration may cause to increase number of runner blades to prevent back flow [15]. Larger number of blades in runner increase the production cost and also reduce the flow passage inside the runner.

e. *Effects of varying height of runner*

Height of runner is the vertical height difference from inlet to outlet. This has to be chosen by the designer. Changing the runner height will not change the remaining main dimensions except the erosion factor. Fig. 9 shows the definition of height of runner and Fig. 10 shows the effect of varying runner height on the erosion factor.

Choosing the height of runner larger than the difference between inlet and outlet radius *(a)* gives lower erosion factor, and vice versa. The higher value of *b* will cause longer blades with more curvature at the outlet. This increases the weight of the runner and may impose manufacturing constraints.

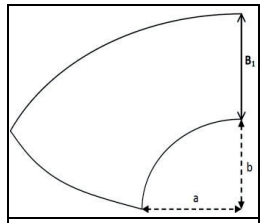

Fig. 9. Definition of runner height, b

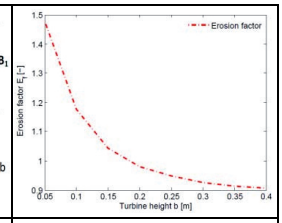

Fig. 10. Effect on erosion factor

f. *Effects of varying shape of blade angle distribution*

Blade angle distribution is the shape in which the runner changes its profile from inlet to outlet. It directly affects the rate of conversion of hydraulic energy to mechanical energy at each section of the runner.

Fig. 11 shows the different nonlinear shape of blade angle distribution considered for this study and Fig.12 shows the effect on erosion factor.

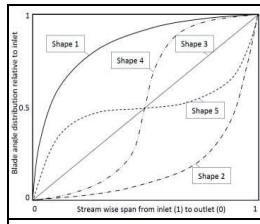

Fig. 11. Different shapes of the blade angle distribution

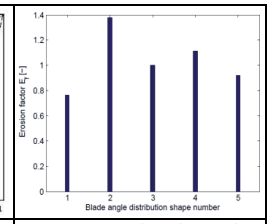

Fig. 12. Erosion factor for different shapes of the blade angle distribution

Linear change of the blade angle (shape 3) has been a commonly accepted blade angle distribution for the design of Francis runners. It is found that with the beta distribution shape 1, there is a drop in erosion factor by almost 30%. This seems to be a very convincing solution, as change in beta distribution has no effects other than change in shape of blade and relative velocities. However, an extreme change in shape of blade may have strength and manufacturing limitations.

CONCLUSIONS:

Standard practice of design of high head Francis turbines has "the highest efficiency without cavitation" as a major design parameter. This fundamentally

isolates sediment erosion from the design process. Erosion factor, as introduced in this paper, can be used as a standard means to compare the relative erosion in runner surface due to variation in the hydraulic design. The major findings of this paper to reduce the sediment erosion in Francis runners by improving the hydraulic design are concluded in Table3.

Table 3. Design modifications for reducing sediment erosion

S.N.	*Proposed Modifications*	*Limitations*
1	Increase outlet diameter of runner	Size of turbine
2	Increase number of pole pairs in generator	Speed number
3	Reduce peripheral velocity at inlet	Reaction ratio
4	Increase acceleration of flow through runner	No of runner blades to prevent back flow
4	Increase blade height of runner	Fabrication
5	Change shape of blade angle distribution	Strength, Fabrication

It is found that multiple parameters of Francis runner can be adjusted to reduce the sediment erosion. There also exist some conditions which impose limits to these adjustments. CFD and CAD analysis for the justifications of these findings would make them more reliable for application in design process.

It is expected that the better hydraulic design of runner, together with hard surface coatings and manufactured with newer methods will be a better and economic solution to reduce the problems of sediment erosion in Francis turbines.

REFERENCES

[1] Thapa B. Sand Erosion in Hydraulic Machinery. Doctoral thesis at NTNU, 2004.

[2] Thapa B, Shrestha R, Dhakal P, Thapa BS. Problems of Nepalese Hydropower Projects due to Suspended Sediments. Journal of Aquatic Ecosystem Health and Management, pp 251-258, 2005.

[3] Sharma HK. Power generation in sediment laden rivers. The International Journal of Hydropower & Dams - Volume Fifteen, pp 112-116, Issue 6, 2010.

[4] Brekke H. Discussion of Pelton turbine versus Francis turbines for high head turbines, IAHR, Colorado, 1978.

[5] Neopane HP, Dhalhaug OG, Thapa B. Alternative Design of a Francis Turbine for Sand Laden Water. International Conference on Hydropower- Hydro Sri Lanka, 2007.

[6] Dahlhaug OG, Skåre PE, Mossing V, Gutierrez A. Sediment resistive Francis runner at Cahua Power Plant", International Journal of Hydropower and Dams, 2010.

[7] Brekke H. Hydraulic design strategy for Francis Turbine, The International Journal of Hydropower & Dams, Issue 3, 1996.

[8] Ståle Risberg, Magnus Jonassen, Roy Jonassen, Design of Francis turbine runners based on a surrogate model approach, The International Journal of Hydropower & Dams - Volume Fifteen, Issue 5, 2008

[9] A.Nourbakhsh , O.Seyed Razavi. H.Khodabakhsh , A.Mehrabadi , New Approach for Hydraulic Design of Francis Runner Based on Empirical Correlations, International Conference on Small Hydropower - Hydro Sri Lanka, 2007

[10] K Daneshkah, M Zangeneh, Parametric design of a Francis turbine runner by means of a three-dimensional inverse design method, 25th IAHR Symposium on Hydraulic Machinery and Systems, Romania, 2010

[11] Truscott GF. A literature survey on abrasive wear in hydraulic machinery. Wear, 1971,

[12] Padhy MK, Saini RP. A Review on silt erosion in hydro turbine. Renewable and Sustainable Energy Reviews, 1974–1987, 2008.

[13] Brekke H. Hydraulic turbines, design, erection and operation, Compendium, NTNU, 2000.

[14] Eltvik M, Olimstad G, Walseth EC. High Pressure Hydraulic Machinery. NTNU, 2009.

[15] Gjosater K. Hydraulic design of Francis Turbine Exposed to Sediment Erosion. Master's Thesis, NTNU, 2011.

CHAPTER XIII

Paper B

Design optimization of Francis runner for sediment handling
Thapa, B.S., Eltvik, M., Dahlhaug, O.G., Thapa, B., Gjøsæter, K.
Fourth International Conference on Water Resources and Renewable Energy Development in Asia, Chiang Mai, Thailand, March 25-26th, 2012

Design Optimization of Francis Runners for Sediment Handling

Biraj Singh Thapa
Turbine Testing Lab
Kathmandu University
P.O. Box 6250
Dhulikhel, Nepal

Mette Eltvik
The Waterpower Laboratory
Norwegian University of Science and Technology
Norway

Kristine Gjøsæter
The Waterpower Laboratory
Norwegian University of Science and Technology
Norway

Ole G. Dahlhaug
The Waterpower Laboratory
Norwegian University of Science and Technology
Norway

Bhola Thapa
Turbine Testing Lab
Kathmandu University
P.O. Box 6250
Dhulikhel, Nepal

Abstract

Growth of energy demands is escalating rapidly. Crisis in conventional sources of energy is urging to expand feasibility limits of the renewable energy resources such as hydropower. New development of hydropower projects is shifting towards the unexplored regions of Asia and South America. These regions have their own specific technical challenges and one of the major problems is sediment erosion of turbine components. Financial feasibility of future hydropower developments across these basins would be largely influenced by technological advancements. New innovations to prevent erosion of mechanical equipment exposed to sediments are important needs at present.

Erosion in hydro turbines is a complex phenomenon, which depends upon several parameters. Design of Francis turbines is unique to each site and hence takes time and effort to produce the best design for specific conditions. This makes design optimization of Francis turbines for erosive environment a challenging task. Several studies have been conducted to estimate erosion behavior in turbines and other components. Recent advancements in computing tools and software have added advantage to these studies. However, the design of Francis turbines to handle large amount of sediments effectively has still not been established.

Kathmandu University, together with Norwegian University of Science and Technology, DynaVec and Nepal Hydro & Electric as partners, has started a unique research project. The goal of the project is to establish a new philosophy for design of Francis turbines effective to handle sediment problems. Jhimruk Hydroelectric Center in Nepal, which represents a typical case of sediment erosion in hydro turbines across the Himalayas, has been taken as the reference case. The research is funded by NORAD supported RenewableNepal Programme. This paper assimilates some of the major findings of the ongoing project.

A new program 'Khoj' has been developed to create and optimize the design of Francis runners. The program is also featured to compare erosion in runner blades for different design cases. The final design can be exported to Computational Fluid Dynamics (CFD) and Fluid Structure Interaction (FSI) for further analysis. Parametric survey was carried out with this program to evaluate the relative effect of each design parameter on sediment erosion. The result was compared with results obtained using CFD analysis to estimate effects of the design variables on hydraulic performance. Several optimized designs were developed and analyzed to fulfill the desired condition of erosion and efficiency.

This paper summarizes the standard procedures used for design of high head Francis runners. Use of computational tools and methods for design optimization of Francis runners for sediment handling is also presented. Application of design program Khoj to identify the effects of design parameters on sediment erosion in Francis runners is explained. Results of CFD analysis of new runner designs, optimized for handling sediments at the reference power plant, are also discussed.

Key Words: Francis runner, design optimization, CFD, erosion, RenewableNepal

1. Introduction

There is a huge potential of new hydropower developments across the basins of Himalaya and Alps of Andes. Nepal, a small south Asian country, alone has more than 6,000 rivers with 42,000 MW of feasible hydropower potential still to be harnessed [1]. However problems due to suspended sediment particles have been one of the technical limiting factors for designers and developers in this region. Almost all the river and rivulets in this region contains 60% -80% of minerals having hardness number above 6 in Moh's scale [2].

Sediment erosion of hydro turbines is a complex phenomenon, as it depends upon various parameters [3, 4]. Several studies have been conducted to quantify the effects of the erosion in hydraulic components of power plants [5, 6, 7]. These studies conclude that sediment erosion removes the base material gradually. This leads to change in flow pattern, losses in efficiency, vibrations and final breakdown of hydro turbine components. This has made sediment erosion of hydro turbines a technical problem with huge economic losses.

Several techniques has been attempted to control the effects of sediment erosion in turbine components. This includes from prevention of sedimentation in the catchment areas to tapping sediments at intakes and applying preventative coatings on the turbine components exposed to high velocity water [3]. However, these and others methods [8] to prevent the sediment erosion in Nepalese power plants have not shown successful results. Change in turbine design philosophy so as to reduce relative velocity of water inside the runner without significant changes in turbine dimensions has been identified as one of the new areas of research in the field of sediment erosion in Francis turbine [9].

2. Sediment Erosion in Francis Turbine

Francis turbines are reaction turbines i.e. turbine components are completely submerged in water. This makes the turbine components more exposed to sediment erosion. Several projects across the Himalayas and Andes regions prove the use of Francis turbines as a bad choice for sediment laden water [10] with occurrence of severe damage in turbine components.

The, use of additional settling basins together with methods of surface coating in runner and guide vanes has been attempted at Jhimruk Power Plant in Nepal [8]. New production method, where runner blades are bolted to hub and shroud instead of welding, which allows applying tungsten carbide based coatings to the whole surface of the runner vanes has been applied at Cahua power plant in Peru [11]. Highly sophisticated settling chambers with continuous flushing mechanism together with HVOF coated runners are used at 1500 MW Nathpa Jhakri power plant in India [12]. The Francis runners at Jhimruk and Nathpa Jhakri power plants are still severely damaged during the monsoon period. However, satisfactory improvements in performance of the Francis runner at Cahua power plant has been reported [10]. Fig. 1 shows the effects of sediment erosion in Francis turbines operating in Himalayan and Andes basins.

(a) **(b)** **(c)** **(d)**

Fig. 1 Francis Turbines performing under basins of Himalaya and Andes: (a) Damage in Runner blade at Jhimruk PP after one year of operation [9]. (b) Runner manufactured with new technology for Cahua PP [10]. (c, d) Damage to guide vanes and cheek plates at Nathpa PP [11].

3. Hydraulic Design of Francis Runners

The hydraulic design procedure of a Francis runner starts with calculating the outlet diameter, D_2, number of poles in the generator, Z_p, and synchronous speed, n. With these values known, the dimensions at the inlet are calculated. These comprises of diameter, D_1, inlet angle, β_1, and inlet height, B_1. Fig. 2 gives an overview of the main dimensions in the runner.

These calculations are based on hydraulic parameters like head and discharge, which are determined by the topography and hydrology of the power plant site. Traditionally, velocity at the inlet and outlet of the runner, triangles as shown in Fig. 3, are used in the design process.

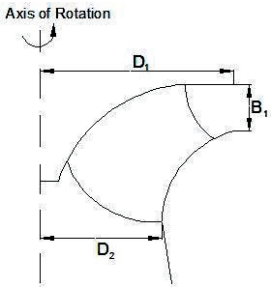

Fig. 2 Axial View of Runner

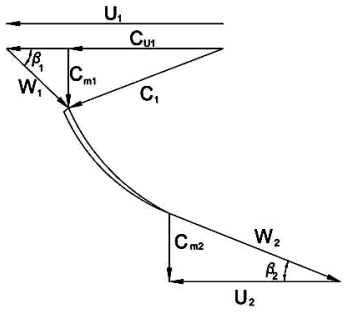

Fig. 3 Velocity triangles

Notations

B	-	Runner height, [m]
C	-	Absolute velocity, [m/s]
D	-	Runner diameter, [m]
U	-	Peripheral velocity, [m/s]
W	-	Relative velocity, [m/s]
N	-	Synchronous speed, [m/s]
Z_p	-	No of poles in generator, [-]
C_m	-	Meridian component of C, [m/s]
C_u	-	Tangential component of C, [m/s]
h_{va}	-	Vapor pressure, [m]
h_b	-	Barometric pressure, [m]
h_s	-	Submergence, [m]
B	-	Angle between the relative and absolute velocity, [degree]
1	-	Inlet Section
2	-	Outlet Section

3.1. Dimensions at Runner Outlet and Inlet:

The dimensioning of the outlet starts with assuming no rotational speed at Best Efficiency Point (BEP) i.e. $C_{u2} = 0$. In addition, the values for outlet angle, β_2, and peripheral speed, U_2, are chosen from empirical data [13]:

$13° < \beta_2 < 22°$ *Lowest value for highest head*

$35 \text{ m/s} < U_2 < 42 \text{ m/s}$ *Highest value for highest head*

The outlet diameter and speed is found by reorganizing the expression for flow rate and peripheral speed, respectively. C_{m2} is obtained from the known geometry in the velocity triangles. The number of poles, Z, in the generator depends on the rotational speed and net frequency. With a grid frequency of 50 Hz, the number of poles is obtained by using equation 4.

$$D_2 = \sqrt{\frac{4 \cdot Q}{\pi \cdot C_{m2}}} \text{ [m]} \quad \text{- (1)} \qquad n = \frac{U_2}{\pi \cdot D_2} \text{ [rpm]} \quad \text{- (2)} \qquad C_{m2} = U_2 \cdot \tan \beta_2 \text{ [m/s]} \quad \text{- (3)} \qquad Z = \frac{50 \cdot 60}{n} \text{ [-]} \quad \text{- (4)}$$

The number of poles should be an integer. The value obtained from equation 4 must therefore be rounded off. With the corrected number of poles, equation 4 is used to find the corrected synchronous speed; this value is again used to calculate the corrected diameter at the outlet.

To avoid the cavitation at the out let of the runner, the required submergence for the runner is calculated using equation 5. The NPSH, called as Net Positive Suction Head, is calculated using empirical equation 6 [13].

$$h_s = h_b - h_{va} - NPSH \text{ [m]} \quad \text{- (5)} \qquad NPSH_{required} = a \cdot \frac{{C_{m2}}^2}{2 \cdot g} - b \cdot \frac{{U_2}^2}{2 \cdot g} \text{ [m]} \quad \text{- (6)} \qquad \eta_k = \frac{C_{u1} \cdot U_1 - C_{u2} \cdot U_2}{g \cdot H} \quad \text{- (7)}$$

At the inlet the values for diameter, D_1, height of the inlet, B_1, and inlet angle, β_1 is calculated. In order to find these values the Euler equation (equation 7) is used. By introducing reduced dimensionless values and assuming no rotation at the outlet, the equation can be rewritten as equation 8. The turbine efficiency, η_t, is generally set to 0.96, and $\underline{U_1}$ is chosen in the interval as given in equation 9. U_1 can be calculated using equation 10.

$$\eta_t = 2 \cdot \underline{U_1} \cdot \underline{C_{U1}} \quad \text{- (8)} \qquad 0.7 < \underline{U_1} < 0.75 \quad \text{- (9)} \qquad U_1 = \underline{U_1} \cdot \sqrt{2 \cdot g \cdot H} \text{ [m/s]} \quad \text{- (10)} \qquad D_1 = \frac{U_1 \cdot 60}{n \cdot \pi} \text{ [m]} \quad \text{- (11)}$$

The inlet diameter can now be found by using equation 11. From the velocity triangles in Fig. 3 an expression for the inlet angle can be derived as given in equation 12. In order to use the equation 12 the value for C_{m1} is calculated by the continuity equation given in equation 13. It is desirable with an acceleration of the water from the inlet to the outlet, in order to avoid backflow through the runner. Therefore, the condition presented in equation 14 is used.

$$\tan\beta_1 = \frac{C_{m1}}{U_1 - C_{u1}} \quad [-] \quad (12) \qquad C_{m1}A_1 = C_{m2}A_2 \quad (13) \qquad C_{m1} = 1.1 \cdot C_{m2} \quad (14) \qquad B_1 = \frac{1.1 \cdot {D_2}^2}{4 \cdot D_1} \quad [\text{m}] \quad (15)$$

The only value left to calculate is the inlet height. By combining equation (13) and equation (14) this value can be obtained as presented in equation 15.

3.2. Shaping of Runner Blade Profile

When the main dimensions of the runner are known, the runner blades can be designed. The design procedure starts by determining the shape of the blade in the axial view, then the radial view is established, and finally the runner blade can be plotted in three dimensions [13-15].

Runner Axial view: At first a streamline along the shroud or along the hub has to be defined. It is most common to define it along the shroud. Traditionally an elliptical or circular shape is chosen for the streamline. Based on the inlet distribution and the definition of the first streamline, the rest of the streamlines can be determined. After the first streamline is defined, the number of streamlines has to be chosen. The distribution of streamlines is determined by the flow rate, Q, at the inlet of the runner, which initially is considered uniform. This gives a uniform distribution of the streamlines between the hub and shroud at the inlet. Fig. 4 shows the axial view of a Francis runner after removing upward curvature at the hub, cutting endpoints and redistributing the remaining points.

Runner Radial view: In order to simplify the design process of going from the axial view to the radial view, a GH-plane is defined, shown in Fig. 5. G is the length of a streamline in the axial plane and H is the length of a streamline in the radial plane. The values of G are calculated by using the values of R and Z from the axial view. Calculating the values of H is more demanding, as they are dependent on the distribution of the blade angle, β. The blade angle is closely linked to the energy distribution along the blade. The energy distribution describes the transformation from pressure energy to rotational energy along the blade. The relation between the energy distribution and the blade angle β is governed by equation 16.

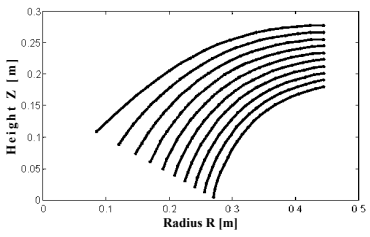

Fig. 4 Axial view

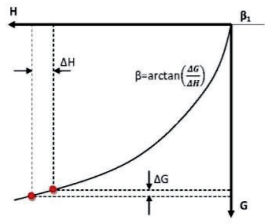

Fig. 5 Definition of GH-plane

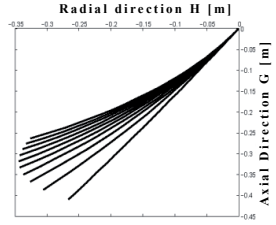

Fig. 6 GH-plane

The blade angles at the inlet and outlet are known from the velocity triangles. The distribution in between has to be determined. This can be done in two ways. Either choosing the $U \cdot C_u$ distribution and then calculating the β distribution, or choosing β distribution and then calculate $U \cdot C_u$ distribution. Choosing the blade angle distribution gives the designer full control of the design outcome. The blade angle distribution is also the most important factor to shape the runner profile.

The values of ΔH corresponding to each ΔG can be obtained using equation 17. When this is performed for each streamline, the G-H plane can be plotted as shown in Fig. 6. Now the radial view of the runner can be established using equation 18, which is defined according to Fig. 7. When knowing all the coordinates for θ and R, the radial view can be plotted as in Fig. 8. Combining the axial coordinates and the radial coordinates, the 3D shape of the runner blade emerges as shown in Fig. 9.

$$\beta = \tan^{-1}\left(\frac{C_m}{U - C_u}\right) \quad [\text{radians}] \quad (16) \qquad \Delta H = \frac{\Delta G}{\tan\beta} \quad (17) \qquad d\theta = \frac{\Delta H}{R} \quad [\text{radians}] \quad (18)$$

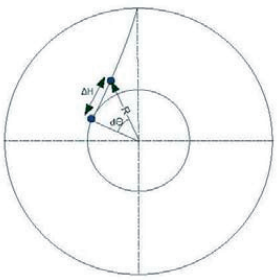

Fig. 7 Definition of radial view

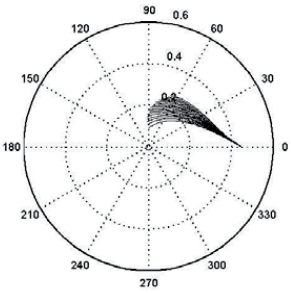

Fig. 8 Radial view of runner

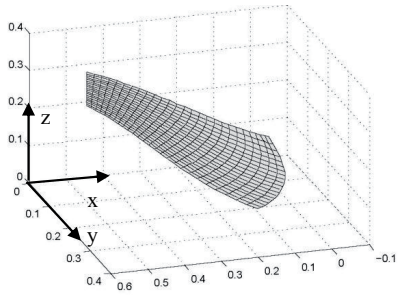

Fig. 9 3D View of runner

4. Method of Design Optimization and Analysis

A graphic user interface (GUI) program to create and modify design of Francis runner has been developed. The methodology and steps discusses in section 3 has been followed to design the runners. The program is named as "Khoj" and is able to create 3-D runner profile based given basic design data. An Analytical design of Francis runner has been made for a reference case. Each hydraulic design parameter is varied within a pre-defined range and change in erosion relative to the reference design has been evaluated. The optimized designs are further analyzed with CFD tools to evaluate its performance in erosive environment.

4.1. Reference Design

JHC is a typical power plant suffering from sediment erosion of Francis turbine in South Asia. It has three units of splitter blade Francis runners of 4.2 MW each. With the basic design data presented in Table 1 and values of hydraulic design parameters presented in Table 2, a reference design to suit this site is created. Full blade runner has been considered as the reference design instead of splitter blade due to limitation in the design program.

Table 1. Basic design data for JHC

S.N.	Parameters	Symbol	Unit	Value
1	Net design head	H	m	201.5
2	Net discharge per unit	Q	m^3/s	2.35
3	Runner efficiency	η	%	96

4.2. Design Optimization Range and Methodology

The hydraulic design parameters are varied within a defined range and its effects on erosion factor is evaluated. Table 2 lists the range of variation of the design parameters considered for this study.

Table 2. Hydraulic design parameters

S.N.	Parameters	Symbol	Unit	Value for Reference design	Range of optimization
1	Outlet diameter	D_2	m	0.54	0.4 - 0.75
2	Number of pole pairs in generator	Z_P	-	3	3 - 12
3	Reduced peripheral velocity at inlet	$\underline{U_1}$	-	0.74	0.65 - 1
4	Acceleration of flow through runner	Acc	%	35	0 - 50
4	Height of runner	b	m	0.16	0.05 - 0.4
5	Blade angle distribution	β	degrees	linear	4 different nonlinear

For evaluating effects of sediment erosions in optimized designs, the following two terms are defined as the indicators and the means of comparison of relative erosion in the Francis turbine runner.

Erosion Tendency (E_t)

It is quantification of tendency of a specific design of runner to be eroded in similar sediment conditions. Erosion tendency is defined as follows:

$$E_t = \frac{\sum_{i=1}^{n} W_i^3 * A_i}{\sum_{i=1}^{n} A_i} \qquad [m^3/s^3] \qquad (19)$$

Where n is the number of segment area (A_i) in the runner blade surface. W_i is the relative velocity of flow in each segment area. The segment area is the area between the intersection of streamlines and stream points in the runner blade surface.

Erosion Factor (E_f)

It is ratio of erosion tendency of each new design with respect to the reference design. Erosion factor is defined as follows:

$$E_f = \frac{(E_t)_{New\ Design}}{(E_t)_{Refrence\ Design}} \quad [-] \qquad (20)$$

The erosion factor estimates a quantitative difference in sediment erosion of runner with the change in hydraulic design alone. In this study the erosion factor is used as a means to compare the relative erosion in the optimized designs of runner with respect to the reference design. The erosion factor for the reference design is 1.

4.3. CFD Analysis

To verify the reference design, a CFD simulation is carried out. Designs from Matlab are exported to Ansys CFX-13. Simulations are done to evaluate the hydraulic performance and erosion on the runner blade surface. Exactly same process has been repeated to all the design analysis to maintain the consistency. Table 3-6 presents the parameters selected for the CFD analysis. Fig 10 shows mesh generated from Ansys Turbo Grid for the reference design for the parameters given in table 3. Fig. 11 shows the computational domain generated by Ansys CFX-Pre for the parameters given in table 4.

Table 3 Parameters for CFX-Turbo Grid

Paramater	Type	Value
Grid Node Count	Fine	250000
Factor Ratio		2
Reynolds No		500000

Table 4 General Parameters for CFX-Pre

Paramater	Type
Turbulence	SST
Flow State	Steady
Flow type	Inviscid
Erosion Model	Tabakoff
Morphology	Particle Transport fluid

Table 5 Parameters for CFX-Pre Sediment Data

Data	Value	Unit
Material	Quartz	
Density	2.65	g/cm^3
Diamter	0.1	Mm
Shape factor	1	
Flow rate	0.07	kg/s

Table 6 Parameters for CFX-Post Erosion Analysis

Paramater	Max value	Unit
Sediment Erosion	3.00E-07	kg/m^{2}s
Rate Density	0.3	mg/m^{2}s

5. Results and Discussion

5.1. Results of design optimization:

Consequences of variation in each design parameter are evaluated from the design program Khoj. Effect of the variation on the erosion factor is of primary interest. However, the effects on other relevant deign parameters are also observed. It is found that the runner outlet diameter, peripheral velocity at inlet, and blade angle distribution have the highest effect on sediment erosion of Francis runner. The results of the study are presented in Table 7. Several methods have been proposed to reduce the sediment erosion in Francis runner. However, each method has its own limiting conditions. Further study is necessary to identify the optimum value of each design parameter for particular site conditions.

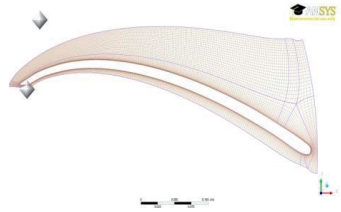

Fig. 10 TurboGrid ATM mesh

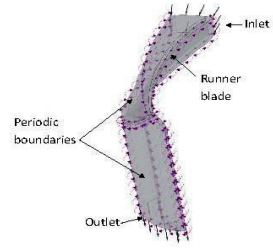

Fig. 11 Computational domain

5.2. Results From CFD Analysis:

CFD Analysis of Reference Design

CFD analysis of reference runner has been done to evaluate the hydraulic parameters and sediment erosion in runner blade surface. This is taken as a reference to compare the same for the optimized designs. Fig. 12 shows the streamlines of flow on the pressure side of the blade. Smooth flow from inlet to outlet section can be observed. Fig. 13 shows the relative velocity on meridional surface from inlet to outlet. It shows the smooth increment of relative velocity from inlet to outlet computational domain. Fig. 14 shows sediment erosion

Table 7. Conclusions from Khoj to reduce sediment erosion

S.N.	Proposed Modifications	Limitations
1	Increase outlet diameter of runner	Size of turbine
2	Increase number of pole pairs in generator	Speed number
3	Reduce peripheral velocity at inlet	Reaction ratio
4	Increase acceleration of flow through runner	No of runner blades to prevent back flow
4	Increase blade height of runner	Fabrication
5	Change shape of blade angle distribution	Strength, Fabrication

rate density on the pressure side of reference runner blade computed by Ansys CFX-Solver for the sediment data presented in table 5. It shows that the erosion pattern spreading at the outlet section of the runner blade, which resembles to the erosion pattern of reference runner as shown in Fig. 1, a.

CFD Analysis of Optimized Designs

Several optimized designs are developed by combining the changes anticipated by the design program to reduce sediment erosion in runner blades. CFD analysis of the optimized designs having erosion factor below 1 has been done to validate the reduction in erosion and also evaluate the effects on other hydraulic parameters. Effects of the variation on other hydraulic parameters have also been computed. Table 8 presents corresponding erosion factors of the two optimized designs calculated by the design program together with respective total runner efficiencies computed by CFD.

Table 8. Optimized designs erosion factors and efficiencies

Design	Reference	Design 1	Design 2
Erosion factor (-)	1.000	0.481	0.395
Total Efficiency (%)	95.05	91.74	90.21

Results of CFD analysis of optimized design 1 is shown in Fig. 15 to Fig. 17. Comparisons with the results for the reference design shows reduction in erosion on the blade surface as predicted by the program. However, there are some irregularities in streamlines at inlet section and transition of relative velocity on meridional surface from inlet to outlet is not smooth. These irrigularities could be possible reasons for drop in total runner efficiency despite of reduction in sediment erosion in runner.

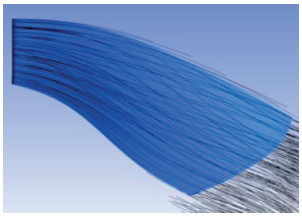

Fig. 12 Streamlines on pressure side

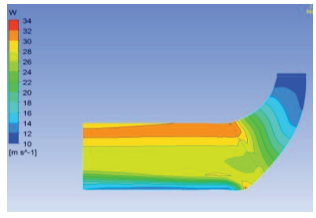

Fig. 13 Relative velocity on Meridional surface

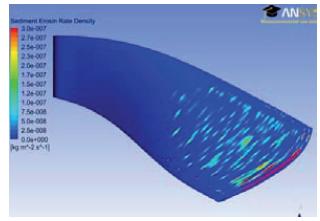

Fig. 14 Sediment erosion on reference runner

Fig. 18 to Fig. 20 shows the results of CFD analysis of optimized design 2. The erosion on the blade surface is less than the reference runner but not lower than that on the optimized design 1 as predicted by the program. Irregularities in the streamlines have further increased and also the rough transitions of the relative velocity. These could have caused to further decrease in the total runner efficiency.

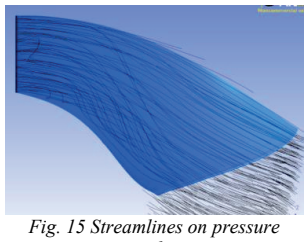

Fig. 15 Streamlines on pressure side

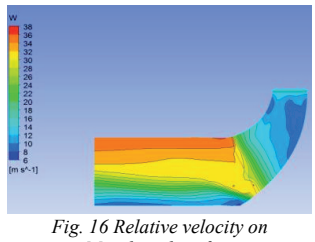

Fig. 16 Relative velocity on Meridional surface

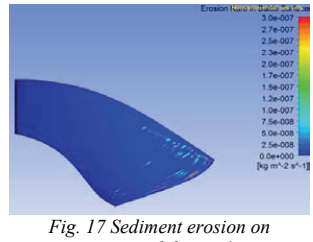

Fig. 17 Sediment erosion on optimized design 1

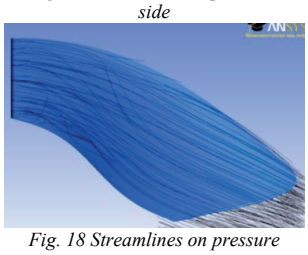

Fig. 18 Streamlines on pressure side

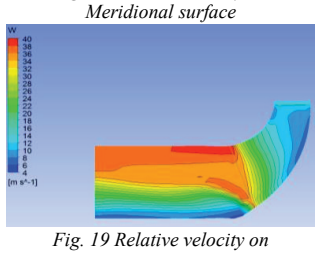

Fig. 19 Relative velocity on Meridional surface

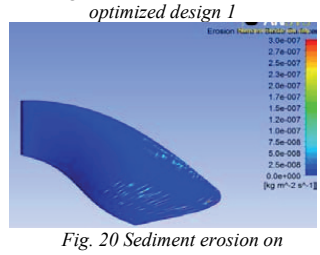

Fig. 20 Sediment erosion on optimized design 2

6. Conclusions

Problem of sediment erosion in turbine components at the hydropower plants across the basins of the Himalayas and the Andes is a technical challenge. Several cases of severe erosion in Francis turbines operating in these regions have been reported. Some attempts to modify manufacturing processes to allow full coating in runner blades has shown an optimistic progress in controlling erosion in Francis turbine. However, new designs of Francis turbines for erosive environments should be explored to make the future of hydropower more economic and sustainable even in the sediment laden projects.

This study makes an attempt to optimize the existing hydraulic design of high head Francis turbines, with the possibility to minimize erosion. The fundamental equations followed for designing a Francis runner has been explored. A reference case has been established and the optimizing parameters with the range of optimization have been identified. Effects of design parameters on sediment erosion in runner blade surface have been estimated by a new design program named as Khoj. Several optimized designs of the runner have been developed and CFD analysis of selected ones has been performed.

From the parametric survey it is found that the runner outlet diameter, peripheral velocity at inlet, and blade angle distribution have the highest effect on sediment erosion of Francis runner. Optimized designs developed show the considerable reduction of erosion in runner blades. Findings of this study will help for further exploration of the research to establish a new design methodology for reduced erosion and increased efficiency of Francis runners.

References

[1] D.P.Sangroula, "Hydropower Development and its Sustainability with respect to Sedimentation in Nepal", *Journal of the Institute of Engineering*, Vol. 7, No. 1, pp. 1-9.

[2] B. Thapa, R. Shrestha, P. Dhakal, B. S. Thapa, "Problems of Nepalese Hydropower Projects due to Suspended Sediments", *Journal of Aquatic Ecosystem Health and Management*, pp 251-258, 2005.

[3] B. Thapa, "Sand Erosion in Hydraulic Machinery", *Doctoral thesis at NTNU*, 2004.

[4] A.A. Hamed, W. Tabakoff, R.B. Rivir, K. Das, P. Arora, "Turbine Blade Surface Deterioration by Erosion", *Journal of Turbomachinery*, 2005, Vol. 127, pp 445-452.

[5] G.F. Truscott, "*A literature survey on abrasive wear in hydraulic machinery*", *Wear*, 1971.

[6] M. Padhy, R.P. Saini, "A Review on silt erosion in hydro turbines"*, Renewable and Sustainable Energy Reviews,* pp. 1974–1987*,* 2008.

[7] Eltvik M., "Sediment Erosion in Francis Turbines", *Master's thesis at NTNU*, 2009.

[8] J. Ruud, "Sediment handling problems Jhimruk Hydroelectric Center", *Master's thesis at NTNU*, 2004.

[9] B.S. Thapa, B. Thapa, O.G. Dahlhaug, "Center of Excellence at Kathmandu University for R&D and Test Certification of Hydraulic Turbine", *Proceeding of International Conference on Hydraulic Efficiency Measurement*, India, 2010.

[10] H. Brekke, Discussion of Pelton turbine versus Francis turbines for high head turbines, IAHR, Colorado, 1978.

[11] O.G. Dahlhaug, P.E. Skåre, V. Mossing, A. Gutierrez, "Sediment resistive Francis runner at Cahua Power Plant, *The International Journal of Hydropower & Dams*, Issue 2, pp109-112, 2010.

[12] H.K. Sharma, "Power generation in sediment laden rivers", *The International Journal of Hydropower & Dams*, Issue 6, pp 112-116, 2010.

[13] H. Brekke, "Hydraulic Turbines Design, Erection and Operation", *NTNU Publication*, 2000.

[14] M. Eltvik, G. Olimstad, E.C. Walseth, "High Pressure Hydraulic Machinery", *NTNU publication*, 2009.

[15] K. Gjosater, "Hydraulic design of Francis Turbine Exposed to Sediment Erosion" *Master's thesis at NTNU*, 2011.

The Authors

Biraj Singh Thapa is a MS by Research student in Mechanical Engineering Department at Kathmandu University (KU) with the topic "Hydraulic Design of Francis Turbine to Minimize Sediment Erosion". He is also a researcher for RenewableNepal Project at KU to develop a new design philosophy for Francis turbine to minimize losses due to sediment erosion.

Corresponding address: bst@ku.edu.np

Mette Eltvik has graduated from the Norwegian University of Science and Technology (NTNU) in 2009. Her field of specialization is sediment erosion in Francis turbines. After one year work as a research assistant in the Waterpower Laboratory at NTNU, she is continuing her research as a PhD candidate in the same field. She is also a supporting researcher for the RenewableNepal Project.

Corresponding address: mette.eltvik@ntnu.no

Kristine Gjosater has obtained her master's degree on 2011 from NTNU with the topic "Hydraulic Design of Francis Turbine Exposed to Sediment Erosion". Currently she is working as a research assistant in the Waterpower Laboratory at NTNU, and is also a supporting researcher for the RenewableNepal Project.

Corresponding address: kristine.gjosater@ntnu.no

Ole G. Dahlhaug obtained his PhD in Mechanical Engineering at NTNU. From 1992 to 1998 he worked at SINTEF as Research Scientist, with research and testing of pumps and turbines. Currently he is Professor at the Waterpower Laboratory at NTNU. He has been actively working with research on sediment erosion of turbine components and efficiency measurements of hydropower plants. He is supervisor of the RenewableNepal project.

Corresponding address: ole.g.dahlhaug@ntnu.no

Bhola Thapa has done Bachelor and Master in Mechanical Engineering from India. He has done PhD from NTNU in the topics "Sand Erosion of Hydraulic Machinery" in 2004. He has been working at Kathmandu University, School of Engineering since 1994. He is a Professor of Mechanical Engineering and he has been serving as Dean of School of Engineering since 2005. He has been involved in research in the field of hydraulic turbines especially in the area design of erosion resistance, operation and maintenance.

Corresponding address: bhola@ku.edu.np

CHAPTER XIV

Paper C

Optimizing runner blade profile of Francis turbine to minimize sediment erosion

Thapa, B.S., Thapa, B., Eltvik, M., Gjøsæter, K., Dahlhaug, O.G.

The 26th IAHR Symposium on Hydraulic Machinery and Systems Beijing, China, August 19 – 23, 2012

The 26th IAHR Symposium on Hydraulic Machinery and Systems
Beijing, China
August 19 – 23, 2012

Paper Number: IAHRXXVI-071

Optimizing runner blade profile of Francis turbine to minimize sediment erosion

Biraj Singh Thapa[1], Bhola Thapa[1], Mette Eltvik[2], Kristine Gjosater[2], Ole Gunnar Dahlhaug[2]

[1]Dept. Mechanical Engineering, Kathmandu University, P.O. Box 6250, Dhulikhel, Nepal
[2] Dept. Energy&Process Engineering, Norwegian University of Science and Technology, NTNU, Trondheim, 7491, Norway

Email: bst@ku.edu.np

Abstract

Hard sediment particles as quartz are present in high amount in the rivers across Asian and Andes mountain ranges. This cause the run-off-river hydropower plants in these regions to suffer from erosion wear. The hydro turbine components erode severely during the monsoon periods. Due to high relative velocity the turbine runners are more vulnerable. Loss of turbine efficiency and high cost of repair and maintenance are the major consequences of the erosion. Several attempts including surface coatings to control the sediment erosion in Francis runners have not shown satisfactory results. One of the emerging solutions is to reduce the relative velocity inside the runner by improving the hydraulic design. This includes optimization of the runner blade profile to reduce sediment erosion, while avoiding cavitation and still maintaining the highest possible efficiency.

This study has been conducted to identify the alternative blade profiles of high head Francis runners and estimate the effects of sediment erosion on each new profile. A new design program named as "Khoj" has been developed to facilitate this study. The program can generate the profiles of Francis runner based on the traditional equations. It is also capable to export the designs for CFD and FEM analysis. Erosion factor has been defined as a means to compare the relative change in sediment erosion due to the variation of the runner design. A reference turbine has been established and alternative blade profiles have been designed. CFD analysis has been conducted to evaluate the performance of the alternative designs relative to the erosive conditions of the reference turbine.

It has been observed that the shape of runner blade has a significant effect on velocity distribution and hence on the sediment erosion of the runner. Results of CFD analysis validates prediction from the design program that the blade profile with higher blade loading at inlet can reduce the sediment erosion in runner up to 33%. It was also observed that this condition improves the runner efficiency without any change in the runner main dimensions. Results of this study can be useful to design Francis turbines operating in sediment conditions.

Key Words: Francis runner**,** erosion, energy distribution, CFD

1. Introduction

The theoretical potential of worldwide hydropower is 2800 GW, which is about four times greater than the amount that has been tapped so far. Much of this potential is found in areas that are exposed to monsoon periods such as the Himalaya and Andes. It is therefore expected that many power plants will be built in these areas in the future. However, rivers in these regions contain high amounts of sediments, which cause rapid erosion of turbine components. Most of the bigger turbines manufactures have developed their turbine designs for the projects with lesser problems of sediments. Consequently proper solution to this age long problem in these parts of world has not been found so far [1]. Growing energy demands in Asia and Latin America has brought up necessity of better designs of hydro turbines, which in particular are capable to handle heavy sediments effectively. Future of sustainable hydropower business in these regions would be largely influenced by the effective solution for the existing problem of turbine erosion.

Sediment erosion of hydro turbines is a complex phenomenon as it depends upon several parameters. Presence of hard particles as quartz in sediment flow removes the base material of turbine gradually. This leads to change in flow pattern, losses in efficiency, vibrations and final breakdown of turbine components. Thus sediment erosion of hydro turbines is a technical problem with major economic losses. Fig. 1 shows the damage in 21 MW Francis runner installed at Cahua power plant in Peru

and Fig. 2 shows the damage in 4.2 MW Francis runner installed at Jimruk Hydroelectric center in Nepal. Both runners are heavily eroded by the sediment particles. Several methods have been attempted to control the effects of sediment erosion in turbine components. This includes, prevention of sedimentation in the catchment areas, tapping sediments at intakes, and applying preventative coatings on the turbine components exposed to high velocity water [2]. However, conventional methods to prevent turbine erosion have not shown successful results. This has created a need for further research to find better solutions to prevent turbine damage from sediments [3].

Standard practice of design of high head Francis turbines has "the highest efficiency without cavitation" as a major design parameter. This fundamentally overlooks considering sediment erosion from the design process. Thus the traditional design methods need optimization for performing satisfactorily in sediment laden projects. Change in turbine design philosophy so as to reduce relative velocity of water inside runner, in addition to the highest efficiency without cavitation criteria, could be one of the new areas of research to minimize sediment erosion in hydraulic turbines.

Recent advancements in computational tools and processors have added advantages to the R&D process of hydraulic turbines. These tools are able not only to compute solutions for the complex design equations but also provide the user friendly virtual environment for performance test and design optimization.

Fig.1 Erosion damage of Francis runner in Peru

Fig.2 Erosion damage of Francis runner in Nepal

2. Research Methodology

2.1. Standard procedure for design of Francis runner

The hydraulic design procedure of a Francis runner starts with calculating the outlet diameter, number of poles in the generator, and synchronous speed. With these values known, the dimensions at the inlet are calculated. These comprises of inlet diameter, inlet angle, and inlet height. These calculations are based on hydraulic parameters like head and discharge, which are determined by the topography and hydrology of the power plant site.

When the main dimensions of the runner are known, the runner blades can be designed. The design procedure starts by determining the shape of the blade in the axial view, then the radial view is established, and finally the runner blade can be plotted in three dimensions. Several equations and intermediate steps are used to develop the 3-D view of Francis runner as discussed in details in [4,5]. This conventional method of design of Francis excludes estimation of erosion in turbine blade in case of sediments in flow.

2.2. Analytical Quantification of Erosion:

In the proposed methodology the following two terms are defined as the indicator and the means of estimating of relative erosion in the Francis turbine runner.

Erosion Tendency (E_t)

It is quantification of tendency of a specific design of runner to be eroded in similar sediment conditions. Erosion tendency is defined as follows:

$$E_t = \frac{\sum_{i=1}^{n} W_i^3 \cdot A_i}{\sum_{i=1}^{n} A} \qquad [\mathrm{m^3/s^3}] \qquad (1)$$

Where n is the number of segment area (A_i) in the runner blade surface. W_i is the relative velocity of flow in each segment area. The segment area is the area between the intersection of stream lines and stream points in the runner blade surface.

Erosion Factor (E_f)

It is ratio of erosion tendency of each new design with respect to the reference design. Erosion factor is defined as follows:

$$E_f = \frac{(E_t)_{New\ Design}}{(E_t)_{Refernce\ Design}} \qquad [-] \qquad (2)$$

The erosion factor estimates a quantitative difference in sediment erosion of runner with the change in hydraulic design alone. Inclusion of erosion factor as a parameter to compare the relative erosion of differently designed turbines for same design conditions can be helpful step to produce better designs for erosive environment.

2.2 Design Program "Khoj"

A graphic user interface (GUI) program to create and modify design of Francis runner has been developed. The program is named as "Khoj" and is able to create a 3-D runner profile based on the design methods and steps discussed in [4,5] and optimize design parameters to reduce erosion factor for the runner designed conventionally. The GUI provides enough flexibility to change

these input parameters and is able to compute the erosion factor for each new design. The program is also featured to save the summary of the design and export it to CFD and CAD programs for further analysis.

The program has been tested and used by the members of the Francis turbine design team at NTNU during spring 2011. The program has been improved and expanded based on the team's findings and needs. Further improvements and expansions might be added in the future. Fig. 3 shows the input data for the main dimension and the velocity triangles generated from the data. Fig. 4 shows the radial view and the 3-D view of runner after several stages of calculations.

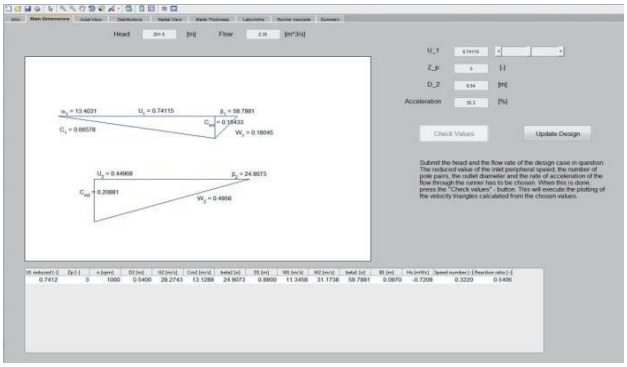

Fig.3 Input tab and velocity triangles

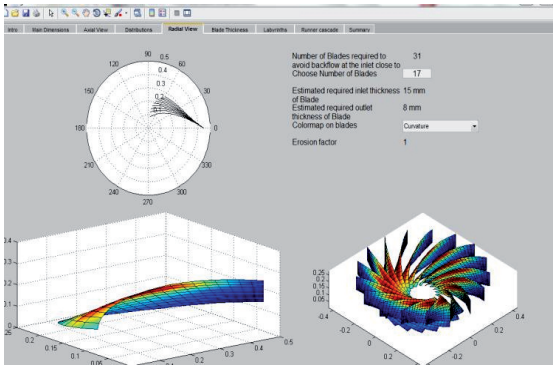

Fig. 4 Radial view and 3-D design

3. Optimization of design

3.1. Reference Design

Jhimruk Hydroelectric Center (JHC) in Nepal is considered as the reference case for this study. JHC is a typical power plant suffering from sediment erosion of high head Francis turbine in South Asia. It has three units of splitter blade Francis runners of 4.2 MW each. With the basic design data presented in Table 1 and values of hydraulic design parameters presented in Table 2, a reference design to suit this site is created. Full blade runner has been considered as the reference design instead of splitter blade due to limitation of the design program. The erosion factor for the reference design is 1.

Table 1 Basic Design Data for JHC

S.N.	Parameters	Symbol	Unit	Value
1	Net design head	H	m	201.5
2	Net discharge per unit	Q	m^3/s	2.35
3	Runner efficiency	n	%	96

Table 2 Hydraulic Design Parameters

S.N.	Parameters	Symbol	Unit	Value for Reference design
1	Outlet diameter	D_2	m	0.54
2	Number of pole pairs in generator	Z_P	-	3
3	Reduced peripheral velocity at inlet	$\underline{U_1}$	-	0.74
4	Acceleration of flow through runner	Acc	%	35
5	Height of runner	b	m	0.16
6	Blade angle distribution	β	^{0}	linear

3.2. Blade angle distribution

Blade angle distribution (or simply beta distribution) is the profile in which the blade angle changes from inlet to outlet. It directly affects the rate of conversion of hydraulic energy to mechanical energy at each section of the runner. It controls how much hydraulic energy in water is converted to the mechanical energy in each section of blade. Linear change of the blade angle from inlet to outlet has been a commonly accepted beta distribution for the design of Francis runners. Various other nonlinear distributions are analyzed in this study to see its effect on efficiency and erosion factor. Fig. 5 shows the liner blade angle distribution for the reference case and its effects on velocity distributions in the blade surface.

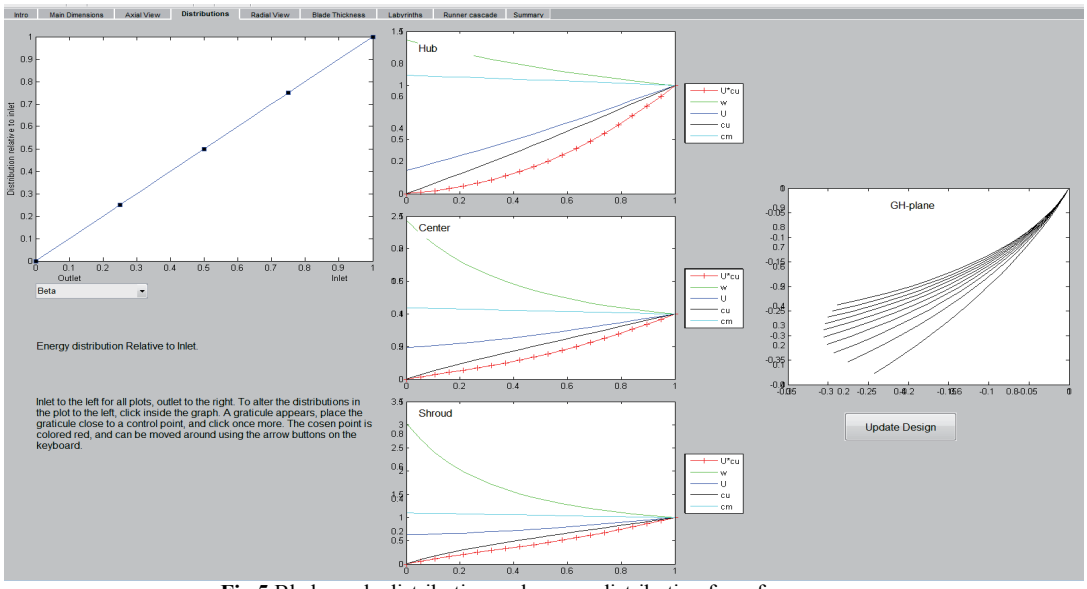

Fig.5 Blade angle distribution and energy distribution for reference case

3.3. Optimization of blade profile

Runner blade profile is optimized by changing blade angle distribution to different non-linear shapes. All other design parameters for the reference design are kept same as presented in Table II. Design program has been featured to generate blade profiles corresponding to the blade angle distribution as an input parameter. Five different blade angle distribution selected for this study is presented in Fig. 6. Selection of blade angle distributions is made to change the amount of energy being extracted from each blade section from inlet to out let. Fig. 6a shows the beta distribution with low energy extraction at runner inlet and high energy extraction at the runner outlet. Fig. 6b shows the beta distribution with high energy extraction at the inlet and low energy extraction at the outlet. Fig. 6c shows the beta distribution with linear energy extraction from the inlet to the outlet. Similarly Fig. 6d and Fig. 6e shows the energy distributions with combinations of high and low energy distribution at the inlet and the outlet respectively.

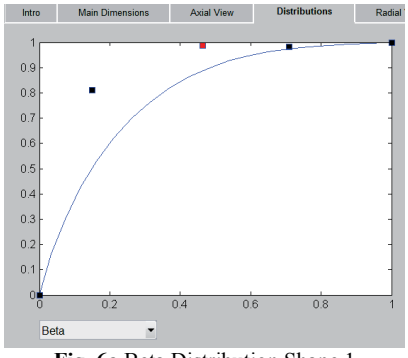

Fig. 6a Beta Distribution Shape 1

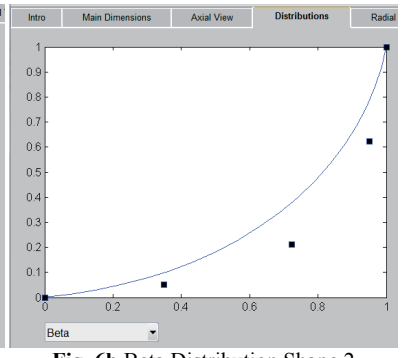

Fig. 6b Beta Distribution Shape 2

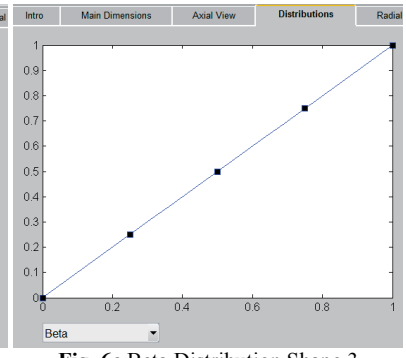

Fig. 6c Beta Distribution Shape 3

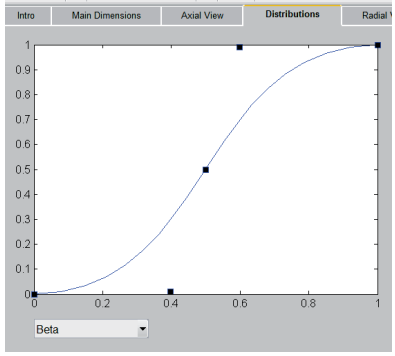

Fig. 6d Beta Distribution Shape 4

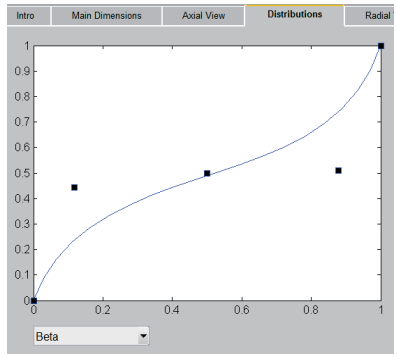

Fig. 6e Beta Distribution Shape 5

4. Numerical Analysis

To verify the reference design, a CFD simulation is carried out. Jhimruk Hydroelectric Center, Nepal has been taken as the reference case. Designs from Matlab are exported to Ansys CFX-13. Simulations are done to evaluate the hydraulic performance and erosion on blade surface. Exactly same process has been repeated to all the Design Analysis to maintain consistency. Comparisons of results are done with that from Matlab for the same designs. Table 3-6 presents the parameters selected for the CFD analysis. Fig. 7 shows the ATM mesh generated by TurboGrid and Fig. 8 shows the computational domain for CFD processing.

CFD analysis of reference runner has been done to evaluate the hydraulic parameters and sediment erosion in runner blade surface as reference value to compare the same for the optimized designs. Fig. 9 shows the pressure distribution on the pressure side of the blade. It shows smooth transition of pressure from inlet to outlet section. Fig. 10 shows the relative velocity at the outlet section of the runner. It shows the average out let velocity at the out let of runner to be in between 30 m/s to 35 m/s. Fig 11 shows sediment erosion rate density on the pressure side of reference runner blade computed by Ansys CFX-Solver for the parameter presented in Table 5 and report generated by the Ansys CFX-Post for the parameters presented in the table 6. It shows that the erosion pattern to be spread at the entire outlet section of the runner blade.

Table 3 Parameters for CFX-Turbo Grid

Paramater	Type	Value
Grid Node Count	Fine	250000
Factor Ratio		2
Reynolds No		500000

Table 4 General Parameters for CFX-Pre

Paramater	Type
Turbulence	SST
Flow State	Steady
Flow type	Inviscid
Erosion Model	Tabakoff
Morphology	Particle Transport fluid

Table 5 Parameters for CFX-Pre Sediment Data

Data	Value	Unit
Material	Quartz	
Density	2.65	g/cm^3
Diamter	0.1	Mm
Shape factor	1	
Flow rate	0.07	kg/s

Table 6 Parameters for CFX-Post Erosion Analysis

Paramater	Max value	Unit
Sediment Erosion	3.00E-07	kg/m^2s
Rate Density	0.3	mg/m^2s

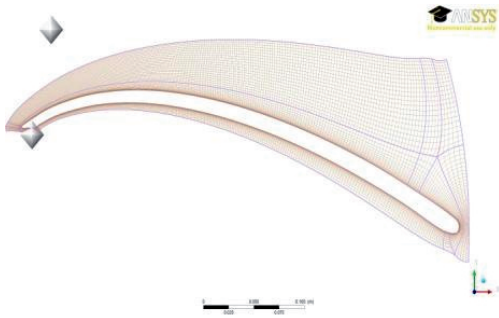

Fig. 7 TurboGrid ATM mesh

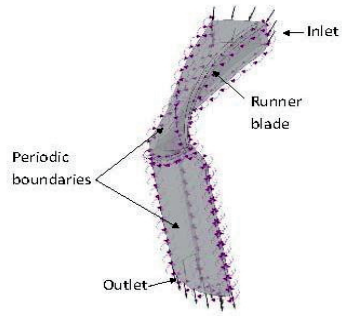

Fig. 8 Computational domain

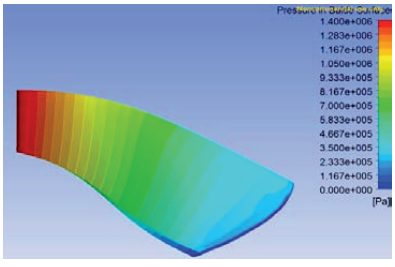

Fig. 9 Pressure distribution in pressure side of blade

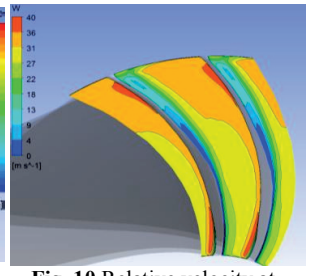

Fig. 10 Relative velocity at blade outlet

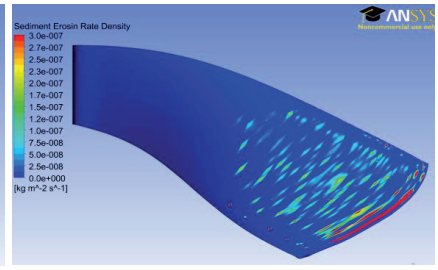

Fig. 11 Sediment erosin on reference runner blade

5. Results and discussions

Consequences of variation Beta distribution are evaluated from the design program Khoj and results are compared with that with CFD analysis. Effect of the variation on the erosion factor is of primary interest. However, the effects on other relevant design parameters are also observed. Fig 12 Shows effect of different shape of beta distribution on velocity distribution at center of the runner blade. It can be observed that the shape of beta distribution has a very strong effect on the velocity and energy

distribution along the blade surface from inlet to outlet. Shape 1 has a very low relative velocity up to its first 80 % of blade surface with high acceleration at the outlet section. This inherently will reduce erosion in balde surface as literatures predict that erosin is proportional to the third power of the relative velocity [6]. Shape 2 has high acceleration at the inlet section relative velocity at almost entire blade surface. Shape 3 has low acceleration at inlet portion and high in the middle. Similarly shape 4 has low acceleration at inlet portion and shape 5 has moderate acceleration at inlet portion and high in end portion.

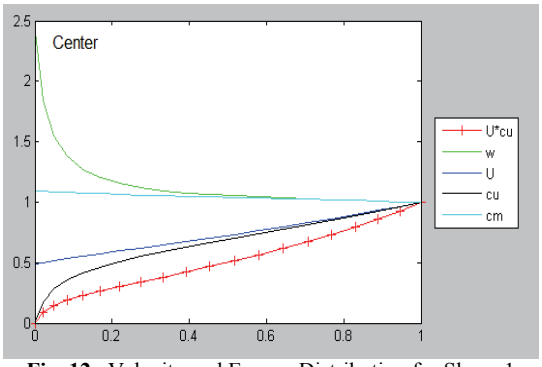

Fig. 12a Velocity and Energy Distribution for Shape 1

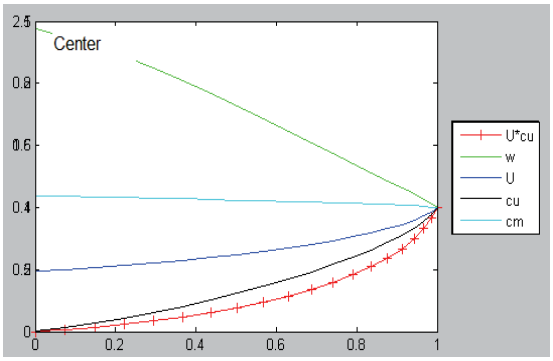

Fig. 12b Velocity and Energy Distribution for Shape 2

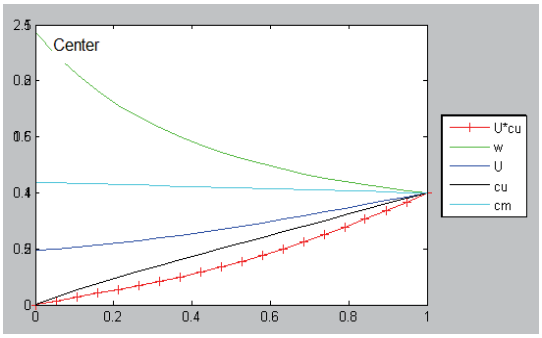

Fig. 12c Velocity and Energy Distribution for Shape 3

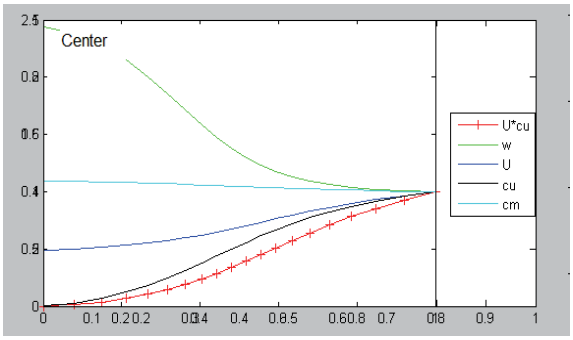

Fig. 12d Velocity and Energy Distribution for Shape 4

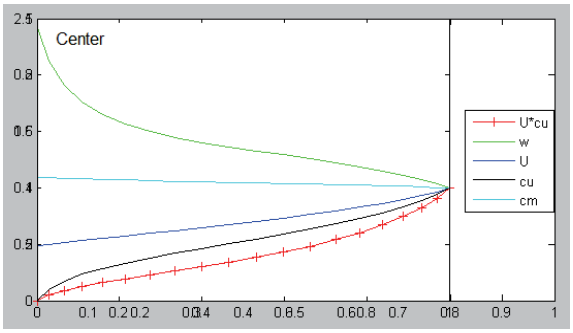

Fig. 12e Velocity and Energy Distribution for Shape 5

Fig. 13 shows the effect of different shape of beta distribution on erosion factor. It can be observed that the erosion factor for the different shapes of beta distribution has strong relation with the relative velocity. Shape with minimum area under relative velocity distribution has the least erosion factor and vice versa. The design program estimates that runner blade with beta distribution shape 1 has erosion factor of 0.67. This suggests 33% of reduction in erosion by changing the runner blade profile alone. Fig. 14 shows the effect of different shape of beta distribution on other design parameters as runner inlet diameter (D1), runner outlet diameter (D2) and submergence (hs). It can be observed that the shape of beta distribution has no effect on other main design parameters. The beta distribution affects only the profile of runner blade from inlet to outlet and hence alters relative velocity and blade loading.

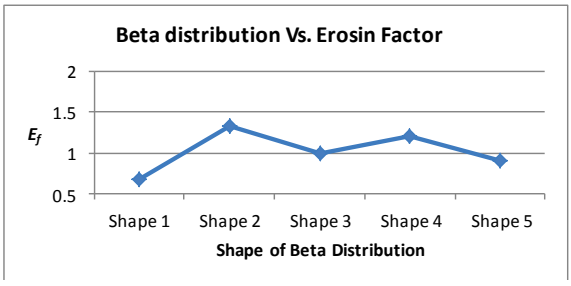

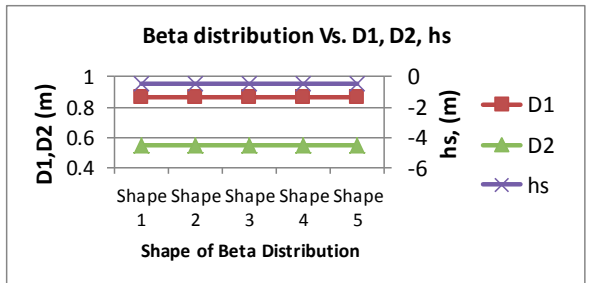

Fig. 13 Effect of Beta Distribution on Erosion Factor

Fig. 14 Effect of Beta Distribution on other design parameters

CFD analysis of runner design for the reference case with different shapes of beta distributions has been done in ANSYS CFX-13. It was observed that the results from CFD analysis matches with the predictions from the design program "Khoj". Fig. 15 shows contour of relative velocity at blade trailing edge from CFD analysis for different shapes of beta distribution. Fig 16 shows sediment erosion pattern on pressure side of runner blade surface. As predicted by the design program shape 1 has the lowest relative velocity at the runner outlet (Fig 15a) and also relatively lower erosion density (Fig 16 a).

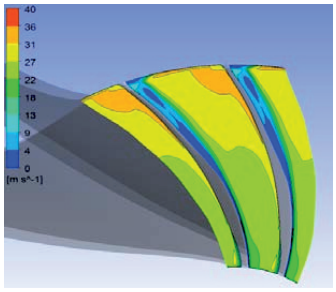

Fig. 15a Relative veocilty at blade trailing edge for Shape-1

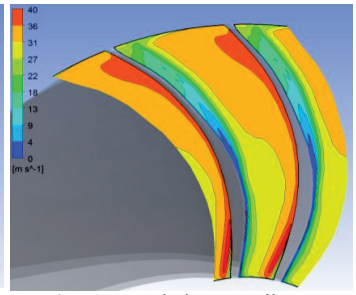

Fig. 15b Relative veocilty at blade trailing edge for Shape-2

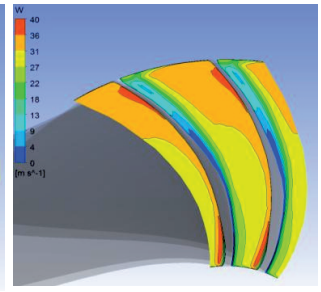

Fig. 15c Relative veocilty at blade trailing edge for Shape-3

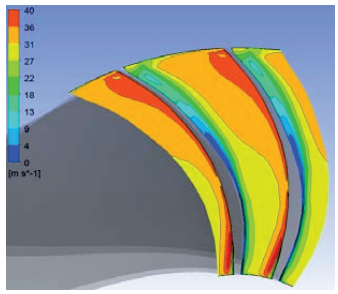

Fig. 15d Relative velocity at blade trailing edge for Shape-1

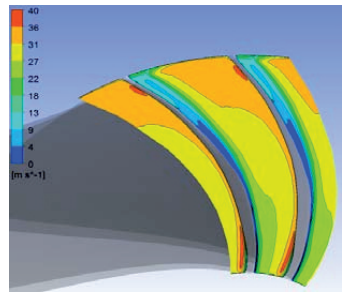

Fig. 15e Relative veocilty at blade trailing edge for Shape-1

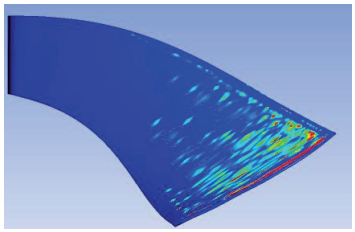

Fig. 16a Sediment erosion in blade surface for Shape-1

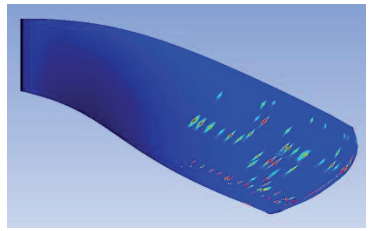

Fig. 16b Sediment erosion in blade surface for Shape-2

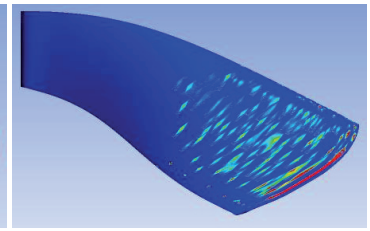

Fig. 16c Sediment erosion in blade surface for Shape-3

The hydraulic efficiency of the runner with the different shapes of beta distributions estimated by CFX has been presented in Table 7.

Table 7 Hydraulic efficiency for runners with different shapes of beta distributions

Parameters	Units	Shape-1	Shape-2	Shape-3	Shape-4	Shape-5
Total Efficiency	%	96.45	93.40	95.05	93.02	95.44

It can be observed that runner profile with beta distribution shape 1 has the highest efficiency and shape 2 and shape 3 have the lowest efficiencies. This result also matches with the trends of erosion factor for the different shapes of beta distribution predicted by the design program.

6. Summary and Conclusions

Computational tools can be used for optimizing designs of hydraulic turbines to suit the specific design needs. This study has been conducted to identify the runner blade profile to minimize the damage of sediment erosion in Francis turbines. A new design program to develop and modify design of Francis turbine and export designs for CFD analysis has been developed and implemented in this study. Results from the design program have been compared to that of CFD analysis. Runner profiles with minimum erosion without losing efficiency and inducing cavitation has been identified.

It has been found that Francis runners' blade profile can be optimized for minimum erosion by modifying the blade angle distribution, which effects the relative velocity distribution along the blade surface. It was also found that change in blade angel distribution has no effect on runner main dimensions and submergence. Both design program and CFD analysis concluded that the runner blade profile with higher blade loading at outlet has lower erosion rates and improved efficiency. It was estimated by the design program that 33% of erosion can be minimized by changing the blade angle distribution alone.

Results from this study can be useful for designing Francis turbines for sediment laden projects and also refurbishing runners damaged by sediment erosion in existing power plants. However, further investigation should be made to verify the findings of this study by means of some experimental verification.

Nomenclature

cm	Meridian component of absolute flow velocity, [m/s]	**cu**	Tangential component of absolute flow velocity, [m/s]
D1	Runner diameter at inlet (m)	**D2**	Runner diameter at outlet (m)
hs	Runner submergence to avoid cavitation (m)	**U**	Runner Peripheral velocity (m/s)
w	Runner relative velocity w.r.t. flow velocity (m/s)		

References

[1] B.S. Thapa, Kristine Gjosoeter, M. Eltvik, O.G. Dahlhaug, B. Thapa. Effects of turbine design parameters on sediment erosion of Francis runner. In *Proc. of 2nd International Conference on the Developments in Renewable Energy Technology,* Bangladesh, 5-7 January 2012.

[2] B. Thapa. Sand Erosion in Hydraulic Machinery. *Doctoral thesis at NTNU*, 2004.

[3] B.S. Thapa, B. Thapa, O.G. Dahlhaug. Center of Excellence at Kathmandu University for R&D and Test Certification of Hydraulic Turbine. In *Proc. of Int. Conf. on Hydraulic Efficiency Measurement*, India, 21-23 October 2010.

[4] M. Eltvik, G. Olimstad, E.C. Walseth. High Pressure Hydraulic Machinery. *NTNU publication*, 2009.

[5] B.S. Thapa M. Eltvik, K. Gjosoeter, O.G. Dahlhaug. Design optimization of Francis runner for sediment handling. In *Proc. of Fourth International Conference on Water Resources and Renewable Energy Development in Asia,* Thailand, 26-27 March 2012.

[6] B.S. Thapa, B. Thapa, O.G. Dahlhaug. Empirical modelling of sediment erosion in Francis turbines. Journal of Energy (2012), Vol. 41, Issue. 1, 386-391.

PART IV

Francis turbine design software KHOJ

Khoj - Francis Turbine Desing Software

KHOJ is a Francis turbine design software developed at the Waterpower Laboratory at the Norwegian University of Science and Technology(NTNU). The software is based on traditional turbine design theory and enables the user to design a Francis turbine. The software creates coordinate files which is requiered by CAD- and CFD-software if mechanical and hydraulic design evaluations is desirable. KHOJ is programmed in Matlab R2010a. The CAD files *.ibl are compatible with Pro/Engineer Wildefire 5.0 (Creo Parametric), and the CFD files *.curve works well with Ansys Workbench v.14.

Acknowledgements

Some Matlab files were found at the *Matlab Central* file exhange web page. Thanks to Shiying Zhao for posting the file uitabpanel.m, which creates the tabs in the figure. This file has been most helpful, and has made the program more user friendly. Thanks the author of the file surfature.m, Daniel Claxton. After struggeling with calculating the curvature of a curved surface for hours, finding this function was a relief.

Many PhD candidates and MSc. students have contributed to accomplish the program with theoretical discussions, matlab programming and debugging. Thanks to Kristine Gjøsæter, Biraj Singh Thapa, Peter Joachim Gogstad, Lars Frøyd, Grunde Olimstad and Mette Eltvik.

Main Dimensions

Designing a Francis turbine starts with calculating the main dimensions. These are based on hydraulic parameters like head H_e and flow rate Q, which are determined by the topography and hydrology of the power plant site. Traditionally, velocity triangles at the inlet and outlet of the runner, as shown in figure 2.1, are used in the design process.

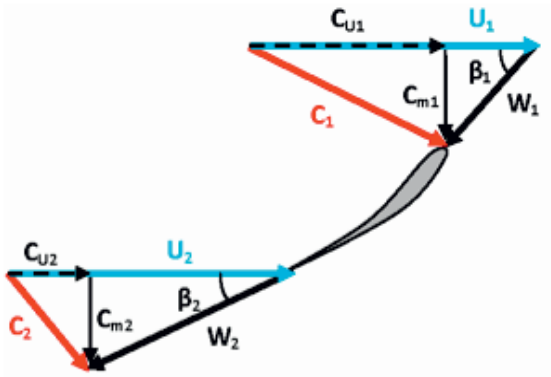

Figure 2.1: Velocity triangles

Dimensions at the runner outlet

As a first attempt, the outlet angle β_2 and peripheral speed U_2 can be chosen based on empirical data. Brekke[1]. states that for traditional Francis runners these values are usually found in the intervals

$$15^\circ < \beta_2 < 22^\circ \tag{2.1}$$
$$35m/s < U_2 < 42m/s \tag{2.2}$$

where β_2 takes lower values for higher heads and U_2 takes higher values for higher heads. The listed intervals should not be considered fixed limits, especially when designing turbines that will be operated in silty water. Measurements at Jhimruk show that the existing runners have a lower outlet peripheral speed than what traditionally is suggested.

At best efficiency point (BEP) no swirl in the draft tube has to be assumed. Hence the peripheral component of the absolute velocity C_{u2} equals zero, and the meridian component of the absolute velocity can be found from the velocity triangles.

$$C_{m2} = U_2 \tan \beta_2 \qquad [m/s] \tag{2.3}$$

With these parameters the outlet diameter D_2 can be calculated from continuity.

$$D_2 = \sqrt{\frac{4 \cdot Q}{\pi \cdot C_{m2}}} \qquad [m] \tag{2.4}$$

However, this is only strictly valid for infinitely thin blades: Due to the thickness of the blades at the trailing edge, the effective outlet area will be smaller. To find a rough estimate of the outlet area, the number of blades and the thickness of the blade at the trailing edge have to be decided or guessed. Because of the outlet blade angle β_2, the lost area must be approximated as the projection of the blade thickness in the outlet plane, as shown in figure 2.2.

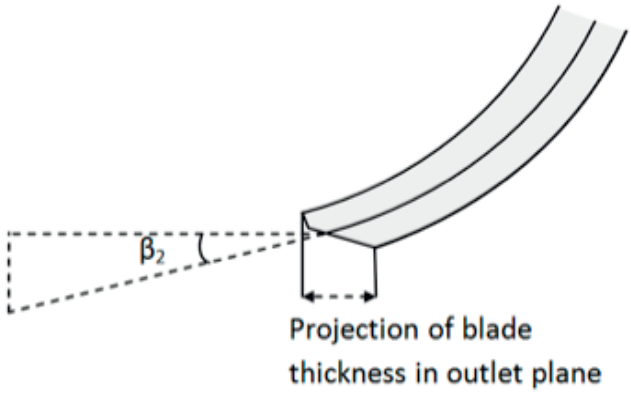

Figure 2.2: Projection of blade thickness into outlet plane

Choosing to keep the value of D_2, the C_{m2} value is recalculated taking the lost area into account. However, because β_2 is dependent on C_{m2}, a small iteration loop is necessary to fulfil the no swirl condition.

Knowing D_2, the rotational speed of the turbine can be calculated according to equation 2.5.

$$n = \frac{U_2 \cdot 60}{\pi D_2} \qquad [rpm] \tag{2.5}$$

The grid frequency f_{grid} in Norway is 50 Hz. In order to obtain a frequency of 50 Hz, the generator rotor has to pass 50 pole pairs in the stator per second.

$$Z_{poles} = \frac{f_{grid} \cdot 60}{n} \qquad [-] \tag{2.6}$$

The number of pole pairs has to be an integer. To fulfil this requirement, the rotational speed has to be corrected to the corresponding synchronous speed found by rearranging equation 2.6. The designer has to choose whether to round up or down the number of pole pairs. Choosing a higher Z_{poles} yields a larger and slower rotating turbine. According to Verma[2], the sediment erosion damage is less in large machines than in smaller ones. By selecting the speed of rotation one or two steps lower than for turbines operated in clean water, the machine size is increased. Thus the relative flow velocities are reduced with consequently less erosion damage.

Dimensions at runner inlet

When the outlet dimensions are set, the inlet of the runner is to be designed. The designer chooses the inlet peripheral speed, and with that the inlet diameter as well.

$$D_1 = \frac{U_1 \cdot 60}{n \cdot \pi} \qquad [m] \tag{2.7}$$

It is convenient to use *reduced values* in the design process because the reduced velocities are dimensionless. The reduced values are denoted by an underscore.

$$\underline{U}_1 = \frac{U_1}{\sqrt{2 \cdot g \cdot H_e}} \qquad [-] \tag{2.8}$$

The Euler equation is commonly used for turbine design, and is defined as shown in equation 2.9.

$$\eta_h = \frac{C_{u1} \cdot U_1 - C_{u2} \cdot U_2}{g \cdot H_e} \qquad [-] \tag{2.9}$$

By introducing reduced values and including the assumption of no swirl flow in the draft tube at BEP, the Euler turbine equation reduces to:

$$\eta_h = 2 \cdot \underline{U}_1 \cdot \underline{C}_{u1} \qquad [-] \tag{2.10}$$

It is common to assume a hydraulic efficiency η_h of 96 %.

In order to avoid back flow in the runner, an acceleration of the flow through the runner is desirable. Generally, ten percent is chosen, but this is up to the designer.

$$C_{m2} = (1 + \frac{Acc}{100}) \cdot C_{m1} \qquad [m/s] \tag{2.11}$$

The inlet area can now be found according to continuity.

$$C_{m1} \cdot A_1 = C_{m2} \cdot A_2 \tag{2.12}$$

As was done at the outlet, the runner blade thickness has to be accounted for also at the inlet. The inlet diameter is fixed due to equation 2.7, so the blade thickness will only affect the runner inlet height B_1, as shown in equation 2.13. By combining equations 2.11 and 2.12, the inlet height can be calculated as

$$B_1 = \frac{A_1}{\pi \cdot D_1 - Z_{blades} \cdot \frac{t_{LE}}{\sin \beta_1}} \qquad [m] \tag{2.13}$$

where β_1 is found from equation 2.14.

$$\tan \beta_1 = \frac{C_{m1}}{U_1 - C_{u1}} \qquad [-] \tag{2.14}$$

Submergence of the turbine

If the water pressure in the runner is lower than the vapor pressure, cavitation may occur. The impact of gas cavities collapsing close to the wall surface causes cavitation erosion. In order to avoid the water pressure to drop below the vapor pressure, the turbine can be submerged. The required level of submergence, expressed as Net Positive Suction Head (NPSH) depends on the main dimensions and the speed number ω of the runner. The speed number is a dimensionless expression for rotational speed at a given head at BEP.

$$\Omega = \underline{\omega} \cdot \sqrt{\underline{^*Q}} \qquad [-] \tag{2.15}$$

Knowing the speed number, the required NPSH can be calculated as

$$\mathrm{NPSH}_{\mathrm{required}} = a\frac{C_{m2}^2}{2g} + b\frac{U_2^2}{2g} \qquad [mWc] \tag{2.16}$$

where the parameters *a* and *b* are empirical constants, and, according to Brekke, dependent on the speed number.

$$\begin{array}{ll} \Omega < 0.55 & \text{gives } a{=}1.12 \text{ and } b{=}0.055 \\ \Omega > 0.55 & \text{gives } a{=}1.12 \text{ and } b{=}0.1{\cdot}\Omega \end{array}$$

NPSH has to fulfil the following requirement to avoid cavitation

$$\mathrm{NPSH}_{\mathrm{required}} < h_{atm} - h_{va} - H_s \qquad [mWc] \tag{2.17}$$

where

h_{atm} - atmospherically pressure, 1 atm = 10.3 mWc
h_{atm} - vapor pressure
H_s - submerging of the turbine. A negative value of H_s implies that the turbine is set below tail water level.

1. Hermod Brekke. *Pumper og turbiner.* Waterpower Laboratory NTNU, 2003. ↩

2. M.C. Verma. Silt friendly design of turbine and other under water components. In *Silting Problems in Hydro Power Plants*, New Dehli, October 1999. Central Board of Irrigation and Power. ↩

Files related to the '*Main dimensions*' tab

- **MainDim.m**
- **Checkvalues.m**
- **MainDimensions.mat**

Functions related to the '*Main dimensions*' tab

In **MainDim.m**

MainDim	Runs the *MakeMainItems* function
MakeMainItems	generates all 'GUI' items on the Man dimesions tab
InitaliseMainDim	Is only executed for new projects. Sets the value of all variables in the Main dimesions tab according to the file MainDimesions.mat if it exists, or to a set of backup data if the file does not exist
HeadEditCallback	Runs the *CheckValues* function
FlowEditCallback	Runs the *CheckValues* function
U1redSliderCallback	Sets the textbox to the corresponding value of the slider, and runs the *CheckValues* function
U1redEditCallback	Sets the slider to the corresponding value of the textbox, and runs the *CheckValues* function
D2EditCallback	Runs the *CheckValues* function
ZpEditCallback	Runs the *CheckValues* function
B1EditCallback	Runs the *CheckValues* function

In **Checkvalues.m**

CheckValues	Calculates the main dimesions according to the theory listed above on this page. Lists the vital values in the bottom table and plots the velocity diagrams.

No functions in **MainDimensions.mat**.

Axial view

The runner axial view is decided by the height of the shroud, denoted *b*, the runner shroud contour and the trailing edge contour.

After setting the height *b*, the shroud contour has to be set to the desired shape. Subsequently, the shape of the trailing edge contour has to be decided.

Based on the inlet distribution and the chosen contour of the streamline along the shroud, the rest of the streamlines can be determined. A point *i* on streamline *j+1* is found by drawing a line between the points *(i+1 , j)* and *(i-1 , j)*. Then the new point, *(i , j+1)*, is placed on an axis orthogonal to this line going through point *(i , j)*, as shown in figure 3.1.

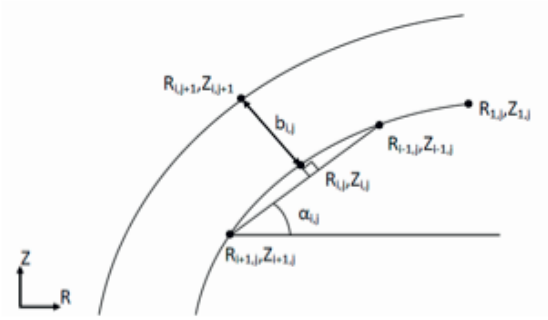

Figure 3.1: Determining a new point in the axial view.
Adapted from Eltvik et al.[1]

From figure 3.1 the following expressions can be derived.

$$\alpha_{i,j} = \tan^{-1}\left(\frac{Z_{i-1,j} - Z_{i+1,j}}{R_{i-1,j} - R_{i+1,j}}\right) \qquad [-] \tag{3.1}$$

$$r_{i,j} = \frac{R_{i,j} + R_{i,j+1}}{2} \qquad [m] \tag{3.2}$$

$$A_{i,j} = 2\pi \cdot r_{i,j} \cdot b_{i,j} \qquad [m] \tag{3.3}$$

$$b_{i,j} = \frac{R_{i,j+1} - R_{i,j}}{\sin \alpha_{i,j}} \qquad [m] \tag{3.4}$$

Combining equations 3.1-3.4 yields:

$$A_{i,j} = 2\pi\left(\frac{R_{i,j+1} + R_{i,j}}{2}\right)\left(\frac{R_{i,j+1} - R_{i,j}}{\sin \alpha_{i,j}}\right) = \frac{\pi}{\sin \alpha_{i,j}}(R_{i,j+1}^2 - R_{i,j}^2) \quad [m^2] \tag{3.5}$$

Equation 3.5 can be rearranged to:

$$R_{i,j+1} = \sqrt{R_{i,j}^2 + \frac{A_{i,j} \cdot \sin \alpha_{i,j}}{\pi}} \qquad [m] \tag{3.6}$$

Finally, the Z coordinate can be found:

$$Z_{i,j+1} = Z_{i,j} - b_{i,j} \cdot \cos \alpha_{i,j} \qquad [m] \tag{3.7}$$

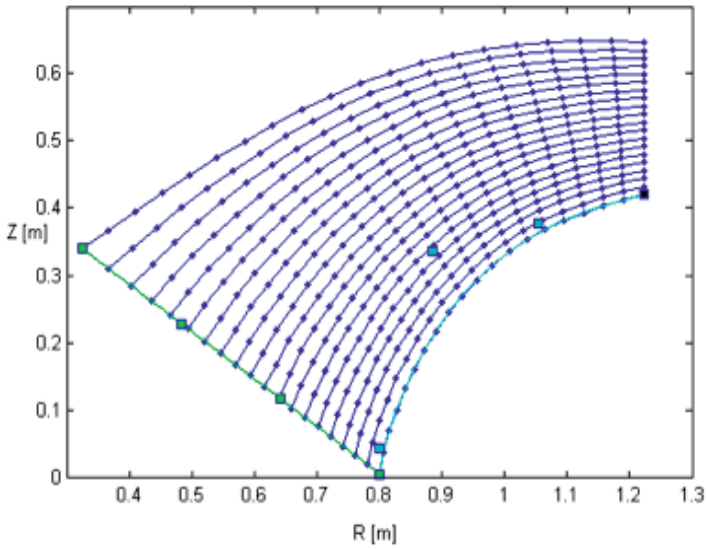

Figure 3.2: Axial view

A common issue when defining the first streamline along the shroud is that the streamlines close to the hub curve upwards at the inlet, instead of going in a straight line, before bending down towards the outlet. This is an undesirable design feature that must be corrected before proceeding with the design. In *Khoj*, this is done by moving the control points on the shroud contour line. or by increasing the height difference b.

1. Mette Eltvik et al. *High pressure hydraulic machinery*. Waterpower Laboratory NTNU, 2009. ↩

Files related to the '*Axial view*' tab

- **Axialview.m**
- **calcAV.m**
- **InitialiseAV.m**
- **plotAxialView.m**
- **UpdateAxial.m**

Functions related to the '*Axial view*' tab

In **AxialView.m**

AxialView	Generates all 'GUI' items on the Man dimesions tab
ResetShroudCallback	Resets the shroud contour to the initial shape for the current value of *b*
ResetOutletCallback	Resets the trailing edge contour to the initial shape for the current value of *b*
nsEditCallback	Sets the position of the slider to the corresponding number of streamlines.
nsSliderCallback	Sets the number of streamlines to the value corresponding to the slider position.
bEditCallback	Sets the position of the slider to the corresponding value of *b*.
bSliderCallback	Sets the value of *b* corresponding to the slider position.

In **calcAV.m**

calcAV	Calculates the R and Z coordinates for the axial view according to the theory (see the above section).

In **IntialiseAV.m**

IntialiseAV	Sets the inital shape of the shroud contour based on the inlet and outlet diameter calculated in the main dimensions tab. This file is only used the first time the axial view tab is opened for each run and if there has been made changes to the main dimensions.

In **plotAxialView.m**

plotAxialView	Plots the axial view.
startdragfcnaxials	Enables moving the control points using the mouse. Finds the coordinates for the chosen point. Valid for the shroud contour control points.
draggingfcnaxials	Tracks the chosen point when it is moved around as long as the left mouse button is pressed. Valid for the shroud contour control points.
startdragfcnaxialo	Enables moving the control points using the mouse. Finds the coordinates for the chosen point. Valid for the trailing edge contour control points.

draggingfcnaxialo	Tracks the chosen point when it is moved around as long as the left mouse button is pressed. Valid for the trailing edge contour control points.
stopdragfcnaxial	Saves the coordintes for the chosen point when the designer lets the left mouse button go. Valid for both the shroud and trailoing edge contour.

In **UpdateAxial.m**

UpdateAxial	Executed when entering the Axial view tab if there has been cahnges to the main dimensions in addition to the first time the axial view tab is opened.

Distributions

In order to smplify the design process of going from the axial view to the radial view, a *GH*-plane is defined. *G* is the length of the streamline in the axial plane and *H* is the length of a streamline in the radial plane.

The values of *G* is calculated directly from *R* and *Z* from the axial view. *G* equals zero at the inlet.

$$G_{i,1} = G_{i-1,1} + \sqrt{(R_{i-1,1} - R_{i,1})^2 + (Z_{i-1,1} - Z_{i,1})^2} \qquad [m] \qquad (4.1)$$

Calculating th values of *H* is more demanding, as they are dependent on the distribution of the blad angle, β. The blade angle is closely linked to the energy distribution along the blade. The energy distribution is often referred to as the U^*C_u distribution, and describes the transformation from pressure energy to rotational energy aalong the blade. The relation between the energy distribution and the blade angle β is governed by the equation 4.2.

$$\beta = \arctan(\frac{C_m}{U - C_u}) \qquad [^\circ] \qquad (4.2)$$

The blade angles at the inlet and outlet are known from the velocity triangles. The distribution in between has to be determined. This can be done in two ways; by choosing the U^*C_u distribution and then calculate the β distribution or choosing the β distribution and then calculate the U^*C_u distribution. Choosing the blade angle distribution gives the designer full control of the design outcome. Choosing the energy distribution and subsequently calculating the blade angle distribution, gives the advantage of full control over the energy distribution, but no control over the blade angle distribution which can lead to some strange designs. A good practice is to control the corresponding distribution afterwards, either if the energy or the blade angle distribution is chosen. A distribution must be specified for each streamline, but you could of course specify the same distribution for all streamlines. The same U^*C_u distribution for all streamlines will give a different distribution of the blade angle for each streamline. Likewise, equal blade angle distribution for all streamlines will give a different energy distribution for each streamline. the corresponding distributions are calculated by equation 4.2.

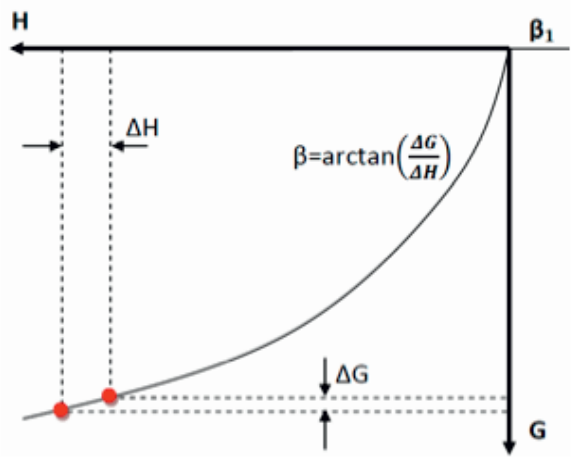

Figure 4.1: Definition of *GH*-plane. Adapted from Eltvik et al.[1]

C_m is the velocity along the streamline, and is found using the continuity equation. The pherpheral velocity U is dependent on the radius R and the angular velocity ω and is thus known for each point.

$$U = \omega \cdot R \qquad [m/s] \tag{4.3}$$

Next the values of ΔH can be obtained using equation 4.4, defined as shown in figure 4.1.

$$\Delta H = \frac{\Delta G}{\tan \beta} \qquad [m] \tag{4.4}$$

When this is performed for each streamline, the *G-H* plane can plotted. The radial view is established using equation 4.5, which is defined according to figure 4.2

$$d\theta = \frac{\Delta H}{R} \qquad [rad] \tag{4.5}$$

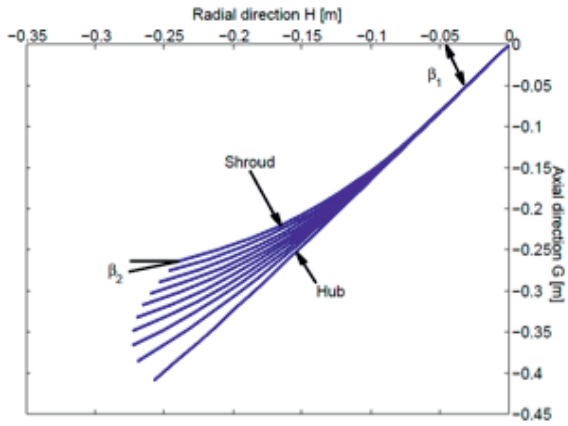

Figure 4.2: *GH*-plane.

1. Mette Eltvik et al. *High pressure hydraulic machinery*. Waterpower Laboratory NTNU, 2009. ↩

Files related to the '*Distribution*' tab

- **plotDistribution.m**

Functions related to the '*Distributions*' tab

In file **Distributions.m**

centerMenuCallback	Executed when changing between energy distribution and blade angle distribution. Runs *plotDistributions.m*
ResetCallback	Resets the energy/blade angle distribution figure to original values

In file **plotDistribution.m**

plotDistribution	Plots the figures in the Distributions tab and executes either *EnergyDistribution* or *BetaDistribution* depending on which option the user has chosen.
EnergyDistribution	Plots the energy distribution in the first figure
BetaDistribution	Plots the blade angle distribution in the first figure

Radial view

From the distributions tab the length of the streamline in the radial view, denoted H, is known. Knowing the radial component from the axial view, the radial view can be established according to figure 5.1.

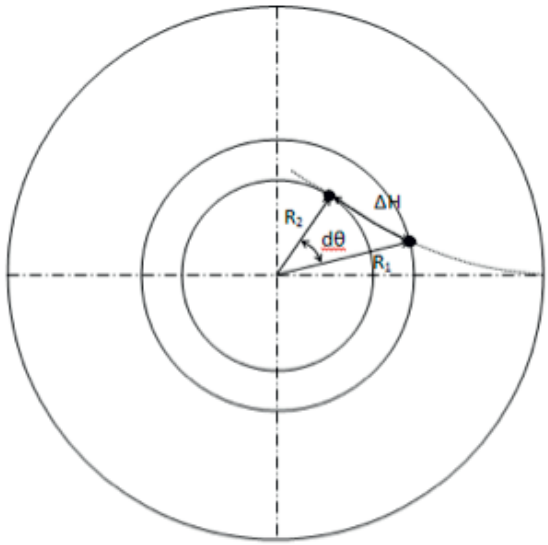

Figure 5.1: Definition of dθ. Distance ΔH and angle dθ is somewhat exaggerated.

$$d\theta = \cos^{-1}\left(\frac{R_2^2 + R_1^2 - \Delta H^2}{2 \cdot R_1 \cdot R_2}\right) \qquad [rad] \tag{5.1}$$

Calculating dθ should be done using the law of cosine, as shown in equation 5.1, but this formula produces high round-off errors in floating point calculations if the triangle is very acute, i.e., if ΔH is small relative to R_1 and R_2 or dθ is small compared to 1. It is even possible to obtain a result slightly greater than one for the cosine of an angle, yielding problems with imaginary numbers for further calculations. Thus is equation 5.2 used instead but this is only valid for small values of ΔH, such that

$$\sin d\theta \approx d\theta = \frac{\Delta H}{R_1} \qquad [rad] \tag{5.2}$$

This gives a radial view of the runner as shown in figure 5.2.

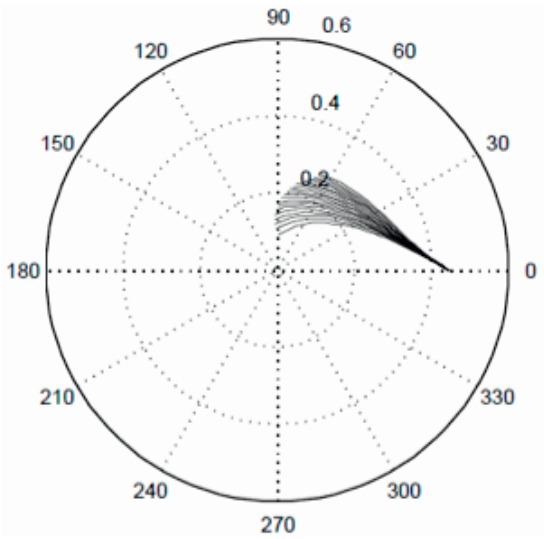

Figure 5.2: Radial view

Blade leaning

Blade leaning is an important means for balancing the pressure distribution on the runner blades. By leaning the inlet of the runner blades, local high or low pressure zones can be shifted towards the hub or shroud both at inlet and outlet. In Khoj, the blade leaning is implemented as an angular displacement of the streamlines. The designer can choose whether to rotate the entire streamline, as shown in fingure 5.4, or to keep the trailing end of the blade fixed and apply a gradual blade leaning from the chosen angular displacement at the inlet to no leaning at the trailing edge, as shown in figure 5.5. With the first method, the shape of the streamlines calculated initially without any blade leaning are kept, but the entire streamlnie is rotated around the runner's axis of rotation. This gives both constant inlet and outlet angles, but alters the pressure on the blade. By choosing the latter method, the streamlines are altered from the initial shape, giving a different inlet angle than what was calculated in the main dimensions tab. This method does however make it possible to shift pressure zones at the inlet and still keep the trailing end of the blade as initially designed, which is particularly interesting if the pressure distribution is good at the trailing end but needs to be altered at the inlet.

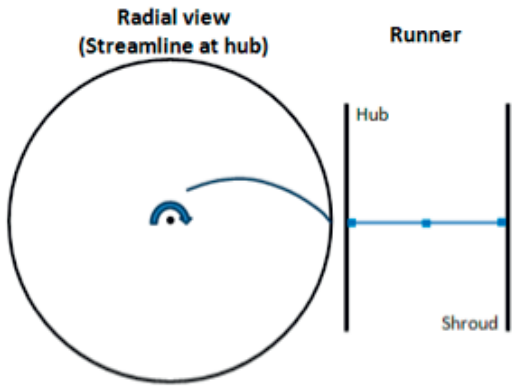

Figure 5.3: Streamline before including blade leaning

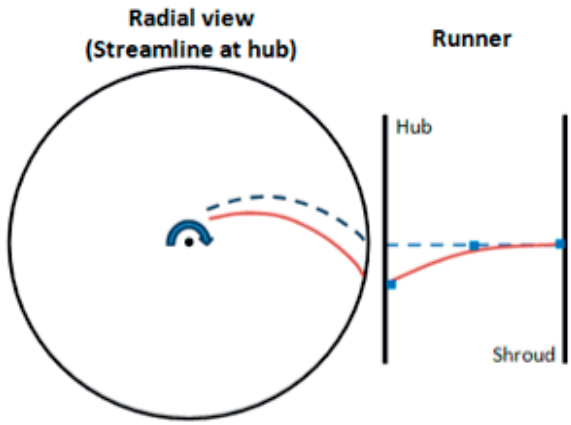

Figure 5.4: Blade leaning option 1; rotate entire streamline around turbine rotational axis

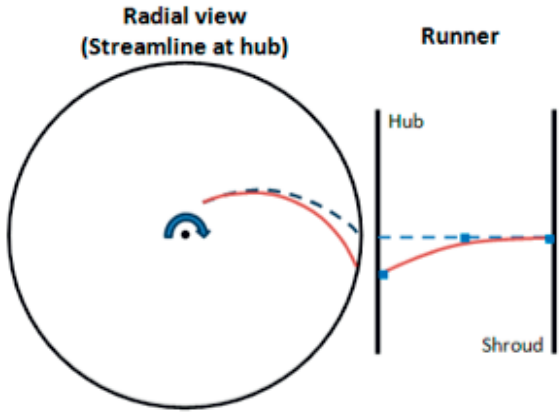

Figure 5.5: Blade leaning option 2; gradual leaning from max at the blade inlet to no leaning at the trailing end

CFD analyses are necessary to map the pressure distribution on the runner blades. It is possible to get a fairly good picture of the pressure distribution from an inviscid CFD analysis performed on a coarse mesh, which will save both time and CPU.

1. Mette Eltvik et al. *High pressure hydraulic machinery*. Waterpower Laboratory NTNU, 2009. ↩

Files related to the '*Radial view*' tab

- **RadialView.m**
- **BladeLeaning.m**
- **InitialiseBL.m**
- **surfature.m**
- **erosionarea.m**
- **plotBG_3D.m**
- **plotUCu3D.m**
- **UpdateRadial.m**

Functions related to the '*Radial view*' tab

In **RadialView.m**

RadialView	Generates all 'GUI' items on the Radial view tab
ResetCallback	Resets the blade leaning graph to no blade leaning. Runs function *Bladeleaning* to update the corresponding plots.
NoBladesCallback	Sets the number of blades to the chosen value, and runs the function *plotBG_3D*.
ColormapBladesCallback	Runs the function *plotBG_3D* to get the chosen colormap on the blades.

In **BladeLeaning.m**

BladeLeaning	Calculates the radial view of the blade with blade leaning. Does also clacuate an estimate of the number of blades required to avoid backflow at the runner inlet, but this estimate should be controlled with CFD analyses of part load operation. Does also run the functions *plotBG_3D* and *plotUCu3D*.
startdragfcnradial	Enables moving the control points for the blade leaning with the mouse.
draggingfcnradial	Thracks the chosen point when it is moved around. Is only active when the left mouse button is pushed in.
stopdragfcnradial	Saves the coordintes for the chosen point when the designer releases he left mouse button. Then the function *BladeLeaning* is executed.

In **surfature.m**

surfature	a

In **erosionarea.m**

erosionarea	b

In **InitialiseBL.m**

IntialiseBL	Plots the hub and shroud lines in the blade leaning figure in axddition to the dashed line indicating no blade leaning. Does also set the title and xlabel of the graph.

In **plotBG_3D.m**

plotBG_3D	Plots the runner blade surface (without thickness) and the full runner with the designers choise of numbers of blades. Colormap on both single blade and runner is default set to grey. Colormap for relative velocity, surface curvature and erosion tendecy as a function of relative velocity is also available.

In **plotUCu3D.m**

plotUCu3D	The $U{\cdot}C_u$ distribution plotted in the distributions tab is the $U{\cdot}C_u$ distribution along the 2D streamline in the axial view, also denoted *G*. When having established the 3D blade, it is possible to find the $U{\cdot}C_u$ distribution along the 3D streamline. By including blade leaning with a gradual leaning from inlet to trailing end, the $U{\cdot}C_u$ distribution along the 3D streamilne is altered. This function calculates the new $U{\cdot}C_u$ distribution along the 3D streamline withand without blade leaning and plots it for the hub, shroud and the middle of the channel, all in absolute values unlike in the distributions tab where the plots are relative to the inlet value.

In **UpdateRadial.m**

UpdateRadial	Calculates the theta components of the radial view for a runner with straight inlet (no blade leaning). Runs function *BladeLeaning*.

Blade thickness

From the radial view tab, the 3D geometry of the runner blade is found, but only as an infinitely thin surface. Having also decided the number of blades decired in the runner, the required thickness of each blade can be determined. The thickness of the runner blade has to be large enough to withstand the hydraulic forces which it is exposed to, being the dynamic pressure pulsations and the static pressure difference between the pressure and suction side of the blade.

Ideally, a full stress analysis would be desirable in order to determine the blade thickness. However, as the geometry are quite complex, a simplified stress analysis is performed to calculate a conservative estimate of the required blade thickness. This value will be a good first guess, and should be corrected after having performed a full Final Element Method (FEM) analysis of the blade.

The simplified stress analysis are performed according to [1]. Modelling the blade as a straight beam between hub and shroud, calssical mechanica are applicable. The hub is considered to be rigid, while the shroud is assumed to be flexible in torsion with respect to the hub. This means that the blade can be modelled as a beam that is clamped at the hub side and guided at the shroud side, as shown in figure 6.1.

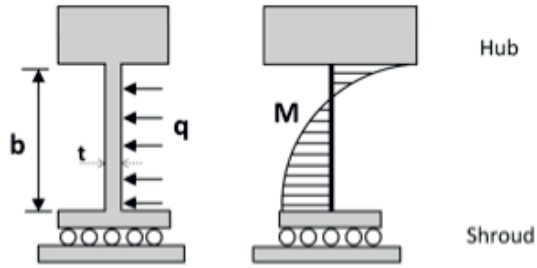

Figure 6.1: Blade modeled as a straight beam between hub and shroud with equally distributed load (left) and corresponding bending moment (right).

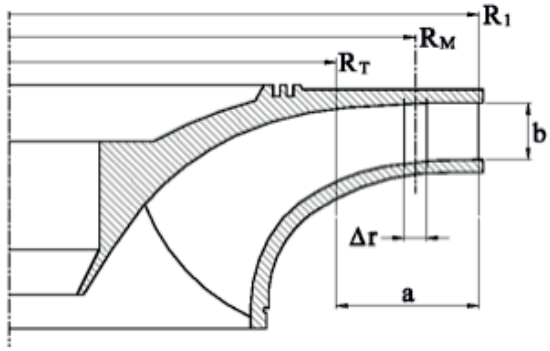

Figure 6.2: Definition of a, b, Δr and R_M

Assuming equally distributed load, $q=\Delta r \cdot \Delta p$, the bending moment, M, is found in mechanical engineering formula books as

$$M = q\frac{b^2}{3} \qquad [Nm] \tag{6.1}$$

The maximum bending stress, σ_{max} is

$$\sigma_{max} = \frac{M}{I}\frac{t}{2} \qquad [Pa] \tag{6.2}$$

with blade thickness, t, and second area moment of inertia, I,

$$I = \frac{\Delta r \cdot t^3}{12} \qquad [m^4] \tag{6.3}$$

Rearranging equations 6.1 - 6.3 gives the minimum blade thikness at the outlet as

$$t_{min} = \sqrt{\frac{\Delta p \cdot 2 \cdot b^2}{\sigma_{max}}} \qquad [m] \tag{6.4}$$

The pressure difference Δp is calculated from the torque on the runner. The length a defined in figure 6.2 is an imaginary length where it is assumed that the entire torque os transferred from the flow to the blade. The value of a has to be chosen, but for the analysis implemented in Khoj, the value of a is set to $1.5 \cdot b$ as sugested by Brekke[1].

$$M_{\text{runner}} = Z_r \cdot a \cdot b \cdot R_M \cdot \Delta p = \frac{P}{\omega} \qquad [Nm] \tag{6.5}$$

$$\Delta p = \frac{P}{Z_r \cdot a \cdot b \cdot R_M \cdot \omega} \qquad [Pa] \tag{6.6}$$

Regarding the thickness distribution from leading to trailing edge of the balde, state of the art is to keep the inlet thickness along the first half lenght of the streamline, before norrowing it in towards the trailing edge. At the trailing edge the blade should not be thinner than 6 mm, and not less than 2 mm at the 30 degree cut end. However, for larger tubines the trailing edge has to be thicker to avoid early fatigue damage.

The method described here is intended as a first guess of the blade inlet thickness, and should ideally be a conservative guess, such that further analysis shold require thinner blades, not thicker. However, other methods for determining a minimum inlet thickness has proven to give more conservative values. Thus a study should be conducted to check if the described method really is conservative, or if a more conservative method is desireable. To do this, FEM analysis is necessary.

Leading and trailing edge

The shape of the trailing edge is fixed as shown in figure 6.3, but with a minimum value of R of 3 mm due to fabrication constraints. This shape is chosen to minimize the amplitude of the von Karman vortices behind the trailing edge. For the leading edge the shape presented in the figure is dependent on the values of a_{ps} and a_{ss}. As default values, a_{ps} is set equal to R and a_{ss} is set equal to 3·R, based on traditional designs. It is however possible for the designer to change the leading edge shape by altering those two values.

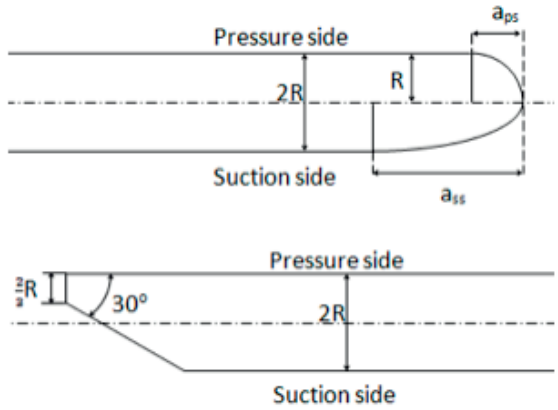

Figure 6.3: Shape of leading and trailing edge

1. Hermod Brekke *Konstruksjon av pumper og turbiner, sec 3.6 (in Norwegian)*. Waterpower Laboratory NTNU, 2000. ↩

Files related to the '*Blade thickness*' tab

- **bladethickness.m**
- **thicknessBT.m**
- **InitialiseBT.m**
- **plotBT.m**
- **plotthicknessBT.m**
- **leading.m**
- **trailing.m**
- **UpdateThickness.m**

Functions related to the '*Radial view*' tab

In **bladethickness.m**

bladethickness	Runs *MakeBTitems*.
MakeBTitems	Generates all 'GUI' items on the Blade thickness tab
ResetCallback	Resets the blade thickness distribution to having a constant thickness from leading edge to 50 % along the blade. Then tapering the blade thikcness to the set leading edge thickness. Subsequently runs *plotthicknessBT*
TleCallback	.
TteCallback	.
aSSSliderCallback	.
aSSEditCallback	.
aPSSliderCallback	.
aPSEditCallback	.

In **thicknessBT.m**

thicknessBT	Adds thickness to the infinitely thin blade generated in the Radial view tab.

In **InitialiseBT.m**

IntialiseBT	Sets the title and the ylabel to the blade thickness distribution figure. Also plots an initial blade thickness distribution based on the thicknesses chosen for last design.

In **plotBT.m**

plotBT	Plots the blade thickness distribution plot with control points.
startdragfcnbt	.
draggingfcnbt	.
dragfcnbtstop	.

In **plotthicknessBT.m**

plotthicknessBT	Plots the 3D blade with thickness. Subsequently runs *PlotBT*.

In **leading.m**

leading	Designs the leading edge of the runner blade according to the values of a_{ps} and a_{ss}, which are chosen by the program user within some preset intervals. The preset intervals are based on the chosen leading edge thickness.

In **trailing.m**

trailing	Designs the trailing edge of the runner blade according to the shape plotted in the lower left graph on the tab. The cut off angle is 30^{o}.

In **Updatethickness.m**

UpdateThickness	.
aBG	.

Labyrinths

The upper and lower labyrinths of a Francis turbine should be located such that the hydrau forces will produce a resultant force acting towards the draft tube. Theory for balancing th turbine by placing of the labyrinths is taken from [1].

$$M = q\frac{b^2}{3} \qquad [Nm] \tag{7.1}$$

1. Hermod Brekke. *Pumper og turbiner*. Waterpower Laboratory NTNU, 2003. ↩

Files related to the '*Labyrinths*' tab

- **labyrinth.m**
- **plotLabyrinth.m**
- **UpdateLabyrinths.m**

Functions related to the '*Labyrinths*' tab

In **labyrinth.m**

labyrinth	Generates all 'GUI' items on the Labyrinths tab
LabEditCallback	Runs *plotLabyrinth* for the new value of T_{shroud}.

In **plotLabyrinth.m**

plotLabyrinth	Calculates the position of the upper labyrinth based on the theory explained above. The position of the lower labyrinth affects the position of the upper labyrinth. For now, the turbine is taken as a vertical axis turbine with a constant weight of 1000 kg independent of unit size. the desired resultant force is set to 1000 N, also independent of size. These variables should be included as user inut for future verisons of the program. Subsequently a simple layout is scetched. Note that this is not real sizes and shapes, and proper drawings should be made with use of CAD tools. In addition, the suggested position of the upper labyrinth should be taken as a first guess for CAD drawings, and further be adjusted based on results from FE and FSI analysis.

In **UpdateLabyrinths.m**

UpdateRadial	Assigns important values from the Blade thickness tab to the 'saved' struct. Saves the keading and trailing edge thickness in the file Thickness.mat for use for next design. Plots one streamline of the runner on the figure in the Guide vanes tab. Subsequently runs *plotLabyrinth*.

Guide vanes, stay vanes and spiral casing

Having designed the runner, the guide vanes stay vanes and spiral casing has to be designed. This process starts with designing the guide vanes. Then the stay vanes and spiral casing can be designed jointly, as the stay vanes design are dependent on the spiral casing dimensions. [1].

Guide Vanes

The number of guide vanes has to be chosen. To minimize the extent of the pressure pulsations that occur when runner vanes pass the guide vanes, the number of guide vanes has to conform to equation 8.1.

$$\alpha_{i,j} = \tan^{-1}\left(\frac{Z_{i-1,j} - Z_{i+1,j}}{R_{i-1,j} - R_{i+1,j}}\right) \qquad [-] \qquad (8.1)$$

To have sufficient distance between the guide vane and the runner, it is common to design the guide vanes outlet diameter at rated power approximately five percent larger than the runner inlet diameter. The gap between the guide vane outlet and the runner inlet is less at full power, and it should be controlled that there is sufficient clearance also at this guide vane position.

As flow in the gap between the guide vane outlet and the runner inlet is unaffected, the free vortex theory is used to find the tangential component of the absolute velocity at the trailing edge of the guide vanes.

$$\alpha_{i,j} = \tan^{-1}\left(\frac{Z_{i-1,j} - Z_{i+1,j}}{R_{i-1,j} - R_{i+1,j}}\right) \qquad [-] \qquad (8.2)$$

The meridional component is found using continuity and the guide vane outlet angle is found from the velocity triangle.

$$\alpha_{i,j} = \tan^{-1}\left(\frac{Z_{i-1,j} - Z_{i+1,j}}{R_{i-1,j} - R_{i+1,j}}\right) \qquad [-] \qquad (8.3)$$

Next, the radial position of the guide vane axis, r_0, has to be determined. When r_0 is known, the length from the trailing edge to the axis of the guide vane, L_0, is found from the law of cosine.

The length of the guide vane is dependent on the number of vanes, as the vanes have to overlap in the closed position. This is to avoid the vane from being able to rotate full circle. It is common to have an overlap with a cover factor, K_{fc}, of approximately 10 - 15 percent [3]. With few vanes, each vane has to be longer. A long vane guides the flow better than a short one, but it also accounts for larger friction losses. Thus the choice of number of guide vanes should be carefully considered.

$$M = q\frac{b^2}{3} \qquad [Nm] \tag{8.4}$$

The guide vane axis should be located somewhere between the middle and three quarters of the vane length upstream from the trailing edge. It is important that both the overlap and axis location criteria are satisfied. The guide vane inlet diameter can now be found using the law of cosine.

To decrease the flow losses in the guide vane cascade, it is desirable to shape the vane as an airfoil. Smooth and symmetrical NACA profiles are often chosen.

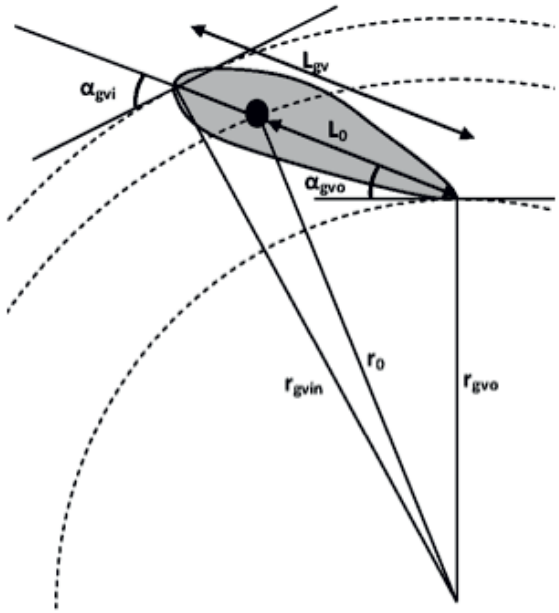

Figure 8.1: Geometry of a guide vane.

Stay Vanes

The stay vanes are designed to have no hydraulic effect, and are present in the turbine cascade just to keep the spiral casing together. Thus the stay vanes have to withstand the maximum hydraulic force acting on the spiral casing.

The shape of the stay vanes follows a free vortex. The outlet diameter is usually chosen 2 percent larger than the guide vane inlet diameter. The design process requires the designer to choose a stay vane inlet diameter. Then the length of the vane can be found, as the length of a streamline following the path of the free vortex from stay vane inlet to stay vane outlet.

The maximum force acting on the spiral casing is the maximum pressure times the area on which the pressure acts. The effective area of the spiral casing and the stay vanes is difficult to determine. As a simplification, the spiral casing and the stay vanes are modeled as an annulus with constant inner and outer diameter.

$$M = q\frac{b^2}{3} \qquad [Nm] \tag{8.5}$$

$$M = q\frac{b^2}{3} \qquad [Nm] \tag{8.6}$$

The maximum pressure acting on the area of the spiral casing occurs if the turbine running at full power is suddenly shut down. This will cause large pressure pulsations, known as the water hammer. The water hammer and the static pressure caused by the head difference give the dimensioning pressure.

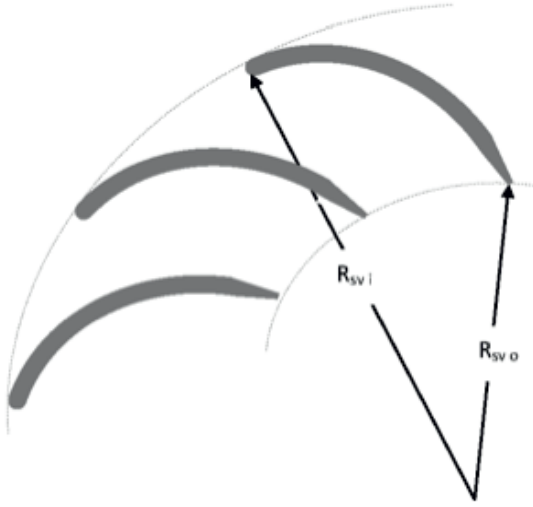

Figure 8.2: Stay vanes.

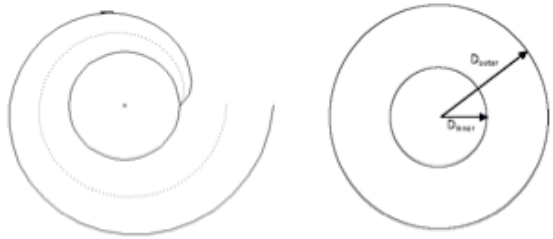

Figure 8.3: Traditional spiral casing and simplified annulus for calculating purposes.

$$M = q\frac{b^2}{3} \qquad [Nm] \tag{8.7}$$

Then the required cross sectional area of the stay vane can be found with maximum bending stress for steel, σ_{max}, equal to 100 MPa. Subsequently the required thickness is calculated.

$$M = q\frac{b^2}{3} \qquad [Nm] \tag{8.8}$$

$$M = q\frac{b^2}{3} \qquad [Nm] \tag{8.9}$$

Spiral Casing

The purpose of the spiral casing is to distribute the flow evenly around the runner. Thus the cross section area of the spiral casing has to decrease downstream, as parts of the water flows through the stay vanes in each section.

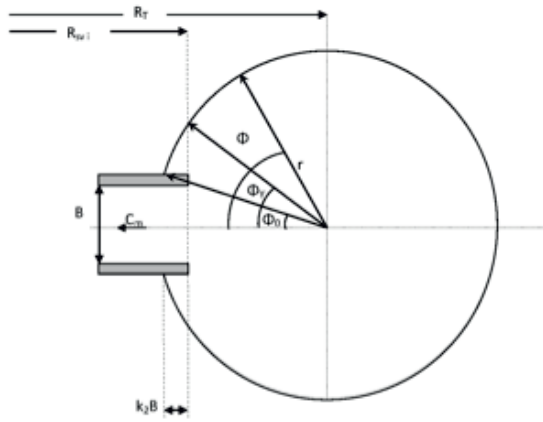

Figure 8.4: Cross section of spiral casing.

The boundary layer in the spiral casing cause an energy loss, but it also induce a secondary flow. To prevent this secondary flow to propagate into the stay vanes and guide vanes, the spiral casing overlaps the stay vane inlet. The overlap factor K_2 is traditionally set to 0.1 for high head Francis turbines. For the design software however, this factor has been set to 0.05.

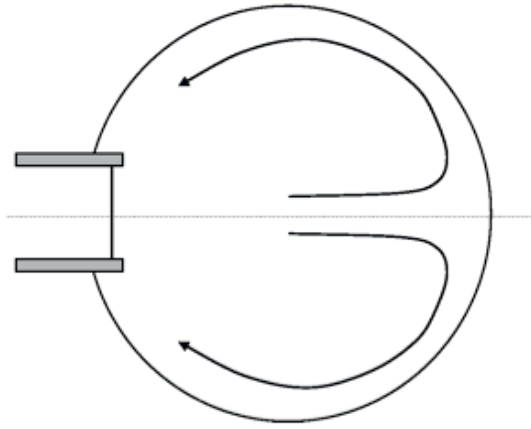

Figure 8.5: Secondary flow in spiral casing.

When designing the stay vanes, the designer has to choose a stay vane inlet radius, R_{svi}. As it is desirable to minimize the flow losses in the spiral casing, the casing is designed so that the flow follows a free vortex. The free vortex constant, K_{FV}, is found from the inlet dimensions of the stay vanes.

$$M = q\frac{b^2}{3} \qquad [Nm] \tag{8.10}$$

The spiral casing is made of a number of sections chosen by the designer. Many sections cause a better and more correct reduction of the flow through the spiral casing, but it is also more expensive to manufacture due to the increased number of weld joints.

R_T and r has to be calculated for each section in order to find the cross section area. This is obtained by at first choosing a starting value of r. Then ϕ_0 and ϕ_y is calculated from geometrical relations according to figure 8.4. Next, R_T is calculated from equation 8.11, and then an new value of r is found by solving equation 8.12 with respect to r. This is an iterative process, which is repeated until the value of r has converged.

$$M = q\frac{b^2}{3} \qquad [Nm] \tag{8.11}$$

$$M = q\frac{b^2}{3} \qquad [Nm] \tag{8.12}$$

When the dimensions of the spiral casing have been found, the thickness of the stay vanes should be calculated. If the required thickness is too small or too large, a new stay vane inlet diameter should be chosen. Subsequently the calculations of stay vane length, spiral casing dimensions and required stay vane thickness should be performed over again. This should be repeated until the required thickness of the stay vanes is acceptable.

1. Hermod Brekke. *Pumper og turbiner*. Waterpower Laboratory NTNU, 2003. ↩

Files related to the '*Guide vanes*' tab

- **guidevanes.m**
- **calcGV.m**
- **calcSV.m**
- **calcSC.m**
- **leadingsv.m**
- **trailingsv.m**

Functions related to the '*Guide vanes*' tab

In **guidevanes.m**

guidevanes	Generates all 'GUI' items on the Radial view tab
airfoilMenuCallback	Resets the blade leaning graph to no blade leaning. Runs function *Bladeleaning* to update the corresponding plots.
DgvaxCallback	Sets the number of blades to the chosen value, and runs the function *plotBG_3D*.
guidevanesCallback	Runs the function *plotBG_3D* to get the chosen colormap on the blades.
k_olCallback	Generates all 'GUI' items on the Radial view tab
t_svCallback	Resets the blade leaning graph to no blade leaning. Runs function *Bladeleaning* to update the corresponding plots.
sigmaCallback	Sets the number of blades to the chosen value, and runs the function *plotBG_3D*.
Z_svCallback	Runs the function *plotBG_3D* to get the chosen colormap on the blades.
Z_scCallback	Runs the function *plotBG_3D* to get the chosen colormap on the blades.

In **calcGV.m**

calcGV	Generates all 'GUI' items on the Radial view tab

In **calcSV.m**

calcSV	Calculates the radial view of the blade with blade leaning. Does also clacuate an estimate of the number of blades required to avoid backflow at the runner inlet, but this estimate should be controlled with CFD analyses of part load operation. Does also run the functions *plotBG_3D* and *plotUCu3D*.

In **calcSC.m**

calcSC	Plots the hub and shroud lines in the blade leaning figure in axddition to the dashed line indicating no blade leaning. Does also set the title and xlabel of the graph.

In **leadingsv.m**

leadingsv	The $U{\cdot}C_u$ distribution plotted in the distributions tab is the $U{\cdot}C_u$ distribution along the 2D streamline in the axial view, also denoted *G*. When having established the 3D blade, it is possible to find the $U{\cdot}C_u$ distribution along the 3D streamline. By including blade leaning with a gradual leaning from inlet to trailing end, the $U{\cdot}C_u$ distribution along the 3D streamilne is altered. This function calculates the new $U{\cdot}C_u$ distribution along the 3D streamline withand without blade leaning and plots it for the hub, shroud and the middle of the channel, all in absolute values unlike in the distributions tab where the plots are relative to the inlet value.

In **trailingsv.m**

trailingsv	The $U{\cdot}C_u$ distribution plotted in the distributions tab is the $U{\cdot}C_u$ distribution along the 2D streamline in the axial view, also denoted *G*. When having established the 3D blade, it is possible to find the $U{\cdot}C_u$ distribution along the 3D streamline. By including blade leaning with a gradual leaning from inlet to trailing end, the $U{\cdot}C_u$ distribution along the 3D streamilne is altered. This function calculates the new $U{\cdot}C_u$ distribution along the 3D streamline withand without blade leaning and plots it for the hub, shroud and the middle of the channel, all in absolute values unlike in the distributions tab where the plots are relative to the inlet value.

Runner Cascade

THis tab shows a 3D view of the runner, guide vanes and stay vanes. There is an option to hide different parts of the turbine.

1. Hermod Brekke *Konstruksjon av pumper og turbiner, sec 3.6 (in Norwegian)*. Waterpower Laboratory NTNU, 2000. ↩

Files related to the '*Blade thickness*' tab

- **bladethickness.m**
- **thicknessBT.m**
- **InitialiseBT.m**
- **plotBT.m**
- **plotthicknessBT.m**
- **leading.m**
- **trailing.m**
- **UpdateThickness.m**

Functions related to the '*Radial view*' tab

In **bladethickness.m**

bladethickness	Runs *MakeBTitems*.
MakeBTitems	Generates all 'GUI' items on the Blade thickness tab
ResetCallback	Resets the blade thickness distribution to having a constant thickness from leading edge to 50 % along the blade. Then tapering the blade thikcness to the set leading edge thickness. Subsequently runs *plotthicknessBT*
TleCallback	.
TteCallback	.
aSSSliderCallback	.
aSSEditCallback	.
aPSSliderCallback	.
aPSEditCallback	.

In **thicknessBT.m**

thicknessBT	Adds thickness to the infinitely thin blade generated in the Radial view tab.

In **InitialiseBT.m**

IntialiseBT	Sets the title and the ylabel to the blade thickness distribution figure. Also plots an initial blade thickness distribution based on the thicknesses chosen for last design.

In **plotBT.m**

plotBT	Plots the blade thickness distribution plot with control points.
startdragfcnbt	.
draggingfcnbt	.
dragfcnbtstop	.

In **plotthicknessBT.m**

plotthicknessBT	Plots the 3D blade with thickness. Subsequently runs *PlotBT*.

In **leading.m**

leading	Designs the leading edge of the runner blade according to the values of a_{ps} and a_{ss}, which are chosen by the program user within some preset intervals. The preset intervals are based on the chosen leading edge thickness.

In **trailing.m**

trailing	Designs the trailing edge of the runner blade according to the shape plotted in the lower left graph on the tab. The cut off angle is 30^{o}.

In **Updatethickness.m**

UpdateThickness	.
aBG	.

Summary

The Summary tab is the last tab and gives a summary of the turbine data is given. The *Save Design* button gives the possibility to save the design as a *.mat*-file containing the design parameters. The design will aslo be exported as *.curve*-files for Turbogrid import and as *.ibl*-files for import in Pro/E.

When the *Save Design* button is executed, a window appears giving the user ability to chose directory and create a folder for the exported files. The exported files will always have the same name, so the name of the folder will separate different designs.

Files related to the '*Summary*' tab

- **Summaryfill.m**

Functions related to the '*Summary*' tab

In **Summary.m**

SaveCallback	The *Save Design* button executes the *SaveCallback*-function. The function write design paramaters to a *.mat*-file and exports the design as *.curve*-files for Turbogrid import and as *.ibl*-files for import in Pro/E.

In **Summaryfill.m**

Summaryfill	Calculates the turbine submergence and creates strings of all calculated values so they can be presented in the Summary tab.